UC Riverside

UC Riverside Electronic Theses and Dissertations

Title

Equilibration of Edge States in the Quantum Hall State at Filling Fraction ν = 5/2

Permalink

https://escholarship.org/uc/item/5hn870hf

Author

Asasi, Hamed

Publication Date

2021

Copyright Information

This work is made available under the terms of a Creative Commons Attribution-NonCommercial-ShareAlike License, availalbe at https://creativecommons.org/licenses/by-nc-sa/4.0/

Peer reviewed|Thesis/dissertation

eScholarship.org Powered by the California Digital Library
University of California

UNIVERSITY OF CALIFORNIA
RIVERSIDE

Equilibration of Edge States in the Quantum Hall State at Filling Fraction $\nu = 5/2$

A Dissertation submitted in partial satisfaction
of the requirements for the degree of

Doctor of Philosophy

in

Physics

by

Hamed Asasi

March 2021

Dissertation Committee:

Professor Michael C. Mulligan, Chairperson
Professor Leonid P. Pryadko
Professor Shan-Wen Tsai

Copyright by
Hamed Asasi
2021

The Dissertation of Hamed Asasi is approved:

Committee Chairperson

University of California, Riverside

Acknowledgments

Studying for a PhD in physics far away from home has been a unique experience for me, and concluding it would have not been possible without the help and support of many. First, I thank my advisor, Michael Mulligan, who has been my main mentor during this period. I am grateful for his help and guidance throughout my research. He supported me both as an advisor and as a friend, and he made sure I had the best means to succeed in my PhD. I really appreciate our engaging meetings, his dedication in explaining his ideas and his help through the details of my research. I also learned a great deal from his lectures on quantum field theory and on topological field theories. I am grateful for his teachings and for his support.

I thank Professor Leonid Pryadko who advised me through my first year at UCR. I learned a lot from him both through his group meetings on quantum error correction, and thought his many informative courses such as quantum field theory and advanced condensed matter. I also thank him as well as Professor Shan–Wen Tsai for being on my dissertation committee and for their helpful suggestions and comments. I am also grateful to the many other teachers that I had during my time at UCR, specially Professor Kirill Shtengel and Professor John Baez. I learned a lot from them.

I thank Professor Dima Feldman for our illuminating correspondence on the details of this project and for his helpful insights on the subject of transport in quantum Hall states.

I am grateful for all the friends that I had during this journey. Either through engaging physics discussions or just hanging out, they made my experience at UCR more gratifying. Their companionship made me feel less away from home. Specially, I thank

Amir, Amin, Razie, Shima, Ali, Abtin, Amartya and Shane. I wish we all come out safe from the other side of this pandemic and that I get to hang out more with my friends.

And as always, I am grateful to my family for their never–ending love and support. I wouldn't be where I am without their help and my success wouldn't be worth without their presence. They always tried their best to make sure I had everything I needed to succeed, and they supported me in all my decisions. I will always have them in my heart.

The following publication is used in this thesis:

- "*Partial equilibration of anti-Pfaffian edge modes at* $\nu = 5/2$", Hamed Asasi and Michael Mulligan, Phys. Rev. B 102, 205104 (2020).

To my parents *Fatemeh* and *Reza* for everthing,

and to *Yasin*, *Hamideh* and *Hakimeh*.

ABSTRACT OF THE DISSERTATION

Equilibration of Edge States in the Quantum Hall State at Filling Fraction $\nu = 5/2$

by

Hamed Asasi

Doctor of Philosophy, Graduate Program in Physics
University of California, Riverside, March 2021
Professor Michael C. Mulligan, Chairperson

Among the most interesting approaches in building fault–tolerant quantum computation is utilizing non–Abelian topological phases of matter. These phases of matter are capable of storing information that is less susceptible to loss due to the interactions between the system and its environment. Furthermore, their non–Abelian characteristics allows for reliable performance of logical operations on the stored information. One of the leading physical systems that can realize such non–Abelian topological phases is the quantum Hall system at filling fraction 5/2. Since the discovery of this state, the nature of the ground state of this system has been the subject of debate. An important development was made recently when the thermal Hall conductance of this state was measured to be $K = 2.5\pi^2 k_B^2 T/3h$ [M. Banerjee *et al.*, Nature **559**, 205 (2018)]. Taken at face value, this result points to the PH–Pfaffian state as the true ground state of the quantum Hall system at filling fraction $\nu = 5/2$. It is the consequence of the assumption that all the modes running along the edge of this system are well–equilibrated with each other. However, as has been pointed out by other authors, this assumption may not be completely justified. In particular, the measured

thermal Hall conductance could also be consistent with the anti–Pfaffian state under some experimental conditions. In this thesis, we study those conditions in detail.

To achieve this, we propose new fixed point theories that describe the low–temperature physics of the anti–Pfaffian state. We demonstrate that these proposed theories could be consistent with the parameters describing the experimental conditions. For each of these fixed points, we identify the effective low–temperature edge modes and study the effect of strong short–range Coulomb interaction and an approximate spin symmetry on the interactions between them.

We derive the kinetic equations that describe the hydrodynamic transport of charge and heat in a general quantum Hall state. This is the expansion of the previous studies and includes the description of transport of strongly coupled edge modes. We use these kinetic equations to describe the hydrodynamic transport of heat and charge in our proposed fixed point theories. We estimate the values of physical parameters in our theory based on the previous experimental studies. This enables us to make meaningful comparisons between our theoretical predictions and the experimental measurements of thermal conductance. We show that there exists an experimentally realistic range of parameters that the anti–Pfaffian state is consistent with the thermal Hall conductance $K = 2.5\pi^2 k_B^2 T/3h$. We identify these ranges of parameters and based upon them, make predictions on the electrical and thermal Hall conductance of the anti–Pfaffian state for a range of temperatures.

Contents

List of Figures

List of Tables

Chapter 1

Introduction

Electrons confined to two spatial dimensions, cooled down to low enough temperatures and subject to a strong transverse magnetic exhibit some of the most interesting and diverse phenomena that has been observed in a condensed matter system. Known as the quantum Hall effect, this phenomena was discovered first in 1980 by von Klitzing, Dorda and Pepper [1], by measuring the electrical Hall resistance of high-purity MOSFET(metal-oxide-semiconductor field-effect transistor) samples. They discovered that the Hall resistance in these samples shows plateaus as a function of the magnetic field, such that the Hall conductance is quantized to integer multiple of e^2/h with a high precision. This phenomena is know as the integer quantum Hall effect (IQHE). While the results of these experiments were explained using the free-electron picture, the more illusive phenomena of fractional quantum Hall (FQHE), discovered in 1982 by Tsui, Stormer and Gossard [2], required a much more elaborate theory. In such a theory, the electron-electron interactions should be included as a necessary ingredient for a successful explanation of this phenomena. The

theoretical studies that followed the discovery of FQHE revealed the prospect for a variety of theoretical approaches that could be employed to explain the fractional Hall effect. Gauge invariance was used to explain the quantized conductance [3, 4]; the role of topology and topological field theories was identified in explaining the observed physics [5–7]; and it was shown that the quasi-particles of these theories exhibit fractional charge and statistics [8–10].

The first Hall plateau at a non–integral filling fraction was discovered at filling fraction $\nu = 1/3$ [2]. Soon, the underlying physics were explained in a pivotal work by Laughlin [8]. More experimental studies revealed a zoo of additional Hall plateaus at fractional filling fraction [11, 12]. These filling fractions shared the property that all have odd denominators. The physics of these states were explained using the extensions of Laughlin's idea which include the hierarchical scheme of D. Haldane and B. Halperin [9, 10] and the J. Jain's concept of composite fermions [13–15].

However, Willet *et al.* discovered a Hall plateau at an even-denominator filling fraction $\nu = 5/2$ [16]. The first explanation for this state, due to Haldane and Rezayi [17], included the role of interaction between electrons with different spins. This contrasts with the odd-denominator hierarchical states which are spin-polarized such that the different spins were living in different Landau levels and their interaction could be ignored. Later, more candidates were suggested for the Hall plateau at filling fraction $\nu = 5/2$. Among them, the Moore-Read Pfaffian state is of particular interest [18, 19]. In contrast to the earlier quantum Hall states, this state has non–Abelian topological order. Over the years, several other candidates for the Hall plateau at $\nu = 5/2$ has been suggested [20–24]. How-

ever, despite many theoretical, numerical and experimental effort, the nature of the ground state of this system is still debated.

Numerical studies point toward either the Moore-Read Pfaffian state [18, 25] or its particle-hole conjugate, the anti-Pfaffian state [20, 21], as the true ground state of the system [17, 26–29]. Both of these states host quasiparticles with non-Abelian statistics. On the other hand, quantum point contact tunneling experiments [30–34] support either the anti-Pfaffian state, the $SU(2)_2$ state, or the Abelian 331 or 113 states. Observation of upstream neutral modes [35, 36] only hints at the realization of a non-Abelian state. In light of these conflicting results, the recent measurement of the thermal Hall conductance in the Hall plateau at $\nu = 5/2$ by Banerjee *et al.* [37] appears highly valuable. Despite this, their result does not completely resolve the existing disagreement.

As first pointed out by Kane and Fisher [38], the thermal Hall conductance K provides a sensitive probe of the topological order of a fractional quantum Hall (FQH) state. In the long wavelength limit, the thermal Hall conductance is predicted to be $K = c_-\kappa_0 T$, where $\kappa_0 = \pi^2 k_B^3/3h$ and c_-, the chiral central charge of the quantum Hall's edge theory, is the difference between the right-moving central charge c_R and the left-moving one c_L. The half-integer value of c_- would suggest the existence of a Majorana edge mode and a non–Abelian topological order in the bulk. The recent measurement which finds the thermal Hall conductance to be $K = 2.5\kappa_0 T$ provides strong evidence for a non-Abelian quantum Hall state. Taken at face value, this result suggests that the recently proposed topological order, the particle-hole symmetric Pfaffian state (PH-Pfaffian) [24] which has chiral central charge $c_- = 5/2$, is realized.

Since the publication of this measurement result, several groups have proposed explanations for its apparent contradiction with the prior studies. One explanation [39] suggests that invoking disorder and Landau Level mixing would stabilize the PH-Pfaffian state in favor of the other candidate such as the Pfaffian and the anti-Pfaffian state. Disorder and Landau Level mixing are inevitably present in any real sample, but they are difficult to include in numerics. Another scenario for explaining $K = 2.5\kappa_0 T$ is that long-range disorder results in puddles of Pfaffian and anti-Pfaffian states, which (intuitively) contribute $(c_-^{\text{Pfaffian}} + c_-^{\text{anti-Pfaffian}})/2 = (7/2 + 3/2)/2$ to the thermal Hall conductance. The resulting state can exhibit the thermal Hall conductance of $K = 2.5\kappa_0 T$ in some parameter regimes [40–42]. However, the conditions for this observation were found to be rather restrictive.

Simon [43] has proposed an alternative interpretation: The experimental measurement may not directly reflect the bulk topological order; instead $K = 2.5\kappa_0 T$ may be due to suppressed thermal equilibration relative to charge equilibration. This partial equilibration is believed to occur at $\nu = 2/3$ and potentially $\nu = 8/3$ [37, 44]. The distinction between various candidate $\nu = 5/2$ states, based on the thermal Hall conductance, is clear only if the different edge channels of the quantum Hall sample are well equilibrated with each other. If instead there's no equilibration between edge modes, the thermal Hall conductance is proportional to the total central charge $c = c_R + c_L$ of the edge state. If the edge modes only partially equilibrate, the thermal Hall conductance can in principle take any value between the fully-equilibrated conductance and the non-equilibrated one.

Among the candidates for the $\nu = 5/2$ state, the anti-Pfaffian state is plausible to fit this picture of partial equilibration. There have been a variety of different scenarios

proposed for partial equilibration of the anti-Pfaffian edge states. Simon [43] originally suggested that the low velocity of the Majorana mode combined with long-range disorder might hinder the equilibration of the Majorana mode with the rest of the edge modes. However, it has been argued that the parameter regime required by this interpretation is not realized experimentally [37, 45]. Partial equilibration in the anti-Pfaffian state can also occur if the modes in the lowest Landau level do not equilibrate with modes in the first Landau level. One possible realization was described by Ma and Feldman [46]. Another mechanism whereby equilibration of the Majorana mode is suppressed was proposed by Simon and Rosenow [47]. There, equilibration between edge modes was assumed to be dominated by scattering via intermediate tunneling to Majorana zero modes localized in the bulk, rather than charge tunneling along the edge, considered in [43, 45, 46].

In this thesis, we continue the study of the role of equilibration in anti-Pfaffian edge-state transport. We do so by expanding the previous studies in two areas. First, we derive the kinetic equations for the transport of charge and heat along the edge of a quantum Hall state, starting from the low-energy field theory of the edge. This effort expands on the prior works in several aspects: through our detailed derivations we are able to relate the transport equations for charge and heat up to numerical coefficients. This allows us to analyze the experimental results one the charge and heat transport, in combination. In turn, we are better equipped to relate the edge theory of the anti-Pfaffian state to the transport measurements and narrow down the range of parameters consistent with them. In addition, our expressions for the kinetic equations are written for a general quantum Hall state. Therefore, they can be readily used for almost any quantum Hall state by simply

plugging in the microscopic theory of the edge.

Second, we pay close attention to the estimation of the non-universal parameters that describe the edge of the anti–Pfaffian state. These parameters include the velocity of the edge modes as well as the strength of Coulomb interaction between them. This lets us comment on the strength of the inter-mode conductivity coefficients and interpret the experimental results at a more granular level.

Furthermore, some of the assumptions we make in modeling the anti-Pfaffian state differs with the previous studies. In contrast to Ref. [43, 47], we assume that electron tunneling, induced by short-range disorder, serves to equilibrate the edge modes. Tunneling between spin-up and spin-down edge modes of the lowest Landau level plays a prominent role in our scenario. These tunnelings were not considered in the previous analysis (Ref. [46]) of transport in the anti-Pfaffian state, as it was argued that weak spin-orbit coupling suppresses such tunnelings. The effective theories we consider are driven by such spin-flip interactions. The resulting low-energy edge states have an approximate spin symmetry in the lowest Landau level that can serve to suppress thermal equilibration while simultaneously allowing complete charge equilibration over a range of experimentally-relevant temperatures, in the presence of a strong Coulomb interaction.

We start in chapter 2 by giving a brief introduction of the classical and quantum Hall effect. In line with our work, we mostly focus on transport phenomena and the role of edge modes in quantum Hall systems. In chapter 3, we expand on the description of edge modes and present the field theory treatment of the edge of a quantum Hall state. This field theory description is needed for the analysis of hydrodynamic transport. In chapter 4 we

present the general framework that we use in order to examine transport of charge and heat in the anti-Pfaffian state. Starting from the effective field theory of a general quantum Hall edge state, we derive the equations that describe charge and heat transport in the ohmic regime. In chapter 5 we discuss the edge theory of the anti-Pfaffian state. We identify low-temperature fixed points of this theory that we argue to be relevant to experiment and discuss two of the fixed points that are driven by spin-flip tunneling. In chapter 6 we apply the framework presented in chapter 4 to these low-energy fixed points. We calculate the electrical and thermal conductances for each of these theories and discuss the regime of parameters consistent with the measured electrical $G = 2.5\sigma_0$ and thermal $K = 2.5\kappa_0 T$ conductances. We discuss the degree to which such parameter regimes are realistic.

Throughout this thesis, we use the notation $\sigma_0 = \frac{e^2}{\hbar}$ and $\kappa_0 = \frac{\pi^2 k_B^2}{3h}$. However, for our calculations we use units where $e = \hbar = k_B = 1$ so that $\sigma_0 = \frac{1}{2\pi}$ and $\kappa_0 = \frac{\pi}{6}$.

Chapter 2

Quantum Hall Effect

In this chapter we give a brief introduction of the classical and quantum Hall effect. Our focus will be the transport properties of quantum Hall states. We start in section 2.1 by introducing the classical Hall effect. In section 2.2 we explain the integer quantum Hall effect (IQHE) and its conduction properties. Study of IQHE would also be useful in understanding the more complicated Hall effect in fractional fillings. In section 2.3 we introduce the fractional quantum Hall effect. This includes the discussion of Laughlin states, hierarchical state, composite fermions and non–Abelian quantum Hall states.

2.1 Classical Hall effect

The classical Hall effect was discovered in 1879 by Edwin Hall [48]. A simple setup to observe this effect is as follows: consider a conductor plate residing in the xy plane and a magnetic field applied in the z direction. The classical Hall effect is the observation that if an electrical current flows in the x direction, a transverse voltage (the Hall voltage) will

be produced in the y direction.

This phenomenon can be easily explained using the Drude model of electron conduction [49–51]. Using this model, the equation of motion of an electron (with mass m and charge $-e$) in the presence of static and uniform electric field $\boldsymbol{E}$ and magnetic field $\boldsymbol{B}$ is

$$m\frac{d\boldsymbol{v}}{dt} = -e(\boldsymbol{E} + \boldsymbol{v} \times \boldsymbol{B}) - m\frac{\boldsymbol{v}}{\tau}. \tag{2.1}$$

The last term on the right–hand–side represents the average effect of collisions experienced by an electron. Under stationary conditions the left–hand–side vanishes, and we easily solve these equations to find the electrical current:

$$\boldsymbol{J} \equiv -ne\boldsymbol{v} = \sigma\boldsymbol{E} \tag{2.2}$$

with the conductance tensor

$$\sigma = \frac{ne^2\tau/m}{1+\omega_B^2\tau^2}\begin{pmatrix} 1 & -\omega_B\tau \\ \omega_B\tau & 1 \end{pmatrix}. \tag{2.3}$$

Here n is the electron density and $\omega_B = |eB|/m$ is the cyclotron frequency of an electron. We can invert the conductivity tensor to find the resistivity tensor

$$\rho = \sigma^{-1} = \frac{1}{ne^2\tau/m}\begin{pmatrix} 1 & \omega_B\tau \\ -\omega_B\tau & 1 \end{pmatrix}. \tag{2.4}$$

Therefore the longitudinal resistivity is $\rho_{xx} = \rho_{yy} = ne^2\tau/m$, independent of the magnetic field while the transverse resistivity

$$\rho_{xy} = -\rho_{yx} = \frac{B}{ne} \tag{2.5}$$

is proportional to the applied magnetic field. What we can hopefully measure in the experiment is the Hall resistance, defined as the Hall voltage produced in the y direction divided

by the applied electrical current in the x direction. If we assume the sample is rectangular with length L_y in the y direction, we have

$$R_{xy} = \frac{V_y}{I_x} = \frac{L_y E_y}{L_y J_x} = -\frac{B}{ne}. \tag{2.6}$$

In the case where the charge carriers are not electrons, we need to replace $-e$ with q, the charge of the carriers, in the above expression. We can see that by measuring the Hall conductance, we can determine the sign of the charge carriers.

2.2 Integer quantum Hall effect

As we saw in the previous section, based on the classical motion of electron we expect that the Hall resistance grows linearly with the applied magnetic field. However, von Klitzing, Dorda and Pepper [1, 52] discovered that at low temperatures (lower than few Kelvins) and High magnetic fields (a few Teslas), the Hall resistance exhibits plateaus as the magnetic field is varied 2.1. At these plateaus, the Hall resistance takes the values

$$R_{xy} = \rho_{xy} = \frac{1}{\nu}\frac{2\pi\hbar}{e^2} \tag{2.7}$$

where ν takes integer values with a high accuracy (about one part per 10^9). The quantity $\frac{2\pi\hbar}{e^2} \equiv \sigma_0$ is called the *quantum of resistivity*. These plateaus could be explained first by looking at the quantum mechanical dynamics of an electron in the presence of a magnetic field. This is the problem of Landau levels.

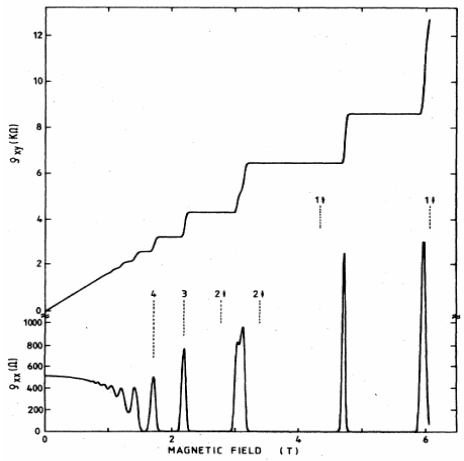

Figure 2.1: Experimental curves for the Hall resistance $R_H = \rho_{xy}$ and the resistivity $\rho_{xx} \sim R_x$ as a function of the magnetic field at a fixed carrier density (temperature $T \approx 8mK$) [52]

.

2.2.1 Landau levels

Consider an electron gas confined to a rectangular box with dimensions L_x, L_y and L_z along the three directions, in the presence of a uniform magnetic field $B_z = B$ along the z direction. The Hamiltonian for this electron is

$$H_0 = \frac{(\boldsymbol{p} - e\boldsymbol{A})^2}{2m} \tag{2.8}$$

where the vector potential is $\boldsymbol{A} = (0, Bx, 0)$ in the Landau gauge. The energy eigenvalues of this Hamiltonian are

$$E_n(k_z) = \hbar\omega_B(n + \frac{1}{2}) + \frac{\hbar k_z^2}{2m}; \qquad n \in \mathbb{Z}; \qquad k_z = \frac{2m_z\pi}{L_z},\ m_z \in \mathbb{Z}. \tag{2.9}$$

For small enough L_z and small enough temperatures, the dynamics in the z direction freezes out and the system becomes effectively two-dimensional. The corresponding eigenfunctions

in the Landau gauge are

$$\psi_{n,k_y}(x,y) \sim \mathrm{e}^{ik_y y}\, H_n(x + k_y \ell_B^2)\, \mathrm{e}^{-(x+k_y\ell_B^2)/2\ell_B^2}\,. \tag{2.10}$$

k_y is the wavevector in the y direction and is a constant of motion, $H_n(x)$ are Hermite polynomials and $\ell_B \equiv \sqrt{\hbar/|eB|}$ is called the *magnetic length*. For a given energy level n and wavevector k_y, the eigenfunction is wave–like in the y direction and localized around $x = -k_y\ell_B^2$ with an approximate spread $\sim \ell_B$. k_y labels the degenerate eigenfunctions at each energy level E_n. To figure out the number of degenerate states at each energy, we first note that due to the limit size of the sample in the y direction, k_y is quantized as

$$k_y = \frac{2m_y\pi}{L_y}, \quad m_y \in \mathbb{Z}. \tag{2.11}$$

On the other hand, the wavefunction should reside inside the sample which implies that the center of the wavefunctions at $\ell_B^2 k_y$ should satisfy

$$-L_x \leq \ell_B^2 k_y \leq 0 \rightarrow -\frac{L_x L_y}{2\pi\ell_B^2} \leq m_y \leq 0. \tag{2.12}$$

Therefore the degeneracy of each of the energy levels is

$$N_{\Phi_0} = \frac{L_x L_y}{2\pi\ell_B^2} = \frac{\mathcal{A}B}{h/e} \tag{2.13}$$

where $\mathcal{A}$ is the area of the two–dimensional sample. The second expression tells us that the degeneracy is equal to the number of flux quanta ($\Phi_0 = h/e$) that penetrates the sample's area.

2.2.2 Conduction of filled Landau levels

Here we discuss the conduction properties of a quantum mechanical sample of effectively two–dimensional electrons in the presence of a perpendicular magnetic field.

There are a few methods that one can use to find the conductance; these include using the Kubo formula and the argument from the gauge invariance [3, 4]. However, we will present an approach that emphasizes the role of the confining potential [53].

First, consider the problem of our free electron with the Hamiltonian H_0, Eq. 2.8, when we add a constant electric field along the x direction (the electrical potential is $V(x, y) = -E_x x$). In this case the Hamiltonian in the Landau gauge is

$$H = \frac{p_x^2}{2m} + \frac{(p_y + eBx)^2}{2m} + eE_x x. \tag{2.14}$$

The energy eigenvalues are

$$E_{n,k_y} = \hbar\omega_B(n + \frac{1}{2}) - \hbar k_y \frac{E_x}{B} - \frac{meE_x^2}{2B^2}. \tag{2.15}$$

Therefore the energy eigenvalues acquire dispersion and their group velocity is

$$v_y = \frac{1}{\hbar}\frac{\partial E_{n,k_y}}{\partial k_y} = -\frac{E_x}{B} = \frac{1}{B}\frac{\partial V}{\partial x}. \tag{2.16}$$

Now, consider a sample that is finite in the x direction ($0 \leq x \leq L_x$) while infinite along the y direction. This means there exists a confining potential at the two edges. Deep inside the sample, the potential is constant and so the group velocity is zero according to 2.16. Assuming the potential at edges are smooth enough so that it can be approximated by a linear potential, the modes along the edge have a finite dispersion: they move along the y direction at the $x = 0$ edge (where $\frac{\partial V}{\partial x} > 0$ to keep the electrons inside the sample) while moving along the $-y$ direction along the $x = L_y$ edge (where $\frac{\partial V}{\partial x} < 0$). These modes are called *chiral* since they are uni–directional and move in opposite directions at the two opposite edges.

Therefore, each state at energy level n and momentum $k_y = 2\nu_y\pi/L_y$ ($n_y \in \mathbb{Z}$) which is centered at $x = -\ell_B^2 k_y$ carries the electrical current density

$$J_y(n,k_y) = -\frac{\mathcal{N}(n,k_y)}{L_xL_y}ev_y = -\frac{\mathcal{N}(n,k_y)}{L_xL_y}\frac{e}{B}\frac{\partial V}{\partial x}|_{x=-\ell_B^2 k_y}. \tag{2.17}$$

$\mathcal{N}(n,k_y)$ is the number of electrons in the state specified by quantum numbers n and k_y. Since electron are fermions, $\mathcal{N}(n,k_y)$ is either zero or one. To find the total current carried by electrons, we just need to sum up the currents from all the filled states inside the sample ($0 \le x \le L_x$). Assuming ν Landau levels are completely filled

$$\begin{aligned} J_{y,\text{total}} &= -\frac{e}{B}\sum_{n=1}^{\nu}\sum_{n_y:0\le x\le L_x}\frac{\mathcal{N}(n,k_y)}{L_xL_y}\frac{\partial V}{\partial x}|_{x=-\ell_B^2 k_y} \\ &\approx -L_x\frac{\nu e}{B}\frac{eB}{2\pi\hbar}\int_0^{L_x}\mathrm{d}x\frac{\partial V}{\partial x} \\ &= \nu\frac{e^2}{2\pi\hbar L_x}\left(V(L_x)-V(0)\right). \end{aligned} \tag{2.18}$$

Therefore the total current is

$$I_{y,\text{total}} = L_xJ_{y,\text{total}} = \nu\frac{e^2}{2\pi\hbar}\left(V(L_x)-V(0)\right). \tag{2.19}$$

which results in the quantized Hall conductance

$$\sigma_{xy} = \frac{I_{y,\text{total}}}{\Delta_x V} = \nu\frac{e^2}{2\pi\hbar}, \qquad \nu \in \mathbb{Z}. \tag{2.20}$$

Therefore, the free electron picture can easily explain the Hall plateaus at integer filling fractions.

2.3 Fractional quantum Hall effect

In 1982, Tsui, Stormer and Gossard discovered an additional plateau at filling fraction $\nu \approx 1/3$ [2]. The corresponding Hall resistance was measured $\rho_{xy} \approx 3h/e^2$. Ad-

ditional plateaus were discovered later mostly in even–denominator filling fractions. These observations could not be explained using the free electron theory. The reason for the failure of the free electron picture is the macroscopic degeneracy of the ground state of the free system. For example, at a non–integral filling fraction $\nu < 1$ there are N_{Φ_0} accessible states in the lowest Landau level while there exists νN_{Φ_0} electrons. So there are $\binom{N_{\Phi_0}}{\nu N_{\Phi_0}}$ ways to fill the available states, and all would have the same energy (in the absence of any external potential). This means that any amount of electron interaction is significant and their effect could not be ignored. It turns out that at certain filling fractions, the electron system becomes gapped and behaves as an *incompressible liquid*. This phenomenon is known as the fractional quantum Hall effect. There exists a variety of such states with differing levels of complexity and sometimes different physical origins. We will introduce some of these states which are going to be useful for later discussions in this thesis.

2.3.1 Laughlin states

The first theoretical explanation of additional plateaus at fractional filling fractions is due to Laughlin [8]. He proposed the following wave–function for the quantum Hall state of N electron at filling fraction $\nu = 1/m$ when m is an odd integer:

$$\Psi_{\text{Laughlin}}(\{z_i\}) \sim \prod_{i<j}^{N} (z_i - z_j)^m \, \mathrm{e}^{-\sum_i |z_i|^2/4\ell_B^2} \, . \tag{2.21}$$

Here $z_i = x_i + iy_i$ is the complex coordinate of the i-th particle. The intuition behind this proposal can be understood as follows. Choosing the symmetric gauge for the vector potential in 2.8 as $\boldsymbol{A} = (-y, x, 0)B/2$, the un–normalized eigenfunctions of a single electron

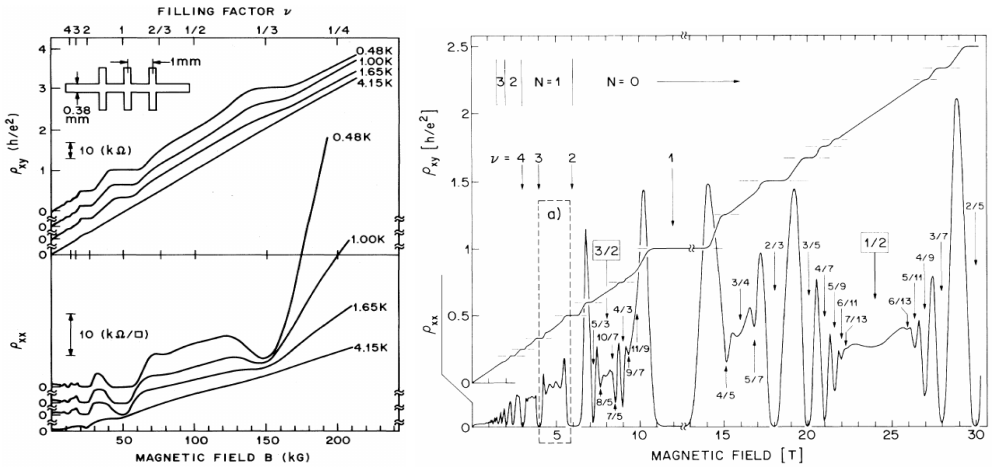

(a) (b)

Figure 2.2: Diagonal resistivity ρ_{xx} and Hall resistance ρ_{xy} in a quantum Hall setting of a $GaAs/AlGaAs$ heterostructure. (a) From [2]. Temperatures are specified on the plot. (b) From [16]. Temperature is $\approx 150mK$ except to the high–field Hall trace at $T = 85mK$.

can be written as

$$\psi_n(z = x + iy) = z^n \, \mathrm{e}^{-|z|^2/4\ell_B^2} \, . \tag{2.22}$$

This wavefunction describes a particle at angular momentum $n\hbar$. For a many–particle system where the electrons are non–interacting, the ground state of the system can be written as the Slater–determinant state

$$\psi(\{z_i\}) \sim \prod_{i<j} (z_i - z_j) \, \mathrm{e}^{-\sum_i |z_i|^2/4\ell_B^2} \, . \tag{2.23}$$

In this state the relative angular momentum of any two–particles cannot be smaller than $\hbar$ due to the Pauli's exclusion principle. Now, if we include the repulsive Coulomb inter–electron interactions, the electrons prefer to be farther away from each other, i.e. have larger relative angular momenta. This is exactly what the Laughlin wavefunctions in Eq.

2.21 describe. In fact, these wavefunctions are the ground state of the toy Hamiltonian [9, 54]

$$H = \sum_{m'=1}^{\infty} \sum_{i<j} v_{m'} \mathcal{P}_{m'}(ij). \tag{2.24}$$

$\mathcal{P}_{m'}(ij)$ is an operator that projects onto the state in which particles i and i have relative angular momenta m and $v_{m'}$ represent the eigenvalues of the repulsive potential $V(\boldsymbol{r} - \boldsymbol{r}')$. We can choose $v_{m'}$ to construct a simple model that describes the physics of the fractional quantum Hall effect. The Laughlin wavefunctions correspond to the choice

$$v_{m'} = \begin{cases} 1 & m' < m \\ \\ 0 & m' \geq m \end{cases} . \tag{2.25}$$

Therefore the Laughlin states describes a system of electrons where the relative angular momenta of any two electron cannot be smaller than m.

On the other hand, we can also check that the Laughlin wavefunction has filling fraction $\nu = 1/m$. The maximum power of z_i is the wavefunction 2.21 is $m(N-1)$. This means each electron has the maximum angular momentum $\hbar m(N-1)$. Therefore, the Hall droplet occupies the area $2\pi\ell_B^2 \times m(N-1)$, which means the electron density is $\approx (2\pi\ell_B^2 m)^{-1}$ in the thermodynamic limit. This corresponds to the filling fraction $\nu = 1/m$.

In addition, the toy Hamiltonian 2.24 implies that any state where two particles have angular momenta less than m would cost a finite amount of energy. This property makes the Laughlin states an *incompressible fluid*. This is a general property of all quantum Hall plateaus and is essential for the description of the edge modes that we will discuss in chapter 3.

Quasi–holes and quasi–particles

The system described by the Laughlin state 2.21 have gapped charge excitations known as quasi–holes and quasi–particles of the FQH state. A quasi–hole at the position $\zeta = \eta$ is described by the wavefunction

$$\psi_{q.h.}(\{z_i\};\eta) \sim \prod_{i=1}^{N}(z_i - \eta)\prod_{i<j}^{N}(z_i - z_j)^m \, \mathrm{e}^{-\sum_i |z_i|^2/4\ell_B^2} \, . \tag{2.26}$$

This quasi–hole has charge e/m. To see this, we put m quasi–holes at η. Following the similar line of arguments as before, the electrons in this new wavefunction have maximum angular momentum $\hbar mN$ and so the droplet with N electrons occupy the area $2\pi\ell_B^2 \times mN$, compared to $2\pi\ell_B^2 \times m(N-1)$ when no quasi–hole is present. That is, in this new wavefunction of m quasi–holes, N electrons occupy the area of $N+1$ electrons. This implies that the new system has the charge deficit of $-e$, or equivalently the wavefunction 2.27 has an extra charge e/m. This is exactly the quasi–hole at η.

In addition to carrying fractional charge, the quasi–holes have fractional statistics. The argument for such statistics is more involved and includes the calculation of Berry phase (See [55, 56]). Following such calculations, we can check that the quasi–holes has statistical angle π/m. This means when we switch the position of two quasi–holes, we get an additional statistical phase $\mathrm{e}^{i\pi/m}$ in the wavefunction. The particles that behave as such are called *Abelian anyons* [57, 58]. The name anyon signifies the fact that the wavefunction does not return to itself when one anyon moves around another anyon, but could acquire "any" phase; a situation that is only possible in two spatial dimensions. Abelian means during this process, the wavefunction only acquires a phase, and does not turn into a linearly independent wavefunction. The latter possibly describes non–Abelian anyons which we will

discuss in section 2.3.4.

Similarly, we can define the wavefunction for a quasi–particle. In the lowest Landau level, the conjugate operator to z is $2\ell_B^2\partial_z$ [8, 67]. Therefore, the wavefunction of the quasi–particle is

$$\psi_{q.p.}(\{z_i\};\eta) \sim \prod_{i=1}^{N}(2\ell_B^2\partial_{z_i} - \bar{\eta}) \prod_{i<j}^{N}(z_i - z_j)^m \, \mathrm{e}^{-\sum_i |z_i|^2/4\ell_B^2} \, . \tag{2.27}$$

Using similar arguments we an show that quasi–particles carry charge $-e/m$ and statistical angle $-\pi/m$.

2.3.2 Hierarchical states

Not all the observed plateaus could be described by the Laughlin wave–functions. These include filling fractions with odd–denominators such as $2/3, 2/5, 5/7$ as well as even–denominator fractions such $5/2$. We will postpone the discussion of the latter to section 2.3.4. One approach to explain the odd–denominator filling fractions besides the Laughlin states is the Haldane–Halperin hierarchy [9, 10]. The idea is that the quasi–particles of the Laughlin state can themselves form quantum Hall liquids. For instance, consider the Laughlin state at filling fraction $1/m$. The quasi–particles/quasi–holes of this state have fractional charge $q = \pm e/m$ and statistical angles $\alpha = \pm\pi/m$. Therefore, if we want to make a liquid state out of these quasi–particles/quasi–holes occupying coordinates η_i, the state with the right statistics would look like

$$\psi(\{\eta_i\};\{z_i\}) \sim \prod_{i<j}(\eta_i - \eta_j)^{2p+\alpha} \, \mathrm{e}^{-\sum_i |\eta_i|^2/4m\ell_B^2} \, \Psi_{\mathrm{Laughlin}}(\{z_i\}) \tag{2.28}$$

with p a positive integer. Note the m factor in the exponential is due the fact that the quasi–particles/quasi–holes have fractional charge. The particles that are described by

such a wave–function have certain maximum angular momentum and therefore occupy a certain area (See section 3.1 for details). We can use this to find the filling fraction of these quasi–particles/quasi–holes and consequently the total filling fraction. The resulting filling fraction is

$$\nu = \frac{1}{m \pm \frac{1}{2p}}. \tag{2.29}$$

These states form the first level of the hierarchy and include states with filling fractions such as $2/3, 2/5, 2/7$ and $6/13$. We can continue and build up higher level of this hierarchy. The filling fractions explained by this hierarchy are of the form

$$\nu = \frac{1}{m \pm \frac{1}{2p_1 \pm \frac{1}{2p_2 \pm \ldots}}}. \tag{2.30}$$

with positive integers p_i.

2.3.3 Composite fermions

There exists another approach for explaining some of the filling fractions other than the Laughlin fractions. This approach is based on the idea of *composite fermions* formulated by Jain [13, 15]. In order to understand the concept of composite fermoins, consider again the Laughlin wavefunction:

$$\Psi_{\text{Laughlin}}(\{z_i\}) \sim \prod_{i<j} (z_i - z_j)^m \, \mathrm{e}^{-\sum_i |z_i|^2/4\ell_B^2}. \tag{2.31}$$

Every particle except the one tat z_i sees the point $z = z_i$ as a vortex of order m: whenever this particle moves around z_i, the wavefunction acquires a $2m\pi$ phase. Of course, one of these vortices is always present due the Pauli exclusion of electron. The other $m - 1$ vortices are due to the repulsive Coulomb interaction. Therefore, we can imagine there

exists a bound state of an electron and $m-1$ vortices at position z_i. This bound state is called the composite fermion. These quasi–particles (the general concept, not to be confused with the quasi–particles of the Laughlin state) are useful since in this picture, the fractional quantum Hall effect of electrons can be thought of as the integer quantum effect of composite fermions. To see this, consider the effect of moving around a composite fermion around a region of area $\mathcal{A}$ inside the sample. Composite fermion has charge $-e$, so it acquires the Aharonov–Bohm phase $-2\pi B\mathcal{A}/\Phi_0$ during this process. In addition, this composite fermion would go around $n\mathcal{A}$ number of other composite fermions (n is the average electron density) and so acquires an additional $2\pi(m-1)n\mathcal{A}$ statistical phase. So the total acquired phase is

$$\gamma = -2\pi\frac{B\mathcal{A}}{\Phi_0} + 2\pi(m-1)n\mathcal{A}. \tag{2.32}$$

The net effect of this process looks as if the composite fermions has acquired only the Aharonov–Bohm phase but in a different effective magnetic field B^* such that

$$\gamma = -2\pi\frac{B^*\mathcal{A}}{\Phi_0} = -2\pi\frac{B\mathcal{A}}{\Phi_0} + 2\pi(m-1)n\mathcal{A} \rightarrow B^* = B - (m-1)n\Phi_0. \tag{2.33}$$

Therefore, we have N (number of electrons) composite fermions experiencing the effective magnetic field B^*. So, they would fill effective Landau levels (called Λ-levels) with the filling fraction

$$\nu^* = \frac{N_e}{|B^*|\mathcal{A}/\Phi_0}. \tag{2.34}$$

Now, if the composite fermions form an integer quantum Hall liquid at filling fraction $\nu^* \in \mathbb{Z}$, based on 2.33 the filling fraction of the electron would be

$$\nu = \frac{\nu^*}{(m-1)\nu^* \pm 1}. \tag{2.35}$$

The plus/minus sign is for positive/negative B^*, respectively. As an example, with $\nu^* = 1$ and $B^* > 0$, we recover the Laughlin states at $\nu = 1/m$. The set of states described by 2.35 are known as the *Jain sequence*, some of which have been observed experimentally.

2.3.4 Non–Abelian quantum Hall states

As we discussed in section 2.3.1, the excitations of the Laughlin states are Abelian anyons. The same is true for the hierarchical states. However, there exists fractional quantum Hall states that host non–Abelian anyons. The Pfaffian state [18, 19], the anti–Pfaffian state [20, 21] the PH–Pfaffian state [24] and the $SU(2)_2$ state [22, 23] are among such states. All of these examples are among the possible candidates for the quantum Hall plateau at filling fraction $\nu = 5/2$ [16]. Since in this thesis we are interested in the transport properties of the anti–Pfaffian state, we will focus mostly on this Hall plateau.

Before introducing the candidates for the Hall plateau at $\nu = 5/2$, we point out that as a zeroth–order approximation the interactions between electrons at the different Landau–levels (called Landau–level mixing) are ignored. With this assumption, we can treat Landau levels as independent which implies that all filling fractions $\nu = 2n + 1/2, n \in \mathbb{Z}$ on the same footing. $2n$ comes from n filled Landau–levels for the two directions of the electron spin. We should also point out that even without Landau–level mixing, the details of the electron interactions could be different from one Landau–level to another.

Moore–Read Pfaffian state

One of the proposed candidates for the observed Hall plateau at $\nu = 5/2$ is the *Moore-Read* or the *Pfaffian* state [18, 19]. The wavefunction of this state is

$$\psi(\{z_i\}) = \mathrm{Pf}\left(\frac{1}{z_i - z_j}\right) \prod_{i<j} (z_i - z_j)^m \, \mathrm{e}^{-\sum_i |z_i|^2/4\ell_B^2} \,. \tag{2.36}$$

The first factor represents the Pfaffian of the matrix with entries $1/(z_i - z_j)$, the Pfaffian of an anti–symmetric matrix being the square root of its determinant. For electrons, m should be even so that this wavefunction is anti–symmetric. Similar to section 2.3.1, we can deduce the filling fraction by counting the power of z_i. The maximum power of each z_i is $m(N-1)$ similar to the Laughlin states. Therefore, the filling fraction is $\nu = 1/m$.

We can interpret the wavefunction 2.36 in terms of composite fermions. We assume m vortices are attached to an electron. For m even, this turns electrons into composite fermions. For $m = 2$, Eq. 2.33 tells us that the composite fermions don't experience any effective magnetic field, i.e. $B^* = 0$. This could potentially mean that the composite fermions are free and have finite dispersion. However, this is not what the wavefunction 2.36 represents. To understand this contradiction, we should look at another state at filling fraction $\nu = 1/2$, the *Rezayi-Read* state [17, 60]. The wavefunction for this state is

$$\psi_{\mathrm{R.R.}}(\{z_i\}; \{\boldsymbol{k}_m\}) = \mathcal{P}_{LLL} \left[\det[\mathrm{e}^{i\boldsymbol{k}_m \cdot \boldsymbol{r}_i}] \prod_{i<j} (z_i - z_j)^2 \, \mathrm{e}^{-\sum_i |z_i|^2/4\ell_B^2} \right] . \tag{2.37}$$

The operator $\mathcal{P}_{LLL}$ projects to the lowest Landau level, $\boldsymbol{k}_m$ are momentum parameters and $\boldsymbol{r}_i$ is the position vector of the i-th particle. This wavefunction indeed describes composite "free" fermions at vanishing effective magnetic field and finite momenta $\boldsymbol{k}_m$. This system has a well–defined Fermi surface that have been confirmed experimentally [14, 61, 62]. More

precisely, it is a system of massive neutral composite fermions forming a Fermi surface that interact via a Chern–Simons gauge field. This description of composite fermions at $\nu = 1/2$ is known as the Halperin–Lee–Read (HLR) theory [63–65].

In light of this picture, the Pfaffian state Eq. 2.36 could be viewed as the BCS (Bardeen–Cooper–Shrieffer) pairing of the composite fermions described by Eq. 2.37. Since the state in Eq. 2.37 is spin–polarized, the spatial part of the wavefunction should anti–symmetric. The Pfaffian state is the result of pairing in the $p_x + ip_y$ angular momentum channel. In addition, the Pfaffian state is a topological superconductor [66]. As a result, the edge of this state host a chiral Majorana fermion. We will discuss edge theory of the Pfaffian state further in section 3.3.

Anti–Pfaffian state

One other consequence of ignoring the Landau–level mixing is that the particle–hole conjugate of a state at filling fraction $n + \tilde{\nu}$ with $\tilde{\nu} < 1, n \in \mathbb{Z}$ is a state at filling fraction $n + 1 - \tilde{\nu}$. The wavefunction for this state can be constructed following Ref. [59, 67]. The particle–hole conjugate of the Pfaffian state is therefore also a state at filling fraction $\nu = 5/2$. The wavefunction of this state is

$$\Psi(\{z_i\}) = \int [\prod_k \mathrm{d}\eta_k \mathrm{d}\bar{\eta}_k] \prod_{i<j} (z_i - z_j)\, \mathrm{e}^{-\sum_i |z_i|^2/4\ell_B^2} \prod_{i,k} (z_i - \eta_k) \prod_{k<l} (\eta_k - \eta_l)\, \mathrm{e}^{-\sum_k |\eta_k|^2/4\ell_B^2}\,. \tag{2.38}$$

As pointed out in Ref. [20, 21], this state is distinct from the Pfaffian state. This can be checked either by looking at the wavefunction 2.38 or by looking at the edge structure under this particle–hole transformation. We will discuss the edge structure of these states

in section 3.3. This new state for at filling fraction $\nu = 5/2$ is called the *anti-Pfaffian* state. The anti–Pfaffian state can also be viewed as a BCS instability of the Fermi surface of composite fermions. In this case, the composite fermions pair in the $p_x - ip_y$ angular momentum channel.

In the absence of interactions that break the particle–hole symmetry, the Pfaffian state and the anti–Pfaffian state are degenerate and are equally valid candidates for the state realized at the $\nu = 5/2$ Hall plateau. However, in practice there always exists some Landau–level mixing that could favor one of these states instead of the other. Numerical studies which include the Landau–level mixing have not been conclusive in determining which of these two states in energetically favorable [17, 26–29, 68, 69], although more recent studies favor the anti–Pfaffian state.

PH–Pfaffian state

More recently, another state was proposed as a candidate for the Hall plateau at $\nu = 5/2$. This state is called the particle–hole symmetric Pfaffian state or *PH-Pfaffian* [24, 39]. As the name suggests, this state is invariant under the particle–hole transformation. To understand the physics of this state, we have to look at its parent state which is a Fermi surface of Dirac composite fermions proposed by D.T. Son [24]. This state describes relativistic massless neutral composite fermions that interact via a statistical gauge field. This is to be contrasted with the HLR theory of massive composite fermions interacting via a Chern–Simons gauge field [64].

These composite fermions can form BCS pairs in a channel with even angular momentum. This evenness is the result of the nontrivial Berry phase of the composite

Fermi surface [24]. The PH–Pfaffian state has been described as the BCS pairing in the zero angular momentum s channel. In section 3.3 we will discuss the edge theory of this state.

Chapter 3

Field Theory of Edge States in Quantum Hall Effect

In the discussion of IQHE in section 2.2, we saw the role of edge states in the transport of charge. As we show in this chapter and the next one, the edge modes of fractional quantum Hall states are similarly responsible for transport. In this chapter, we focus on the field theory of these edge modes and the role of interactions. These studies would build the ground for studying the low–temperature transport of quantum Hall states that we get to in the next chapter.

3.1 Current algebra and Laughlin states

As we mentioned in section 2.3.1, the states describing the quantum Hall plateaus are incompressible. This means there can be no low–energy density excitations inside the bulk of the quanum Hall state. The only possible excitations happen at the edge of the

quantum Hall droplet. These take the form of changes in the shape of the boundary of the droplet. Following [6, 70–74], in order to describe the quantum mechanics of these boundary waves, we first write down the Hamiltonian of the edge classically, and then we will quantize the theory.

The energy of the droplet due to the confining potential $V(x, y)$ is

$$E = -e \int_{-\infty}^{\infty} \mathrm{d}x \int_{-\infty}^{\infty} \mathrm{d}y \ \rho(x, y) V(x, y), \tag{3.1}$$

where $\rho(x, y)$ is the two–dimensional electron density. Its value is $n = \nu |B| \mathcal{A}/\Phi_0$ inside the droplet and zero outside the droplet (See section 2.2.1 for notations). Now, let's assume for simplicity that the droplet occupies the $y < 0$ region so that the boundary is situated at $y = 0$. Also assume that the shape of the boundary wave at $y = 0$ is such that it can be written as a single–valued function $h(x)$; the density is n for $y \leq h(x)$ and zero for $y > h(x)$:

$$\rho(x, y) = n\theta(h(x) - y). \tag{3.2}$$

$\theta(x)$ is the step function. Therefore, the energy is

$$E = -ne \int_{-\infty}^{\infty} \mathrm{d}x \int_{-\infty}^{h(x)} \mathrm{d}y \ V(x, y). \tag{3.3}$$

The fact that the edge is at $y = 0$ implies that the confining potential does not change in the x direction at $y = 0$. Now, assume the confining potential is smooth enough (compared to the scale determined by $h(x)$) that it can be approximated with the linear potential

$$V(x, y) \approx \frac{\partial V}{\partial y}|_{y=0} y. \tag{3.4}$$

Note that since the droplet of negatively charged liquid occupies $y < 0$ we should have

$\frac{\partial V}{\partial y}|_{y=0} < 0$. Subtracting the energy of the un–distributed edge ($h(x) = 0$) we find

$$E = -\frac{ne}{2}\frac{\partial V}{\partial y}|_{y=0}\int_{-\infty}^{\infty} \mathrm{d}x\ h(x)^2. \tag{3.5}$$

We can relate the slope of the potential to the velocity of edge modes according to 2.16. We also define the one–dimensional density as $\rho(x) = nh(x)$. Overall we find

$$E = \frac{\pi\hbar}{\nu}|v_x|\int_{-\infty}^{\infty} \mathrm{d}x\ \rho(x)^2. \tag{3.6}$$

where v_x is the velocity of the edge waves.

On the other hand, the density wave described by $\rho(x,t)$ should also satisfy the chiral wave equation

$$\partial_t\rho(x,t) + v_x\partial_x\rho(x,t) = 0. \tag{3.7}$$

Therefore, in the momentum space ($k = 2n\pi/L$ with $n \in \mathbb{Z}$)

$$\rho(x) = \frac{1}{\sqrt{L}}\sum_k \mathrm{e}^{ikx}\,\rho_k \tag{3.8}$$

we have

$$E = \frac{2\pi\hbar}{\nu}|v_x|\sum_{k>0}\rho_{-k}\rho_k \tag{3.9}$$

$$\dot{\rho}_k = -iv_xk\rho_k. \tag{3.10}$$

To write down the energy as a Hamiltonian, we identify ρ_k as the coordinate. This means its conjugate momentum is

$$p_k = \mathrm{sign}(v_x)\frac{2\pi i\hbar}{\nu k}\rho_{-k}. \tag{3.11}$$

Now we can quantize this theory by requiring the commutation relation $[\rho_k, p_{k'}] = i\hbar\delta_{kk'}$. This implies

$$[\rho_k, \rho_{k'}] = \text{sign}(v_x)\frac{\nu k}{2\pi}\delta_{k+k'} \tag{3.12}$$

This algebra is known as the $U(1)$ Kac–Moody algebra.

The density operators $\rho(x,t)$ represent the neutral low–energy excitations of the edge. However, there also exists charge excitations of the edge represented by adding or removing electrons from the edge. Let's represent the creation operator for such electrons as $\psi^\dagger(x)$. We then expect

$$[\rho(x), \psi^\dagger(x')] = \delta(x - x')\psi^\dagger(x). \tag{3.13}$$

We can satisfy this relation by using the bosonized version of these fields (See [75–79]).

$$\psi^\dagger(x) = \frac{\gamma}{\sqrt{2\pi a}}\,\mathrm{e}^{-i\eta\phi(x)/\nu} \tag{3.14a}$$

$$\rho(x) = \frac{1}{2\pi}\partial_x\phi(x). \tag{3.14b}$$

$\eta = \text{sign}(v_x)$ is the chirality of the edge mode, γ is a Majorana fermion operator that ensures the correct anti–commutation of different species of fermion operators, and a is the short–distance cutoff. The chiral bosonic fields $\phi(x)$ satisfy

$$[\phi(x), \phi(x')] = \pi i\eta\nu\,\text{sign}(x - x'). \tag{3.15}$$

The fermion operators satisfy the correct anti–commutation relations

$$\{\psi(x), \psi^\dagger(x')\} = \delta(x - x') \tag{3.16a}$$

$$\{\psi(x), \psi(x')\} = \{\psi^\dagger(x), \psi^\dagger(x')\} = 0 \tag{3.16b}$$

only when $1/\nu$ is an odd number. This means the above formalism is only valid for the Laughlin states. As we will discuss in the next section, to accommodate for the other filling fractions we need to consider several branches of edge modes.

In addition to the fermion operators, there are operators $\mathrm{e}^{\pm i\eta_i\phi_i(x)}$ which annihilate/create quasi–particle/quasi–holes of the Laughlin state at the edge. These operators are the most basic set of operators that we can build our theory upon. One implication of this is that the bosonic fields ϕ should satisfy the periodicity conditions

$$\phi(x) \sim \phi(x) + 2n\pi, \quad n \in \mathbb{Z}. \tag{3.17}$$

3.1.1 Lagrangian formulation

In terms of the bosonic field $\phi(x)$, the Hamiltonian density of the edge mode of a Laughlin state is ($v = |v_x|$ is the magnitude of the edge mode velocity)

$$\mathcal{H} = \frac{v}{4\pi\nu} \left(\partial_x \phi(x)\right)^2 . \tag{3.18}$$

In some circumstances, it is more convenient to work with the Lagrangian formulation of this bosonic theory. To find the conjugate momentum to $\phi(x)$, we take the derivative of Eq. 3.15 with respect to x':

$$[\phi(x), \partial_{x'}\phi(x')] = -2\pi i\eta\nu\delta(x - x'). \tag{3.19}$$

Therefore the conjugate momentum to $\phi(x)$ would be $\pi(x) \equiv -\eta\partial_x\phi(x)/2\pi i\nu$. The usual procedure for writing down the Lagrangian would tell us that the action for this theory is

$$\mathcal{L} = \pi(x,t)\partial_t\phi - \mathcal{H} = -\frac{\eta}{2\pi\nu}\partial_t\phi\partial_x\phi - \frac{v}{4\pi\nu}(\partial_x\phi)^2. \tag{3.20}$$

However, this is not the correct theory as it would not produce the correct equation of motion for $\phi(x,t)$. This inconsistency is due to the non–local/self–dual nature of the field $\phi(x)$ [80–82]. The correct Lagrangian is

$$\mathcal{L} = \frac{1}{2}\pi(x,t)\partial_t\phi - \mathcal{H} = \frac{1}{4\pi\nu}\left(-\eta\partial_t\phi\partial_x\phi - v(\partial_x\phi)^2\right). \tag{3.21}$$

3.2 Hierarchical states

The field theory of the edge modes in a hierarchical state is a simple generalization of the above construction: at level N of the hierarchy, there are N droplets: each of these droplets has a specific filling fraction and its corresponding edge mode. In the first approximation we assume that these edges are far enough from each other so that we can treat them as independent. Therefore, we have N bosonic fields $\phi_i(x)$ with filling fractions ν_i and chirality η_i moving with the speed v_i. Assuming $B > 0$, the chirality of the edge mode is positive (negative) if the droplet is a condensate of negatively–charged quasi–particles (positively–charged quasi–holes). Therefore, these bosonic field satisfy the commutation relations

$$[\phi_i(x), \phi_j(x')] = \delta_{ij}\pi i\eta_i\nu_i\,\mathrm{sign}(x-x'), \tag{3.22}$$

and the total Hamiltonian in the absence of any extra interactions is

$$H = \sum_i H_i \tag{3.23a}$$

$$H_i = \frac{v_i}{4\pi\nu_i}\int \mathrm{d}x\ \left(\partial_x\phi_i(x)\right)^2. \tag{3.23b}$$

The electron operator corresponding to the i^{th} edge mode and its charge density (in units of $-e$) are

$$\psi_i^\dagger(x) = \frac{\gamma_i}{\sqrt{2\pi a}}\, \mathrm{e}^{-i\eta_i\phi_i(x)/\nu_i} \tag{3.24}$$

$$\rho_i(x) = \frac{1}{2\pi}\partial_x\phi_i(x). \tag{3.25}$$

with Majorana fermions satisfying $\{\gamma_i, \gamma_j\} = 2\delta_{ij}$. The basis represented by the fields ϕ_i is called the "symmetric" basis. It is also possible to use a different basis for describing the same theory. In general, the universal/topological nature of a chiral bosonic theory is described by the combination of a K matrix and a charge vector $\boldsymbol{t}$[5, 83]. The K matrix is defined by

$$[\phi_i(x), \phi_j(x')] = \pi i K_{ij}^{-1}\, \mathrm{sign}(x - x'). \tag{3.26}$$

In the symmetric basis of fields ϕ_i, the K matrix is $K_{ij} = \delta_{ij}\eta_i/\nu_i$. The charge vector represents the fact that the charge density carried by the edge mode ϕ_i is

$$\rho_i(x) = \frac{t_i}{2\pi}\partial_x\phi_i. \tag{3.27}$$

In the "symmetric" basis the charge vector is $\forall i : t_i = 1$. Therefore in the symmetric basis, the total charge density along the edge is

$$\rho(x) = \sum_i \rho_i(x) = \frac{1}{2\pi}\sum_i \partial_x\phi_i. \tag{3.28}$$

3.3 Non–Abelian states

Deriving the edge theory of the non–Abelian states is a more subtle problem. To achieve this, one has to study the excitations of the ground state wavefunction when quasi–holes are added near the edge [7, 18, 84]. Since in this thesis we are interested in QHE at

filling fraction $\nu = 5/2$, we only focus on the edge theory of a few of the potential candidates for this system: the Pfaffian state, the anti–Pfaffian state and the PH–Pfaffian state.

Pfaffian state

For the Moore–Read Pfaffian state at filling fraction $\nu = 1/2$, the spectrum of edge excitations correspond to a bosonic field representing the charge density fluctuations of the edge plus a Majorana fermion [7, 84]. These two edge excitation are moving in the same direction. This means that edge theory of the Pfaffian state consists of a chiral bosonic field $\phi(x)$ with $\eta = 1$ and $\nu = 1/2$ and a chiral Majorana fermion $\psi(x)$ with $\nu = 1$. The action for this theory is $S = S_\phi + S_\psi$ with

$$S_\phi = -\frac{1}{4\pi\nu} \int \mathrm{d}t \int \mathrm{d}x \; \partial_x\phi \left[\eta\partial_t\phi + v\partial_x\phi\right], \tag{3.29a}$$

$$S_\psi = \frac{1}{4} \int \mathrm{d}t \int \mathrm{d}x \; i\psi(\partial_t\psi + u\partial_x\psi). \tag{3.29b}$$

u is the velocity of the Majorana mode. The quasi–particle excitations can be created by either charge $e/2$ operators $\mathrm{e}^{i\phi}$ or $\psi\,\mathrm{e}^{i\phi}$, or by the charge $e/4$ operator $\sigma\,\mathrm{e}^{i\phi/2}$. The operator σ twists the boundary condition for the Majorana mode ψ. The anyons ψ and σ form the Ising topological quantum field theory with fusion rules (1 is the vacuum)

$$\psi \times \psi = 1, \quad \psi \times \sigma = \sigma, \quad \sigma \times \sigma = 1 + \psi. \tag{3.30}$$

When we are concerned with the Pfaffian state at filling fraction $\nu = 5/2$, we just need to add the edge modes for the two filled Landau levels. Denoting these bosonic field by ϕ_1 and ϕ_2 ($\nu_1 = \nu_2 = \eta_1 = \eta_2 = 1$) and the bosonic field at the half–filled second Landau level by

ϕ_3, the action in the absence of inter–mode interactions is

$$S = \sum_{i=1}^{3} S_i + S_\psi, \tag{3.31a}$$

$$S_i = -\frac{1}{4\pi\nu_i} \int \mathrm{d}t \int \mathrm{d}x \; \partial_x \phi_i \left[\eta_i \partial_t \phi_i + v_i \partial_x \phi_i\right], \tag{3.31b}$$

$$S_\psi = \frac{1}{4} \int \mathrm{d}t \int \mathrm{d}x \; i\psi(\partial_t \psi + u\partial_x \psi). \tag{3.31c}$$

Anti–Pfaffian state

As we pointed out in section 2.3.4, The Pfaffian state is not particle–hole symmetric and its particle–hole conjugate is the anti–Pfaffian state. This fact can be used to write down the edge theory for the anti–Pfaffian state. In fact, this is the first approach that was used in Ref. [20] to study this new state. In the Pfaffian state at $\nu = 1/2$, the edge states separate the vacuum ($\nu = 0$) from the bulk at $\nu = 1/2$. The particle–hole conjugate of this edge is realized by putting a narrow region with $\nu = 1$ between the vacuum and the anti–Pfaffian bulk at $\nu = 1/2$. In this setup, the edge modes that sit between the $\nu = 1$ state and the $\nu = 1/2$ state are the same modes as the ones for the Pfaffian state but now moving in the opposite direction (upstream). In addition, there exists a $\nu = 1$ edge mode that sits between the vacuum and the $\nu = 1$ state. Therefore, the edge theory of the anti–Pfaffian state at $\nu = 1/2$ consists of a $\nu_3 = 1, \eta_3 = 1$ chiral boson ϕ_3, a $\nu_4 = 1/2, \eta_4 = -1$ chiral boson ϕ_4 and a $\eta = -1$ chiral Majorana. Similar to the previous section, to get the edge modes for the anti–Pfaffian state at $\nu = 5/2$ we add the two edge modes of the Lower Landau levels ϕ_1 and ϕ_2 with $\nu_1 = \nu_2 = \eta_1 = \eta_2 = 1$. Therefore, the action for the edge of the anti–Pfaffian state at $\nu = 5/2$ in the absence of additional interactions is

$S = \sum_{i=1}^{4} S_i + S_\psi$ with

$$S_{\phi_i} = -\frac{1}{4\pi\nu_i} \int \mathrm{d}t \int \mathrm{d}x \; \partial_x \phi_i \left[\eta_i \partial_t \phi_i + v_i \partial_x \phi_i)\right], \tag{3.32a}$$

$$S_\psi = \frac{1}{4} \int \mathrm{d}t \int \mathrm{d}x \; i\psi(\partial_t \psi - u\partial_x \psi). \tag{3.32b}$$

PH–Pfaffian state

The basic excitations of the PH–Pfaffian state are quasi–particle/quasi–hole of charge $\mp e/4$ [24]. However, since they are half–vortex excitations, they must be created in pairs. So, we might conclude that we cannot have edge modes with filling fraction $\nu = 1/4$ and only an edge mode with filling fraction $\nu = 1/2$ is possible. Also, the existence of a half–vortex quasi–hole implies the presence of Majorana zero modes. Therefore, the PH–Pfaffian state is non–Abelian and its edge has a chiral Majorana mode.

The chirality of these edge modes are determined by imposing the particle–hole symmetry on the edge structure of this state and on its electrical and thermal Hall conductance [39]. The transport properties of quantum Hall states will be explained in the next chapter. For now, we only need to know the following: for an edge theory with a set of chiral bosons ϕ_i (with filling fraction ν_i and chirality η_i) and a chiral Majorana fermion ψ (with chirality η) the electrical conductance G and the thermal conductance K are

$$G = \frac{e^2}{h}\nu = \frac{e^2}{h}\Big|\sum_i \eta_i \nu_i\Big| \tag{3.33}$$

$$K = \frac{\pi^2 k_B^2}{3h} T \Big|\eta c_\psi + \sum_i \eta_i c_i\Big|. \tag{3.34}$$

$c_i = 1$ is the central charge of a bosonic mode and $c_\psi = 1/2$ is the central charge of a Majorana mode.

To determine the chirality of the $\nu = 1/2$ bosonic mode η_ϕ and also that of the Majorana mode η_ψ, we look at the behavior of the electrical and thermal conductance under the particle–hole transformation. Under this transformation, the chirality of all the edge modes are reversed and an edge mode corresponding to a filled Landau level (with $\nu = \eta = c = 1$) is added. Therefore, under the particle–hole transformation

$$G = \frac{e^2}{h}.\left|\frac{1}{2}\eta_\phi\right| \rightarrow G' = \frac{e^2}{h}\left|1 - \frac{1}{2}\eta_\phi\right| \tag{3.35a}$$

$$K = \frac{\pi^2 k_B^2}{3h}T\left|\eta_\psi\frac{1}{2} + \eta_\phi\right| \rightarrow K' = \frac{\pi^2 k_B^2}{3h}T\left|1 - \eta_\psi\frac{1}{2} - \eta_\phi\right|. \tag{3.35b}$$

Particle–hole symmetry of the PH–Pfaffian state implies $G = G'$ and $K = K'$. Based on the above expressions we can deduce that $\eta_\phi = 1$ and $\eta_\psi = -1$. Calling the $\nu = 1/2$ bosonic mode ϕ_3 and including the edge modes from the lower filled Landau–levels ϕ_1 and ϕ_2 ($\nu_1 = \nu_2 = \eta_1 = \eta_2 = 1$), the action for the PH–Pfaffian state at $\nu = 5/2$ is $S = \sum_{i=1}^{3} S_i + S_\psi$ with

$$S_{\phi_i} = -\frac{1}{4\pi\nu_i}\int \mathrm{d}t \int \mathrm{d}x\ \partial_x\phi_i\left[\eta_i\partial_t\phi_i + v_i\partial_x\phi_i)\right], \tag{3.36a}$$

$$S_\psi = \frac{1}{4}\int \mathrm{d}t \int \mathrm{d}x\ i\psi(\partial_t\psi - u\partial_x\psi). \tag{3.36b}$$

3.4 Interactions

There are different ways that the edge modes of a quantum Hall system can interact. One possibility is that an edge mode has interaction with itself. For example, we can include higher order density–density interactions in 3.6, which might play an important role when the confining potential is not smooth enough. This can lead to a reconstruction of the edge where one edge mode is broken into several edge modes [85–91]. For the pur-

poses of this thesis, we ignore such interactions and focus on the inter–edge interactions and their effect on the low–energy/low–momentum physics. In this section, we will only discuss interactions in a hierarchical state. Though, these treatments can be easily generalized to include the Jain states and non–Abelian states. In particular, we will discuss interactions in the edge theory of the anti–Pfaffian state in chapter 5.

3.4.1 Coulomb interactions

Since the edge mode are charged, there exists Coulomb interactions between them. We only consider the short–ranged density–density interactions with interaction potential

$$H_{\text{Coulomb}} = \frac{1}{4\pi} \sum_{i \neq j} v_{ij} \int \mathrm{d}x \; \partial_x \phi_i(x) \partial_x \phi_j(x). \tag{3.37}$$

The positive values v_{ij} quantify the magnitude of these Coulomb interactions. In the language of renormalization group, these interactions are marginal relative to the fixed point of the "free" theory given by Eq. 3.23. This can be easily checked by observing that the bosonic fields have zero scaling dimension. Therefore, these Coulomb interactions could affect the low–energy physics. However, it is easy to include the effects of such interaction. First, we note that the Hamiltonian $H_0 + H_{\text{Coulomb}}$ is a quadratic theory

$$H_0 + H_{\text{Coulomb}} = \frac{1}{4\pi} \sum_{ij} V_{ij} \int \mathrm{d}x \; \partial_x \phi_i(x) \partial_x \phi_j(x) \tag{3.38}$$

with velocity matrix

$$V_{ij} = \begin{cases} \frac{v_i}{\nu_i} & i = j \\ v_{ij} & i \neq j \end{cases}. \tag{3.39}$$

Using a linear transformation $\phi_i = \Lambda_{i\alpha}\tilde{\phi}_\alpha$ we can easily diagonalize this theory [92]. We should point out that this transformation is not a typical diagonalization where orthogonal/unitary transformations are employed. The transformations Λ should be canonical, i.e. preserve the structure of the commutation relations in Eq. 3.26 (although we allow for the scaling of the bosonic fields for convenience).

To proceed, we first perform a scaling of the fields as $\phi \equiv \sqrt{\nu_i}\phi_i'$ so that the commutation relations for the new fields are

$$[\phi_i'(x), \phi_j'(x')] = \delta_{ij}\pi i\eta_i \,\mathrm{sign}(x - x'). \tag{3.40}$$

Then we transform these fields as $\phi_i' = \tilde{\Lambda}_{i\alpha}\tilde{\phi}_\alpha$ and require the matrix $\tilde{\Lambda}_{i\alpha}$ to diagonalize $H_0 + H_{\mathrm{Coulomb}}$ as

$$H_0 + H_{\mathrm{Coulomb}} = \frac{1}{4\pi}\int \mathrm{d}x \ \left[\sum_\alpha \tilde{v}_\alpha \partial_x\tilde{\phi}_\alpha \partial_x\tilde{\phi}_\alpha)\right]. \tag{3.41}$$

This means we should have

$$\Lambda^T V \Lambda = \tilde{V} \tag{3.42}$$

with diagonal matrix $\tilde{V}_{\alpha\beta} = \delta_{\alpha\beta}\tilde{v}_\alpha$. The requirement that the transformation $\tilde{\Lambda}$ be canonical means

$$[\tilde{\phi}_\alpha(x), \tilde{\phi}_\beta(x')] = \delta_{\alpha\beta}\pi i\tilde{\eta}_\alpha \,\mathrm{sign}(x - x'), \tag{3.43}$$

or equivalently

$$\tilde{\Lambda}^T \eta \tilde{\Lambda} = \tilde{\eta} \tag{3.44}$$

where $\eta_{ij} = \delta_{ij}\eta_i$, $\tilde{\eta}_{\alpha\beta} = \delta_{\alpha\beta}\tilde{\eta}_\alpha$. Overall, we can write the resulting action as

$$S_0 + S_{\mathrm{Coulomb}} = -\frac{1}{4\pi}\int \mathrm{d}t \int \mathrm{d}x \left[\sum_\alpha \partial_x\tilde{\phi}_\alpha(\tilde{\eta}_\alpha\partial_t\tilde{\phi}_\alpha + \tilde{v}_\alpha\partial_x\tilde{\phi}_\alpha)\right]. \tag{3.45}$$

This theory in terms of the set of free chiral bosons $\tilde{\phi}_\alpha$ is a conformal field theory where the chiral fields have zero scaling dimension.

3.4.2 Tunneling interactions

Another form of interaction along the edge of a quantum Hall state is tunneling between the edge modes. In general electrons can tunnel between different edge modes. Quasi–particles can also tunnel provided the region between the two modes allow the existence of such particles. At low energies, these tunnelings should always be assisted by a disorder potential that breaks the translational symmetry of the edge [46, 93]. The reason is that the different edge modes have different Fermi momenta. So a translationally invariant edge cannot provide the momentum mismatch between the different modes. The momentum difference is due to the magnetic flux that penetrates the area between the edge modes. If the distance between the two edge modes is d, then the difference in their Fermi momenta is

$$\Delta k_F = \frac{eB}{\hbar} d. \tag{3.46}$$

Therefore the disorder should vary considerably at least over the length scale $1/\Delta k_F$. To get a sense of the order of magnitude of the numbers involved, let's take the example of $\nu = 2/3$ of Fig. 2.2a where $B \approx 18T$. Taking $d \sim \ell_B$ we get $\Delta k_F \sim 1/\ell_B \approx (6nm)^{-1}$.

Estimates based on experimental parameters (see [45]) suggest that disorder satisfies this requirement. Relaxation of such an assumption, however, has interesting consequences for the equilibration of edge modes, as suggested by Simon [43]. If the disorder can indeed provide this momentum difference, then we can assume that the tunneling be-

tween the edge modes happen in practice. In this case, for simplicity, we take the disorder potential to be a random field $\xi(x)$ with Gaussian distribution and correlation

$$\overline{\xi(x)\xi^*(x')} = W\delta(x-x'). \tag{3.47}$$

W quantifies the strength of the tunnelings. Now we can write down the tunneling interaction term as (h.c. stands for Hermitian conjugate)

$$H_{\text{tunneling}} = \int \mathrm{d}x \left[\xi(x)\, \mathrm{e}^{i\sum_i m_i\phi_i(x)} + \text{h.c.}\right]. \tag{3.48}$$

These interactions should conserve the total charge in the process. The operator $\mathrm{e}^{i\eta_i\phi_i}$ annihilates a quasi–particle of charge ν_i. Therefore, we should have

$$\sum_i \eta_i\nu_i m_i = 0. \tag{3.49}$$

The inclusion of the effect of these tunneling interactions in describing the low–energy physics of the edge is, in general, a nontrivial problem. In order to analyze the effect of these tunnelings, we first write the action of the theory. Including the short–ranged Coulomb interactions and the tunnelings we have $S = S_{F.P.} + S_{\text{tunneling}}$ with (*F.P.* stands for fixed point)

$$S_{F.P.} = -\frac{1}{4\pi}\int_{t,x}\left[\sum_i \frac{1}{\nu_i}\partial_x\phi_i(\eta_i\partial_t\phi_i + v_i\partial_x\phi_i) + \sum_{i\neq j} v_{ij}\partial_x\phi_i\partial_x\phi_j\right], \tag{3.50a}$$

$$S_{\text{tunneling}} = -\int_{t,x}\sum_{p\in P}\left[\xi_p(x)\, \mathrm{e}^{i\sum_j m_j\phi_j} + \text{h.c.}\right]. \tag{3.50b}$$

We used the shorthand notation $\int_{t,x} = \int \mathrm{d}t \int \mathrm{d}x$. As we demonstrated in the previous section, the theory described by the action $S_{F.P.}$ is completely solvable and describes a set of independent chiral bosonic field $\tilde{\phi}_\alpha$. So, the first step in analyzing S is to consider the

effect of $S_{\text{tunneling}}$ near the fixed point described by $S_{F.P.}$. First, we look at the scaling dimension of the tunneling operator $\mathcal{O}(x) = \mathrm{e}^{i\sum_i m_i\phi_i(x)}$. Denoted by $\Delta_{\mathcal{O}}$, it is defined by the correlation function

$$\left\langle \mathcal{O}(x,t)\mathcal{O}^{\dagger}(x,t=0)\right\rangle \sim |t|^{-2\Delta_{\mathcal{O}}}. \tag{3.51}$$

We can find its value at the fixed point theory described by $S_{F.P.}$ (See Appendix A). Its value is

$$\Delta_{\mathcal{O}} = \frac{1}{2}\sum_{i,j,\alpha} m_i m_j \Lambda_{i\alpha}\Lambda_{j\alpha}. \tag{3.52}$$

where the transformation $\phi_i = \Lambda_{i\alpha}\tilde{\phi}_\alpha$ diagonalizes $S_{F.P.}$. Now, by a simple counting of scaling dimensions and considering Eq. 3.47, we can find the scaling dimension of W

$$[W] = 2\Delta - 3. \tag{3.53}$$

This implies that the renormalization group (RG) equation to linear order near the $S_{F.P.}$ fixed point is

$$-\frac{dW}{d\ln\Lambda} = (3-2\Delta)W, \tag{3.54}$$

with Λ being the momentum scale. Therefore, for $\Delta > 3/2$ the tunneling strength W is irrelevant at low momenta/low energies, and we can treat the tunneling term $S_{\text{tunneling}}$ in perturbation theory. On the other hand, when $\Delta > 3/2$ the tunneling strength W becomes relevant at low energies and the theory described by $S_{F.P.} + S_{\text{tunneling}}$ is no longer a good starting point for the study of the low energy physics. For certain edge theories, there exists emergent fixed points know as the *disordered fixed points* which could be written as a simple quadratic theory of chiral bosons, similar to $S_{F.P.}$ [93]. These fixed point theories

will be useful in describing the edge theory of the anti–Pfaffian state that we will describe in chapter 5.

3.4.3 Disordered fixed point

The disordered fixed point was introduced by Kane, Fisher and Polchinski [93] in order to analyze the low energy physics of the edge of FQHE at filling fraction $\nu = 2/3$. In the absence of edge reconstruction [89–91, 94], the edge of this Hall state consists of a $\nu_1 = 1$ downstream ($\eta_1 = 1$) chiral boson ϕ_1 and a $\nu_2 = 1/3$ upstream ($\eta_2 = -1$) chiral boson ϕ_2. Considering the most relevant tunneling term, the action for the Hall bar edge is $S = S_{F.P.} + S_{\text{tunn.}}$ with

$$S_0 = -\frac{1}{4\pi}\int_{t,x}\Big[\sum_{i=1}^{2}\nu_i\partial_x\phi_i(\eta_i\partial_t\phi_i + v_i\partial_x\phi_i) + 2v_{12}\partial_x\phi_1\partial_x\phi_2\Big], \tag{3.55a}$$

$$S_{\text{tunn.}} = -\int_{t,x}\left[\xi(x)\,\mathrm{e}^{i(\phi_1+3\phi_2)} + \text{h.c.}\right], \quad \overline{\xi(x)\xi^*(x')} = W\delta(x-x'). \tag{3.55b}$$

In order to identify the disordered fixed point, we write this theory in terms of the charge mode and the neutral mode. The total charge mode is $\phi_\rho = \sqrt{\frac{3}{2}}(\phi_1 + \phi_2)$ while the neutral mode is $\phi_\sigma = \frac{1}{\sqrt{2}}(\phi_1 + 3\phi_2)$. In this basis, we have $S = S_\sigma + S_\rho + S_{\sigma\rho}$ with

$$S_\rho = -\frac{1}{4\pi}\int_{t,x}[\partial_x\phi_\rho(\partial_t\phi_\rho + v_\rho\partial_x\phi_\rho)] \tag{3.56a}$$

$$S_\sigma = S_{\sigma,0} + S_{\text{tunn.}} \tag{3.56b}$$

$$S_{\sigma,0} = -\frac{1}{4\pi}\int_{t,x}\left[\partial_x\phi_\sigma(\eta_\sigma\partial_t\phi_\sigma + v_\sigma\partial_x\phi_\sigma\right], \tag{3.56c}$$

$$S_{\text{tunn.}} = -\int_{t,x}\left[\xi(x)\,\mathrm{e}^{i\sqrt{2}\phi_\sigma} + \text{h.c.}\right] \tag{3.56d}$$

$$S_{\rho\sigma} = -\frac{1}{4\pi}v_{\rho\sigma}\int_{t,x}[\partial_x\phi_\rho\partial_x\phi_\sigma)] \tag{3.56e}$$

where $\eta_\sigma = -1$. When Δ, the scaling dimension of $e^{i(\phi_1+3\phi_2)}$, is smaller than 3/2 the edge is driven out of the free fixed point (described by S_0) to a new fixed point where $v_{\rho\sigma} = 0$. In order to see this, first note that at $v_{\rho\sigma} = 0$ the neutral and charge modes are decoupled. Also it is easy to see that $\Delta = 1$ (See Appendix A). As a result, the operators $\partial_x\phi_\sigma$, $e^{i\sqrt{2}\phi_\sigma}$ and $e^{-i\sqrt{2}\phi_\sigma}$ all have scaling dimension one and therefore, form the generators for an $\mathfrak{su}(2)_1$ algebra. More specifically, the current operators (a is the short–distance cutoff) [92, 95, 96]

$$J^x = \frac{1}{2\pi a}\cos(\sqrt{2}\phi_\sigma) \tag{3.57a}$$

$$J^y = \frac{1}{2\pi a}\sin(\sqrt{2}\phi_\sigma) \tag{3.57b}$$

$$J^z = \frac{1}{2\pi\sqrt{2}}\partial_x\phi_\sigma \tag{3.57c}$$

satisfy a $\mathfrak{su}(2)_1$ current algebra as

$$\Big[J^a(x), J^b(x')\Big] = -\frac{i}{4\pi}\eta_\sigma\delta^{ab}\partial_x\delta(x-x') + i\epsilon^{abc}J^c(x)\delta(x-x'). \tag{3.58}$$

We can use this fact to write the action of the neutral mode S_σ in Eq. 3.56 as a free theory. In terms of the currents 3.57, the Hamiltonian of the neutral field is

$$H_\sigma = \int \mathrm{d}x \left[\frac{2\pi v_\sigma}{3}J^2 + 2\xi^a J^a\right], \tag{3.59}$$

with

$$J^2 = (J^x)^2 + (J^y)^2 + (J^z)^2 \tag{3.60a}$$

$$\boldsymbol{\xi} = \Big(\frac{\xi+\xi^*}{2}, \frac{\xi-\xi^*}{2i}, 0\Big). \tag{3.60b}$$

Now, note that the algebra Eq. 3.58 is preserved under the $SO(3)$ gauge transformation

$$J^a(x) = O^{ab}(x)\tilde{J}^b(x) + h^a(x), \quad h^c(x) = \frac{1}{8\pi}\epsilon^{abc}(O(x)\partial_x O^T)^{ab}. \tag{3.61}$$

This means the currents $\tilde{J}^b$ satisfy the same algebra as J^a. The Hamiltonian of the neutral mode H_σ is invariant (up to inconsequential additive constants) under this gauge transformation, provided the disorder transforms as

$$\xi^a(x) \to \tilde{\xi}^a(x) = \left(\xi^b(x) + \frac{2\pi v_\sigma}{3} h^b\right) O^{ba}. \tag{3.62}$$

We can require $\tilde{\xi}(x) = 0$ in order to eliminate the tunneling term from H_σ. This amounts to the specific choice of O^{ab}

$$O(x) = S(x, x_0)O(x_0), \quad S(x, x_0) \equiv P_x e^{\frac{6}{v_\sigma}\int_{x_0}^{x} \mathrm{d}x' \ \boldsymbol{\xi(x')}.\boldsymbol{L}}. \tag{3.63}$$

$O(x_0)$ is an arbitrary $SO(3)$ rotation, P_x is the path ordering operator putting operators with larger x to the left, and $L^a, a = x, y, z$ are the three generators of $SO(3)$. After this transformation we express the currents $\tilde{J}^a$ in terms of a new bosonic field $\tilde{\phi}_\sigma$, similar to 3.57. In terms of $\tilde{\phi}_\sigma$

$$H_\sigma = \frac{v_\sigma}{4\pi} \int \mathrm{d}x (\partial_x \tilde{\phi})^2. \tag{3.64}$$

Therefore, the resulting action for the whole edge theory is $S = S_\sigma + S_\rho + S_{\sigma\rho}$ with

$$S_\rho = -\frac{1}{4\pi} \int_{t,x} [\partial_x \phi_\rho (\partial_t \phi_\rho + v_\rho \partial_x \phi_\rho)] \tag{3.65a}$$

$$S_\sigma = -\frac{1}{4\pi} \int_{t,x} \left[\partial_x \tilde{\phi}_\sigma (\partial_t \tilde{\phi}_\sigma + \eta_\sigma v_\sigma \partial_x \tilde{\phi}_\sigma\right] \tag{3.65b}$$

$$S_{\rho\sigma} = -\frac{2v_{\rho\sigma}}{4\pi} \int_{t,x} \partial_x \phi_\rho \left(\frac{\sqrt{2}}{a} O^{zx} \cos(\sqrt{2}\tilde{\phi}_\sigma) + \frac{\sqrt{2}}{a} O^{zy} \sin(\sqrt{2}\tilde{\phi}_\sigma) + O^{zz} \partial_x \tilde{\phi}_\sigma\right). \tag{3.65c}$$

Here, we also used the following transformation in order to eliminate the term proportional to $h^z(x)$:

$$\phi_\rho(x,t) \to \phi_\rho(x,t) + 2\sqrt{2}\pi \frac{v_{\rho\sigma}}{v_\rho} \int_{-\infty}^{x} \mathrm{d}x \ h^z(x). \tag{3.66}$$

$S_\sigma + S_\rho$ describes the disordered fixed point that we promised; a free theory around which we can analyze the effect of $S_{\rho\sigma}$ and possibly other interaction terms. In order to see the effect of $S_{\rho\sigma}$, first write (we use $\tilde{J}^a$ only as a shorthand here)

$$S_{\rho\sigma} = -\frac{1}{2\pi}\int_{t,x} \partial_x \phi_\rho(\boldsymbol{\xi}_\sigma . \tilde{\boldsymbol{J}}(x)), \qquad \xi^a_\sigma \equiv 2\pi\sqrt{2} v_{\rho\sigma} O^{za}(x). \tag{3.67}$$

Since $\xi(x)$ is a quenched (time–independent) random field, so is the field $\xi^a_\sigma(x)$. The auto–correlation of this field decays on the length scale $\sim v_\sigma^2/W$. We can see this by looking at the solution Eq. 3.63 and considering 3.47. This decay of auto–correlation of $\xi_\sigma(x)$ renders $S_{\rho\sigma}$ irrelevant on length scales larger than v_σ^2/W. Assuming v_σ^2/W is small enough, for simplicity we take ξ^a_σ to have Gaussian correlation $\overline{\xi^a_\sigma(x)\xi^b_\sigma(x')} = \delta^{ab} W_\sigma \delta(x-x')$ where $W_\sigma \approx 8\pi^2 v_{\rho\sigma}^2 v_\sigma^2/W$. Dimensional analysis shows that the scaling dimension of the coupling W_σ is 1 so that the interaction term $S_{\rho\sigma}$ is irrelevant at low energies, about the disordered fixed point.

Therefore, for the edge theory of FQHE at $\nu = 2/3$ we have a line of fixed points when $\Delta > 3/2$ described by S_0 and a fixed point at $\Delta = 1$ described by $S_\sigma + S_\rho$. An RG analysis around $\Delta = 3/2$ [93] suggests that the $\Delta = 1$ point is the attractive fixed point for all $\Delta < 3/2$.

This analysis can be generalized to all the states in the Jain series with filling fractions $\nu = n/(pn+1)$ [92] (p is an even integer. See section 2.3.3). In this case, the edge theory possesses an emergent $SU(n)$ symmetry. We can readily see this for the simple case of $p = 0$ i.e. the integer QHE at $\nu = n$. In this case we have n chiral bosons with $\forall i: \ \eta_i = \nu_i = 1$. The most relevant tunnelings are of the form $\mathcal{O}_{ij} = \mathrm{e}^{i(\phi_i - \phi_j)}$. The total charge mode along the edge is $\phi_\rho = (\sum_i \phi_i)/\sqrt{\nu}$ while we can define the $n-1$ neutral modes

as

$$\phi_{\sigma_m} = \sum_j D^m_{jj} \phi_j, \tag{3.68}$$

where D^m for $m = 1, ..., n-1$ are the diagonal generators of the $\mathfrak{su}(n)$ algebra. The diagonal entries of D^m starting from the top are m ones, then one $-m$ and the rest zero. Now, the neutral density operators $\partial_x \phi_{\sigma_m}$ form the $n-1$ mutually commuting generators of the current algebra $\mathfrak{su}(n)_1$ (its Cartan sub–algebra). Then, the $n(n-1)$ raising/lowering operators are defined as

$$i \neq j: \quad J^{ij} \sim \mathrm{e}^{i(\phi_i - \phi_j)}. \tag{3.69}$$

Overall, the density operators and the raising/lowering operators constitute the $n^2 - 1$ generators of the $\mathfrak{su}(n)_1$ current algebra. This emergent symmetry can be used to eliminate the tunneling terms $\mathrm{e}^{i(\phi_i - \phi_j)}$ from the action. Therefore, we find a quadratic theory describing the disordered fixed point at which the scaling dimension of the tunneling operators are $\Delta_{\mathcal{O}_{ij}} = 1$.

Chapter 4

Transport in quantum Hall states

In this chapter, we derive the kinetic equations that describe the low–temperature dc transport of charge and heat along the edge of a quantum Hall state. Ultimately, we are interested in setting up a machinery that allows us to find the two–terminal electrical and thermal conductance of a quantum Hall state. However, these methods can be readily used to study other transport phenomena in quantum Hall states. These might include finding the multi–terminal Hall conductance [92, 97] or investigations of equilibration in more complex geometries [98–100].

An example of a setup that we are interested in is shown in Fig. 4.1. It represents a quantum Hall bar at filling fraction $\nu = 2/3$ and two contacts that are used to measure the two–terminal Hall electrical and thermal Hall conductance. The left and right edges of the Hall bar are coupled to leads held at chemical potentials μ_L and μ_R and temperatures T_L and T_R, respectively. The two edge modes carry charge and heat along the edge and result in a net charge and heat current from one contact to the other. These net currents

depend on the edge structure of the Hall bar (i.e. the filling fraction of the edge modes, their chiralities and their central charges) as well as on the interactions between the modes that equilibrate charge and heat. The universal conductance values that are usually measured in quantum Hall states are the result of effective equilibration of the edge modes. The universal value of the electrical conductance of a quantum Hall plateau at filling fraction ν is $G = \nu e^2/h$ while the universal value of the thermal conductance is $K = c\frac{\pi^2 k_B^2}{3h}T$ where c is the chiral central charge of the edge theory. In this chapter, we will discuss these values and the conditions under which such values are measured.

In section 4.1 we consider the simplest situation when no equilibration occurs between the edge modes. Then in section 4.2 we present a phenomenological description of equilibration and what we expect to happen when the edge modes equilibrate. In section 4.3, we study how the microscopic interactions between the modes drive the equilibration of charge and heat and then derive the kinetic equations describing the hydrodynamic transport of charge and heat. Our derivation is the generalization of the previous studies [92, 101–104] to multiple number of edge modes. Also, we will discuss how the equilibration of charge and heat are related and we highlight the dependence of the kinetic equations on the low–temperature fixed point of the edge theory. In section 4.6, we will apply these results to transport in the quantum Hall plateau at filling fraction $\nu = 5/2$ and discuss electrical and thermal conductance in some candidate states for this Hall plateau. The detailed application the kinetic equations to the anti–Pfaffian edge theory will be the subject of chapter 6.

Throughout this chapter we use the system of units where $e = \hbar = k_B = 1$ unless

explicitly mentioned otherwise.

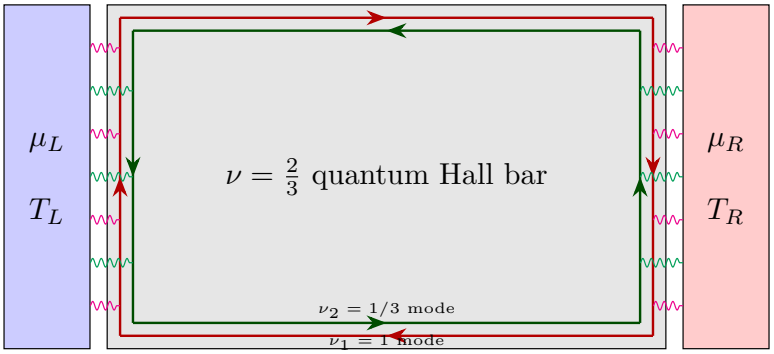

Figure 4.1: Schematic geometry for the measurement of two–terminal Hall conductance of quantum Hall state at filling fraction $\nu = 2/3$. The two counter–propagating modes (red and green directed lines) of the edge theory of $\nu = 2/3$ QHE are shown (See section 3.4.3). The wiggly lines represent tunnelings from the contacts to the edge modes along left and right line junctions.

4.1 Transport without equilibration

4.1.1 Charge transport

As we discussed in 3.1, the charge density fluctuations along the edge of a quantum Hall state are described by chiral bosonic modes ϕ that carry charge density $n(x) = \frac{1}{2\pi}\partial_x\phi(x)$. Indeed, starting from the Lagrangian Eq. 3.21 we can view the charge conservation as the result of the shift symmetry (c is a constant)

$$\mathcal{L}(\phi(x) + c) = \mathcal{L}(\phi(x)) \tag{4.1}$$

and the Noether's theorem. Applying Neother's theorem to the Lagrangian of Eq. 3.21 we find the conservation law

$$\partial_t n(x,t) + \partial_x I(x,t) = 0 \tag{4.2}$$

with charge current operator

$$I(x) = -\frac{1}{2\pi}\partial_t \phi(x). \tag{4.3}$$

In the absence of any tunneling between the edge modes, the current in each mode is separately conserved. Therefore, to find the electrical conductance we can simply add up the contributions from the different modes. Focusing on only one edge mode, we first calculate the charge current along the Hall bar in a setup similar to Fig. 4.1. We can do this using the Kubo formula [103, 105]. Assume we bias the edge with electrical potential $\mu(x,t)$. The perturbed Hamiltonian is

$$H = \int \mathrm{d}x \left[\frac{v}{4\pi\nu}\partial_x\phi(x)^2 - \mu(x)\frac{1}{2\pi}\partial_x\phi(x)\right]. \tag{4.4}$$

Kubo formula for calculating the effect of $\mu(x,t)$ on the electrical current, to linear order is

$$I(x,t) \equiv \left\langle \hat{I}(x,t)\right\rangle = -i\int \mathrm{d}x' \int_{-\infty}^{t} \mathrm{d}t' \left\langle [-\frac{1}{2\pi}\partial_t\phi(x,t), -\frac{1}{2\pi}\partial_x\phi(x,t)]\right\rangle \mu(x,t). \tag{4.5}$$

It is most convenient to find the above correlation function using the imaginary time Matsubara formalism where $t = -i\tau$ and $\omega + i\delta \to i\omega_n$ ($\omega_n = 2\pi n/\beta,\ n \in \mathbb{Z}$ are the Matsubara frequencies and $\beta = 1/k_B T$). In the frequency domain we have:

$$I(x, i\omega_n) = i\int \mathrm{d}x' \int_0^{\beta} \mathrm{d}\tau\, \mathrm{e}^{i\omega_n\tau} \left\langle T\partial_\tau\phi(x,-i\tau), \partial_x\phi(x,-i\tau)\right\rangle \mu(x, i\omega_n). \tag{4.6}$$

Using the Green functions introduced in Appendix A and after a few steps we find

$$I(x, i\omega_n) = \frac{\eta\omega_n}{2\pi v}\int \mathrm{d}x'\ \ \mathrm{e}^{-\omega_n\eta(x-x')/v}\,\theta(\eta(x-x'))\mu(x', i\omega_n). \tag{4.7}$$

We can observe the chiral nature of the edge mode in this expression: for a downstream edge mode with $\eta = 1$ (upstream edge mode with $\eta = -1$), the current at point x only depends on the applied voltage in the region $x' < x$ ($x' > x$). In order to apply this expression to the two–terminal geometry, consider the voltage

$$\mu(x', i\omega_n) = \begin{cases} \mu_L & x' < 0 \\ \mu_R & x' > L \\ 0 & 0 < x' < L. \end{cases} \tag{4.8}$$

We find

$$\begin{cases} \eta = 1 : & I(x, i\omega_n) = \frac{\nu}{2\pi}\mu_L \, \mathrm{e}^{-\omega_n x/v} \\ \eta = -1 : & I(x, i\omega_n) = -\frac{\nu}{2\pi}\mu_R \, \mathrm{e}^{\omega_n (x-L)/v} \end{cases} . \tag{4.9}$$

Now, an issue comes up when we want to find the DC current ($i\omega_n = 0$) far away from the contacts at $x' < 0, x' > L$. We have to take two limits: $i\omega_n \to 0$ and $x \to \infty$ for $\eta = 1$ ($(L - x) \to \infty$ for $\eta = -1$). The order of taking these two limits would change the final result. This issue has been discussed before [38, 77, 106]. The resolution is that one should take the limit $i\omega_n \to 0$ first, in order the get the correct result for the Hall conductance. Doing so we find

$$I(x, i\omega_n = 0) = \begin{cases} \frac{\nu}{2\pi}\mu_L & \eta = 1 \\ -\frac{\nu}{2\pi}\mu_R & \eta = -1 \end{cases} . \tag{4.10}$$

Therefore in a two–terminal setup (Fig. 4.1) a downstream (upstream) edge mode carries the electrical currents $\frac{\nu}{2\pi}\mu_L$ ($-\frac{\nu}{2\pi}\mu_R$) along the top edge and the current $\frac{\nu}{2\pi}\mu_R$ ($-\frac{\nu}{2\pi}\mu_L$) along the bottom edge. Note that we take the clockwise direction to be positive. Therefore,

the total current transported from the left contact to the right contact is

$$I_{\text{total}} = \frac{\nu}{2\pi}(\mu_L - \mu_R) \tag{4.11}$$

irrespective of the chirality. This merely represents the fact that negative charges move from lower potentials to higher potentials. The two–terminal conductance of a single edge mode with filling fraction ν and chirality η is

$$G_{\text{single mode}} = \frac{(\mu_L - \mu_R)}{I_{\text{total}}} = \frac{\nu}{2\pi}. \tag{4.12}$$

If the quantum Hall bar consists of N non–interacting edge modes with filling fraction ν_i and chiralities η_i, the two–terminal electrical conductance is the sum of the contributions from each mode:

$$G = \sum_i G_i = \frac{1}{2\pi} \sum_{i=1}^{N} \nu_i. \tag{4.13}$$

Unless all the edge modes propagate in the same direction, this is not a result that is observed in the measurements of electrical conductance. Instead the experiments measure the conductance

$$G = \frac{1}{2\pi}\nu = \frac{1}{2\pi}|\sum_{i=1}^{N} \eta_i \nu_i|. \tag{4.14}$$

In order to explain the experiments we need to include the effects of the interactions between edge modes and their effect on the equilibration.

4.1.2 Heat transport

Heat or thermal currents are also conserved due to the time translation symmetry of the edge theory (Lagrangian Eq. 3.21 for a chiral boson and Eq. 3.29b for a Majorana

mode). Using Noether's theorem we can identify the heat/energy density $\mathcal{H}$ and heat current J^Q which satisfy the conservation equation

$$\partial_t \mathcal{H}(x,t) + \partial_x J^Q(x,t) = 0. \tag{4.15}$$

For a single bosonic edge mode with filling fraction ν and chirality η

$$\mathcal{H}(x) = \frac{v}{4\pi\nu} \left(\partial_x \phi(x)\right)^2, \tag{4.16}$$

$$J^Q(x) = \frac{\eta}{4\pi\nu} \left(\partial_t \phi(x)\right)^2, \tag{4.17}$$

while for a Majorana fermion of chirality η

$$\mathcal{H}(x) = \frac{i\eta u}{4} \psi(x) \partial_x \psi(x), \tag{4.18}$$

$$J^Q(x) = -\frac{i\eta u}{4} \psi(x) \partial_t \psi(x). \tag{4.19}$$

The edge modes carry heat only if they are at finite temperature. Temperature is not exactly an external field that we can simply add its contribution by adding a term to the Hamiltonian. Therefore, it is not immediately obvious how one can use the Kubo formula for calculating the heat current. However, as was suggested by Luttinger, one can indeed treat the temperature as an external field that couples to the stress–energy tensor [105, 107, 108]. This basically renders a temperature field as equivalent to a gravitational field.

Although, it is possible to use the Kubo formula for finding the heat current, we can use a simpler approach when dealing with quantum Hall states, following Ref. [38]. A chiral edge mode with velocity v and chirality η at momentum k carries the energy $E_k = \eta v k$ ($\hbar = 1$). Also, in thermal equilibrium at temperature T the number of bosons at energy

E_k is given by the Bose–Einstein distribution for the chiral bosons and by the Fermi–Dirac distribution for the Majorana fermions. Therefore, we can simply add the expectation value of the energy for each momentum to get the total energy. For a chiral boson in a system of size L we have (See Eq. A.6. We use the units where $k_B = \hbar = 1$)

$$\langle H_\phi \rangle = \sum_{\eta k>0} \eta v k \left\langle b_k^\dagger b_k \right\rangle = \frac{L}{2\pi} \int_{\eta k>0} \mathrm{d}k \frac{\eta v k}{\mathrm{e}^{\eta v k/T} - 1} = \frac{L\pi}{6v} \frac{T^2}{2}, \tag{4.20}$$

While for a Majorana fermion

$$\langle H_\psi \rangle = \sum_{\eta k>0} \eta v k \left\langle \psi_k^\dagger \psi_k \right\rangle = \frac{L}{2\pi} \int_{\eta k>0} \mathrm{d}k \frac{\eta v k}{\mathrm{e}^{\eta v k/T} + 1} = \frac{L\pi}{12v} \frac{T^2}{2}. \tag{4.21}$$

Therefore, we can write the energy density generally as

$$\mathcal{H} = c \frac{\pi}{6v} \frac{T^2}{2}, \tag{4.22}$$

where c is the central charge of the edge mode: $c = 1$ for bosons and $c = 1/2$ for Majorana fermions. For chiral modes, the energy current is related to the energy density simply as

$$J^Q = \eta v \mathcal{H} = \eta c \frac{\pi}{6} \frac{T^2}{2}. \tag{4.23}$$

We define the coefficient $\kappa_0 = \pi/6$. In SI units it is $\kappa_0 = \pi^2 k_B^2 / 3h$.

Now, assuming there are no interactions between the edge modes, we can find the total heat current carried in a two–terminal setup. Similar to the previous section, we find the total current carried by N edge modes

$$J^Q_{\text{total}} = \frac{\kappa_0}{2} (\sum_{i=1}^{N} c_i) \left(T_L^2 - T_R^2 \right). \tag{4.24}$$

Therefore, for small temperature differences ($|T_R - T_L| \ll T_{L/R}$), the thermal Hall conductance is

$$K = \frac{T_L - T_R}{J^Q_{\text{total}}} = \kappa_0 \bar{T} (\sum_{i=1}^{N} c_i), \tag{4.25}$$

with the average temperature $\bar{T} = (T_L + T_R)/2$. Experimental measurements of thermal Hall conductance are a relatively new achievement [37, 44]. The results that has been gathered so far contradict the above expression for K. Kane and Fisher [38] predicted that the thermal conductance is indeed quantized but with the value

$$K = \frac{T_L - T_R}{J^Q_{\text{total}}} = \kappa_0 \bar{T} \Big| \sum_{i=1}^{N} \eta_i c_i \Big|. \tag{4.26}$$

This is the result when the edge modes are fully equilibrated with each other. Indeed, for the quantum Hall states for which the ground state is well known, the experimental measurements are very close to the fully equilibrated prediction. On the other hand, there are quantum Hall plateaus for which there is not a unanimous agreement on what ground state is realized in experimental conditions. The most notable of such states is the quantum Hall system at filling fraction $\nu = 5/2$. We will discuss the transport characteristics of some candidates for this state in section 4.6.

4.2 Equilibration: phenomenology

When we add tunneling between the edge modes, the charge and energy on any individual edge is no longer conserved, and we need to modify the conservation equations 4.2 and 4.15. To start with a simple setup, consider two bosonic edge modes ϕ_1 and ϕ_2 that interact only through an impurity at $x = x_0$ along the edge. First, we look at charge equilibration. The impurity at x_0 drives a tunneling current $I_{\text{tunneling}}$ from mode ϕ_1 to mode ϕ_2. At the phenomenological level, we can write the DC (static) tunneling term using

the Ohm's law as

$$I_{\text{tunneling}} = G\left(\mu_2(x_0) - \mu_1(x_0)\right), \tag{4.27}$$

where μ_i is the electrical potential of edge mode ϕ_i and $G > 0$ is the conductance of the impurity and its value depends on the strength of tunnelings at $x = x_0$. The conservation of total charge current along the edge implies

$$I_1(x_0 + \delta x) - I_1(x_0 - \delta x) = -I_2(x_0 + \delta x) + I_1(x_0 - \delta x) = I_{\text{tunneling}}, \tag{4.28}$$

where δx represents a small distance along the edge. Combined with 4.27

$$\Delta I_1(x_0) \equiv I_1(x_0 + \delta x) - I_1(x_0 - \delta x) = G\left(\mu_2(x_0) - \mu_1(x_0)\right) \tag{4.29a}$$

$$\Delta I_2(x_0) \equiv I_2(x_0 + \delta x) - I_2(x_0 - \delta x) = -G\left(\mu_2(x_0) - \mu_1(x_0)\right). \tag{4.29b}$$

In addition, assuming local equilibrium we can use the result of section 4.1.1 and relate the local charge current $I_i(x)$ to the local potential $\mu_i(x)$ as:

$$I_i(x) = \frac{\eta_i \nu_i}{2\pi} \mu_i(x). \tag{4.30}$$

Using this, we can solve Eq. 4.29 to find the outgoing currents $I_i(x_0 + \delta x)$ in terms of the incoming currents $I_i(x_0 - \delta x)$:

$$\begin{pmatrix} I_1(x_0 + \delta x) \\ \\ I_2(x_0 + \delta x) \end{pmatrix} = \frac{G}{\sigma_0} \begin{pmatrix} 1 - \frac{\eta_1}{\nu_1} & \frac{\eta_2}{\nu_2} \\ \\ \frac{\eta_1}{\nu_1} & 1 - \frac{\eta_2}{\nu_2} \end{pmatrix} \begin{pmatrix} I_1(x_0 - \delta x) \\ \\ I_2(x_0 - \delta x) \end{pmatrix}. \tag{4.31}$$

If instead of a single impurity there exists tunnelings across all the edge, we can write down a similar set of equations but in the differential form

$$\partial_x I_1(x) = g\left(\mu_2(x) - \mu_1(x)\right) \tag{4.32a}$$

$$\partial_x I_2(x) = -g\left(\mu_2(x) - \mu_1(x)\right), \tag{4.32b}$$

where now $g > 0$ represents conductance coefficient per unit length. Note that these equations are the modification of conservation law Eq. 4.2: the conservation law of an independent edge mode ϕ_i, in frequency space (Fourier transform of time) is

$$-i\omega n_i(x,\omega) + \partial_x I_i(x,\omega) = 0. \tag{4.33}$$

So, in the DC limit $\omega = 0$ we should have $\partial_x I_i(x, \omega = 0) = 0$.

Along with Eq. 4.30 we can solve the kinetic equations 4.32 along the edge of the quantum Hall bar in order to find the total current carried along the edge. We will explain the calculation in more details in section 4.5.

In a two–terminal setup similar to Fig. 4.1, when the two edge modes are co–propagating, they are populated at the same contact, and so they always have the same voltage. This means no effective current is transferred between them. In this case, we can just use the results of section 4.1 to find

$$G = \frac{1}{2\pi}(\nu_1 + \nu_2). \tag{4.34}$$

On the other hand, when the modes are counter–propagating ($\eta_1\eta_2 = -1$) they are biased differently at the two terminals and therefore they exchange charge according to Eq. 4.32. By solving this equation we find the two–terminal electrical conductance ($\nu_1 \neq \nu_2$ is assumed)

$$G = \frac{\nu_1 + \nu_2\, \mathrm{e}^{-\tilde{g}L}}{\nu_1 - \nu_2\, \mathrm{e}^{-\tilde{g}L}} \frac{(\nu_1 - \nu_2)}{2\pi}, \quad \tilde{g} = \frac{\nu_1 - \nu_2}{\nu_2\nu_1} g. \tag{4.35}$$

L is the length of the top and bottom edge in the setup of Fig. 4.1. When gL is very small, the tunneling is not effective in equilibrating the edge modes, and we recover the result of

the previous section

$$G = \frac{\nu_1 + \nu_2}{2\pi}. \tag{4.36}$$

In the other limit where $gL \gg 1$ the equilibration is effective, and we find

$$G = \frac{|\nu_1 - \nu_2|}{2\pi}, \tag{4.37}$$

a result that agrees with the experimental measurement of conductance in Hall plateaus [2, 16].

A similar discussion can be used for the heat transport: tunneling between the edge modes transfers heat current between them. On average there will be a net heat current $j^Q_{\text{tunneling}}$ between the modes provided they are at different temperatures. Looking at the example of two edge modes, the heat current $j^Q_{\text{tunneling}}$ due to an impurity–induced tunneling at x_0 is related to the temperature difference, to linear order, as

$$j^Q_{\text{tunneling}}(x_0) = G^Q \left(\frac{T_2^2(x_0) - T_1^2(x_0)}{2} \right). \tag{4.38}$$

The positive heat conductance coefficient G^Q depends on the strength of the tunneling and could potentially depend on the temperature as well. This phenomenological expression is known as the Newton's law or Fourier's law of cooling. In the continuum limit of many impurities we get

$$\partial_x J_1^Q(x) = g^Q \left(\frac{T_2^2(x_0) - T_1^2(x_0)}{2} \right) \tag{4.39}$$

$$\partial_x J_2^Q(x) = -g^Q \left(\frac{T_2^2(x_0) - T_1^2(x_0)}{2} \right). \tag{4.40}$$

Assuming local equilibrium, heat currents $J_i^Q(x)$ and local temperatures $T_i(x)$ are related as Eq. 4.23. We can use this to solve equations 4.39. For two co–propagating modes with

central charges c_1 and c_2 we find in a two–terminal setup we find

$$K = (c_1 + c_2)\kappa_0 T. \tag{4.41}$$

On the other hand, for two counter–propagating we find

$$K = \frac{c_1 + c_2\, \mathrm{e}^{-\tilde{g}^Q L}}{c_1 - c_2\, \mathrm{e}^{-\tilde{g}^Q L}} \frac{(c_1 - c_2)}{2\pi}, \quad \tilde{g}^Q = \frac{c_1 - c_2}{c_2 c_1} g. \tag{4.42}$$

For ineffective equilibration $\tilde{g}^Q L \ll 1$ we have $K = (c_1 + c_2)\kappa_0 T$ while for effective equilibration $\tilde{g}^Q L \gg 1$ have $K = |c_1 - c_2|\kappa_0 T$

The kinetic equations that we discuss in this chapter are the derivation of the equations such as Eq. 4.32 and Eq. 4.39 starting from the low–energy field theory of a quantum Hall edge described in chapter 3.

4.3 Kinetic equations

In this section, we derive the kinetic equations for a hierarchical FQH state. The field theory for the edge of such states were described in section 3.2. We include the short–ranged Coulomb interaction and the tunneling interactions between the different edge modes and discuss their effect on the equilibration along the edge.

Consider a hierarchical quantum Hall state with edge modes at filling fractions ν_i for $i = 1, \ldots, N$. The action for the chiral boson edge modes ϕ_i is $S_{\text{edge}} = S_0 + S_{\text{tunneling}}$ where

$$S_0 = -\frac{1}{4\pi} \int_{t,x} \left[\sum_i \frac{1}{\nu_i} \partial_x \phi_i (\eta_i \partial_t \phi_i + v_i \partial_x \phi_i) + \sum_{i \neq j} v_{ij} \partial_x \phi_i \partial_x \phi_j \right], \tag{4.43a}$$

$$S_{\text{tunneling}} = -\int_{t,x} \sum_{p \in P} \left[\xi_p(x)\, \mathrm{e}^{i \sum_j^N m_j^{(p)} \phi_j} + \text{h.c.} \right]. \tag{4.43b}$$

To recap from the previous chapter, v_{ij} parameterizes the short–ranged Coulomb interaction coupling the edge–mode charge densities $\frac{1}{2\pi}\partial_x\phi_i$; the velocities v_i are non–negative; $\int_{t,x} = \int dtdx$; P is the set of charge–conserving processes that tunnel $\nu_j m_j^{(p)}$ electrons/bosons between the edge channels; and ξ_p is a Gaussian random field with statistical average $\overline{\xi_p(x)\xi_{p'}^*(x')} = \delta_{pp'}W_p\delta(x-x')$. To study the transport properties of S_{edge} it is convenient to diagonalize S_0 using the transformation $\phi_i = \Lambda_{i\alpha}\tilde{\phi}_\alpha$ (summation over repeated indices are implied):

$$S_0 = -\frac{1}{4\pi}\int_{t,x}\left[\sum_\alpha \partial_x\tilde{\phi}_\alpha(\tilde{\eta}_\alpha\partial_t\tilde{\phi}_\alpha - \tilde{v}_\alpha\partial_x\tilde{\phi}_\alpha)\right]. \tag{4.44}$$

This transformation is of the form $\Lambda_{i\alpha} = \sqrt{\nu_i}\tilde{\Lambda}_{i\alpha}$ where $\tilde{\Lambda}_{i\alpha}$ satisfies $\tilde{\Lambda}^T\eta\tilde{\Lambda} = \tilde{\eta}$ ($\eta_{ij} = \delta_{ij}\eta_i$, $\tilde{\eta}_{\alpha\beta} = \delta_{\alpha\beta}\tilde{\eta}_\alpha$). Throughout the rest of this thesis, we will use Latin indices i, j for the fractional modes and Greek indices α, β, γ for the bosonic modes that diagonalize the action.

The action S_0 describes a set of non–interacting edge modes $\tilde{\phi}_\alpha$. Therefore, transport in the absence of any tunneling between the modes can be treated similar to section 4.1. This will result in the same result as the non–interacting edge: electrical conductance is given by Eq. 4.13 while the thermal conductance is given by Eq. 4.25. Therefore, it is necessary to include the tunneling interactions $S_{\text{tunneling}}$ in order to explain the universal transport results Eq. 4.14 and 4.26.

To understand the effect of the tunnelings, we first need to check whether they change the low–energy physics or not. In other words, we need to check whether the tunneling strengths W_p are relevant. The leading order renormalization group equation for W_p is

$$-\frac{dW_p}{d\ln\Lambda} = (3-2\Delta_p)W_p \tag{4.45}$$

with Δ_p the scaling dimension of the tunneling operator $\mathcal{O}_p = \mathrm{e}^{i\sum_j m_j^{(p)}\phi_j} = \mathrm{e}^{i\sum_{j,\alpha} m_j^{(p)}\Lambda_{j\alpha}\tilde{\phi}_\alpha}$ (See Eq. 3.52). When all tunneling operators appearing in $S_{\text{tunneling}}$ are irrelevant, $\Delta_p > \frac{3}{2}$, the fixed point action is S_0. At zero temperature, the currents $\tilde{I}_\alpha = -\frac{1}{2\pi}\partial_t\tilde{\phi}_\alpha$ and $\tilde{J}_\alpha(x) = \frac{\eta_\alpha}{4\pi}(\partial_t\tilde{\phi}_\alpha)^2$ (no sum over α) associated to each mode are separately conserved. In particular, the static components of these currents satisfy for each α,

$$\partial_x\tilde{I}_\alpha(x,\omega=0) = 0, \tag{4.46}$$

$$\partial_x\tilde{J}_\alpha(x,\omega=0) = 0. \tag{4.47}$$

At low temperatures, the irrelevant terms in $S_{\text{tunneling}}$ perturbatively correct these conservation equations to allow equilibration between the different edge channels.

On the other hand, If any of the tunneling operators in $S_{\text{tunneling}}$ is relevant, $\Delta_p \leq \frac{3}{2}$, we have to determine the resulting low–energy fixed point in order to derive the appropriate transport equations. In some cases, those tunneling terms could drive the edge towards a disordered fixed point (See section 3.4.3). These situations should be treated on the case by case basis. However, through the study of the disordered fixed point of the FQHE at filling fraction $\nu = 2$ (section 4.4) and the anti–Pfaffian state at $\nu = 5/2$ (chapter 6), we find that there exists a similar set of conserved charge and heat currents, and we can treat the leading irrelevant terms (with respect to the corresponding disordered fixed point) perturbatively. The difference compared to a clean fixed point lies in the set of processes that drive inter–mode equilibration and the details of the expressions of the kinetic equations.

In the rest of this section, we derive the kinetic equations for charge and heat. Although we demonstrate the concepts using the clean fixed point theory S_0, similar dis-

cussions can be made about the disordered fixed points.

4.3.1 Charge transport

We calculate how the conservation equation 4.2 changes when we include the tunneling interactions $S_{\text{tunneling}}$. Clearly, the charge is no longer conserved when charge density and charge current are defined as

$$\tilde{n}_\alpha = \frac{1}{2\pi}\partial_x\tilde{\phi}_\alpha, \qquad \tilde{I}_\alpha = -\frac{1}{2\pi}\partial_t\tilde{\phi}_\alpha. \tag{4.48}$$

Instead we take $\tilde{n}_\alpha$ to have the above form, but define $\tilde{I}_\alpha$ such that the conservation law Eq. 4.2 is valid. This means we define $\tilde{I}_\alpha$ by

$$-\partial_x\tilde{I}_\alpha(x,t) \equiv \partial_t\tilde{n}_\alpha(x,t). \tag{4.49}$$

To understand the physics of equilibration, we first consider the discretization of $S_{\text{tunneling}}$: instead of the continuous disorder fields $\xi_p(x)$ we assume there exists a series of impurities at discrete positions $x_n = n\Delta x,\ n \in \mathbb{Z}$ [101]. So, the tunneling Hamiltonian is

$$H_{\text{tunneling}} = \int_t \sum_n \sum_{p\in P} \left[\xi_p(x_n)\, \mathrm{e}^{i\sum_j^N m_j^{(p)}\phi_j(x_n)} + \text{h.c.}\right]. \tag{4.50}$$

Also, the Hamiltonian term corresponding to S_0 of Eq. 4.44 is

$$H_0 = \frac{1}{4\pi}\int_x \left[\sum_\alpha \tilde{v}_\alpha(\partial_x\tilde{\phi}_\alpha)^2\right]. \tag{4.51}$$

As we discussed in section 4.2, at a point x_n along the edge there exists a net tunneling current between the modes only when the modes have different chemical potentials at x_n. Let's denote by $\tilde{\mu}_\alpha(x)$ the local chemical potential of the mode $\tilde{\phi}_\alpha$. Since the charge current $\tilde{I}_\alpha(x)$ changes along the edge due to tunneling, so does the chemical potential $\tilde{\mu}_\alpha(x)$. We

relate these two quantities as follows: assume we know $\tilde{I}_\alpha(x)$ and $\tilde{\mu}_\alpha(x)$ at $x = x_0 - \mathrm{d}x$ for all α ($\mathrm{d}x$ is an infinitesimal distance). For example $x_0 - \mathrm{d}x$ could be in the contact regions which we know their chemical potentials. We use can use this to find the tunneling current between all the modes at x_0 (described below), and consequently $\tilde{I}_\alpha(x_0 + \mathrm{d}x)$. Then, we assume the mode $\tilde{\phi}_\alpha$ comes to local equilibrium before the next tunneling at $x = x_1 - \mathrm{d}x$. This implies we can use an expression similar to Eq. 4.10 and write

$$\tilde{I}_\alpha(x_1 - \mathrm{d}x) = \frac{1}{2\pi}\tilde{\eta}_\alpha\tilde{\mu}_\alpha(x_1 - \mathrm{d}x). \tag{4.52}$$

Therefore, we know the chemical potentials during the tunneling at x_1 and so we can find the tunneling current. We can continue this process for all n's and find the charge currents $\tilde{I}_\alpha(x)$ along the edge. This is the setup and the assumptions that we have in mind whenever we write down the kinetic equations. In practice, including the variation in chemical potential is done as follows: add the bias term

$$H_\mu = -\frac{1}{2\pi}\int \mathrm{d}x \ \sum_\alpha \tilde{\mu}_\alpha \partial_x \tilde{\phi}_\alpha \tag{4.53}$$

to the Hamiltonian. Assuming $\tilde{\mu}_\alpha$ is constant on the scale Δx, we find the tunneling currents at all points x_n along the edge. This result depends on $\tilde{\mu}_\alpha$. Then we relate the currents and the chemical potentials as Eq. 4.52 and solve the for $\tilde{I}_\alpha(x)$.

Now, in order to actually find the tunneling currents, we continue from Eq. 4.49 and use the Heisenberg's equation of motion for $\tilde{n}_\alpha$ to write

$$\begin{aligned} -\partial_x \tilde{I}_\alpha(x,t) = \partial_t \tilde{n}_\alpha(x,t) &= -i[H_0 + H_{\text{tunneling}}, \tilde{n}_\alpha(x,t)] \\ &= -\tilde{\eta}_\alpha \tilde{v}_\alpha \partial_x \tilde{n}_\alpha(x,t) - i[H_{\text{tunneling}}, \tilde{n}_\alpha(x,t)]. \end{aligned} \tag{4.54}$$

The first term represents the propagation of the density wave $\tilde{n}_\alpha(x,t)$ along the edge while the second term represents change in charge density due to tunneling. Since the current $\tilde{I}_\alpha$ varies along the edge, so does $\tilde{n}_\alpha$ and so the first term in the above equation is non–zero. However, we are interested in DC transport. In this case, assuming the second term is small enough, the change in $\tilde{I}_\alpha$ is also small. And since $\tilde{I}_\alpha$ and $\tilde{n}_\alpha$ are related as

$$\tilde{I}_\alpha(x) = \tilde{\eta}_\alpha \tilde{v}_\alpha \tilde{n}_\alpha(x) \tag{4.55}$$

between the impurities, the change in $\tilde{n}_\alpha$ is also small, and we can drop the first term in the first order approximation.

At the end, we are interested in the expectation value of the tunneling currents. Taking all the above into account, we need to find

$$-\partial_x \left\langle \tilde{I}_\alpha(x,t) \right\rangle_{\rho_{H_0}} = -i \left\langle [H_{\text{tunneling}}, \tilde{n}_\alpha(x,t)] \right\rangle_{\rho_{H_0}}, \tag{4.56}$$

where ρ_{H_0} means the expectation value is taken in the thermal ensemble $\rho_{H_0} \sim \mathrm{e}^{-H_0/T}$ at temperature T. In practice, we find these expectation values using the Keldysh technique [109–112] to first order approximation in W_p. The details of the derivations are carried out in Appendix C.1. In the ohmic regime $\tilde{\mu}_\alpha \ll T$ we find (See Eq. (C.16)):

$$\partial_x \left\langle \tilde{I}_\alpha(x) \right\rangle = -\sigma_0 \tilde{\eta}_\alpha \sum_{p\in P} \left[g_p (\sum_i m_i^{(p)} \Lambda_{i\alpha}) \left(\sum_j \tilde{\eta}_\beta m_j^{(p)} \Lambda_{j\beta} \tilde{\mu}_\beta(x) \right) \right], \qquad g_p \propto W_p T^{2\Delta_p - 2}. \tag{4.57}$$

Following Eq. 4.52 we have $\left\langle \tilde{I}_\alpha(x) \right\rangle = \tilde{\eta}_\alpha \sigma_0 \tilde{\mu}_\alpha(x)$. These equations are more transparent physically in the original basis where $I_i = \Lambda_{i\alpha} \tilde{I}_\alpha$ and $\tilde{\mu}_\alpha = \mu_i \Lambda_{i\alpha}$:

$$\partial_x \langle I_i(x) \rangle = -\tilde{\eta}_i \nu_i \sum_{p\in P} g_p m_i^{(p)} \left(\sum_{\text{J}} m_j^{(p)} \langle I_j(x) \rangle \right) \tag{4.58}$$

or in matrix form (dropping expectation value signs),

$$\partial_x \boldsymbol{I} = G^e \boldsymbol{I}, \tag{4.59a}$$

$$G^e_{ij} = -\eta_i \nu_i \sum_{p \in P} g_p m_i^{(p)} m_j^{(p)}. \tag{4.59b}$$

These equations constitute the kinetic equations for dc charge transport about the S_0 fixed point. Equilibration of charge is parameterized by the charge matrix G^e_{ij}.

4.3.2 Heat transport

Following a similar process, we can find the heat tunneling currents between the different edge modes. The conservation of heat implies

$$-\partial_x \tilde{J}^Q_\alpha(x,t) = \partial_t \mathcal{H}_\alpha(x,t) = -i[H, \mathcal{H}_\alpha(x,t)], \tag{4.60}$$

where the energy density is

$$\mathcal{H}_\alpha(x) = \frac{\tilde{v}_\alpha}{4\pi}(\partial_x \tilde{\phi}_\alpha)^2. \tag{4.61}$$

Since we are interested in these tunneling currents to linear order, we can ignore the variation of chemical potential along the edge. Therefore, we use the Hamiltonian $H = H_0 + H_{\text{tunneling}}$. Assuming small variations in $\tilde{J}^Q_\alpha(x)$ along the edge we can ignore $[H_0, \mathcal{H}_\alpha(x,t)]$ in Eq. 4.60 (See the discussion after Eq. 4.54). Taking the expectation value

$$-\partial_x \left\langle \tilde{J}^Q_\alpha(x,t) \right\rangle_{\rho_{H_0}} = -i \left\langle [H_{\text{tunneling}}, \mathcal{H}_\alpha(x,t)] \right\rangle_{\rho_{H_0}}. \tag{4.62}$$

Here, we find the expectation values in the ensemble $\rho_{H_0} \sim \mathrm{e}^{-\sum_\alpha H_\alpha/T_\alpha}$ where T_α represents the local temperature of mode $\tilde{\phi}_\alpha$ and $H_\alpha = \int \mathrm{d}x\ \mathcal{H}_\alpha(x)$. We find these expectation values

using the Keldysh technique. The details are relegated to Appendix C.2. To linear order in $(T_\alpha - T_\beta)/T_\alpha$, we find

$$\partial_x \left\langle \tilde{J}_\alpha(x) \right\rangle = \kappa_0 \sum_{\beta \neq \alpha} g^Q_{\alpha\beta} \frac{T^2_\beta(x) - T^2_\alpha(x)}{2}, \qquad g^Q_{\alpha\beta} = \sum_{p \in P} g_p \frac{12 d^{(p)}_\alpha d^{(p)}_\beta}{1 + 2\Delta_p}. \tag{4.63}$$

The constants $d^{(p)}_\alpha = \frac{1}{2}(\sum_i m^{(p)}_i \Lambda_{i\alpha})^2$. Similar to charge transport, the set of processes P and conductivity coefficients $g^Q_{\alpha\beta}$ depend on the low–temperature fixed point of the theory. Assuming local equilibrium we express the local currents $\tilde{J}_\alpha(x)$ in terms of local temperatures $T_\alpha(x)$ as ($\tilde{c}_\alpha$ is the central charge of mode α—See Eq. 4.23)

$$\left\langle \tilde{J}_\alpha(x) \right\rangle = \frac{1}{2} \kappa_0 \tilde{\eta}_\alpha \tilde{c}_\alpha T^2_\alpha(x). \tag{4.64}$$

The resulting kinetic equations take the form (again dropping the expectation value signs):

$$\partial_x \tilde{\boldsymbol{J}} = G^Q \tilde{\boldsymbol{J}}, \tag{4.65a}$$

$$G^Q_{\alpha\beta} = \frac{\tilde{\eta}_\beta}{\tilde{c}_\beta} (g^Q_{\alpha\beta} - \delta_{\alpha\beta} \sum_\gamma g^Q_{\alpha\gamma}). \tag{4.65b}$$

Similar to the charge kinetic equations, equilibration of heat is controlled by $G^Q_{\alpha\beta}$.

4.4 Edge–state transport at $\nu = 2$

We now illustrate kinetic equations by looking at the case of QHE at $\nu = 2$. The reason that for choosing this state is two–fold: first, it is an example of a state where the low–energy theory is a disordered fixed point. Therefore, we can demonstrate that the kinetic equations can be written using a similar procedure as the clean fixed points described in section 4.3. Second, it allows us to offer an alternative explanation for the

large equilibration lengths reported in [98, 100]. This explanation will be relevant to our study of the anti–Pfaffian edge–state theory and its transport in chapters 5 and 6.

Consider the action for the edge modes of the integer quantum Hall state at $\nu = 2$. Ignoring possible edge reconstruction, $S = S_0 + S_{\text{tunneling}}$:

$$S_0 = -\frac{1}{4\pi}\int_{t,x}\Big[\sum_{i=1}^{2}\partial_x\phi_i(\partial_t\phi_i + v_i\partial_x\phi_i) + 2v_{12}\partial_x\phi_1\partial_x\phi_2\Big], \tag{4.66a}$$

$$S_{\text{tunneling}} = -\int_{t,x}\left[\xi_{12}(x)\,\mathrm{e}^{i(\phi_1-\phi_2)} + \text{h.c.}\right], \quad \overline{\xi_{12}(x)\xi_{12}^*(x')} = W_{12}\delta(x-x'). \tag{4.66b}$$

Here, the most relevant tunneling term transfers a spin–up electron of the first edge channel ϕ_1 into a spin–down electron of the second edge channel ϕ_2. Because $\mathrm{e}^{i(\phi_1-\phi_2)}$ has scaling dimension $\Delta_{12} = 1$ (for any value of v_{12}) and is therefore relevant, it drives the system to an IR disordered fixed point (See section 3.4.3 for the discussion of disordered fixed points and also Appendix B). To identify this disordered fixed point, we first write the action S in terms of the total charge mode $\phi_{\rho_{12}} = \frac{1}{\sqrt{2}}(\phi_1 + \phi_2)$ and the spin mode $\phi_{\sigma_{12}} = \frac{1}{\sqrt{2}}(\phi_1 - \phi_2)$. Then we use a gauge transformation similar to section 3.4.3 to eliminate the disordered tunneling term. We can then write the action as $S = S_{\Delta_{12}=1} + S_{\text{int}}$ [92] with:

$$S_{\Delta_{12}=1} = -\frac{1}{4\pi}\int_{t,x}[\partial_x\phi_{\rho_{12}}(\partial_t\phi_{\rho_{12}} + v_{\rho_{12}}\partial_x\phi_{\rho_{12}})] - \frac{1}{4\pi}\int_{t,x}\left[\partial_x\tilde{\phi}_{\sigma_{12}}(\partial_t\tilde{\phi}_{\sigma_{12}} + v_{\sigma_{12}}\partial_x\tilde{\phi}_{\sigma_{12}}\right], \tag{4.67a}$$

$$S_{\text{int}} = -\frac{2v_{\sigma_{12},\rho_{12}}}{4\pi}\int_{t,x}\partial_x\phi_{\rho_{12}}\left(\frac{\sqrt{2}}{a}O^{zx}\cos(\sqrt{2}\tilde{\phi}_{\sigma_{12}}) + \frac{\sqrt{2}}{a}O^{zy}\sin(\sqrt{2}\tilde{\phi}_{\sigma_{12}}) + O^{zz}\partial_x\tilde{\phi}_{\sigma_{12}}\right), \tag{4.67b}$$

where $\tilde{\phi}_{\sigma_{12}}$ is the gauge–transformed spin mode and

$$v_{\rho_{12}} = \frac{v_1+v_2}{2} + v_{12}, \quad v_{\sigma_{12}} = \frac{v_1+v_2}{2} - v_{12}, \quad v_{\sigma_{12},\rho_{12}} = \frac{v_1-v_2}{2}. \tag{4.68}$$

$S_{\Delta_{12}=1}$ describes the disordered fixed point about which $S_{\rm int}$ is irrelevant. The modes $\phi_{\rho_{12}}$ and $\tilde{\phi}_{\sigma_{12}}$ constitute the low–energy modes of this theory that we can use as the starting point for writing down the kinetic equations. In particular, the conservation law for the total charge density $n_{\rho_{12}} = \partial_x \phi_\rho / 2\pi$ and the transformed spin density $\tilde{n}_{\sigma_{12}} = \partial_x \tilde{\phi}_{\sigma_{12}} / 2\pi$ is

$$-\partial_x I_{\rho_{12}} = \partial_t n_{\rho_{12}} \tag{4.69}$$

$$-\partial_x \tilde{I}_{\sigma_{12}} = \partial_t \tilde{n}_{\sigma_{12}}. \tag{4.70}$$

Since the total charge is always conserved $\partial_x I_{\rho_{12}}(x, \omega = 0) = 0$. On the other hand, the interaction term $H_{\rm int}$ (corresponding to $S_{\rm int}$) causes the spin current to decay along the edge. We treat the effect of $H_{\rm int}$ similar to section 4.3.1 and write

$$-\partial_x \tilde{I}_{\sigma_{12}} = \partial_t \tilde{n}_{\sigma_{12}} = -i[H_{\rm int}, \tilde{n}_{\sigma_{12}}]. \tag{4.71}$$

We find the expectation value of this expression in Appendix C.1.2. In the Ohmic regime ($\tilde{I}_{\sigma_{12}}/\sigma_0 \ll T$) we find (See Eq. C.29)

$$\partial_x \left\langle \tilde{I}_{\sigma_{12}} \right\rangle = -g \left\langle \tilde{I}_{\sigma_{12}} \right\rangle, \qquad g = \frac{2 v^2_{\sigma_{12},\rho_{12}} T^2}{3 v^2_{\rho_{12}} W_{12}}. \tag{4.72}$$

This simply represents the exponential decay of the spin current along the edge with equilibration length $\ell_{eq} = 1/g$. In the linear regime we find it more convenient to express the kinetic equation for $I_{\rho_{12}}$ and $\tilde{I}_{\sigma_{12}}$ in terms of a basis similar to the original fractional modes. We define the "slow" fractional basis as

$$I'_1 = \frac{1}{\sqrt{2}}(I_\rho + \tilde{I}_\sigma) \tag{4.73a}$$

$$I'_2 = \frac{1}{\sqrt{2}}(I_\rho - \tilde{I}_\sigma). \tag{4.73b}$$

In this basis the kinetic equation is

$$\partial_x \begin{pmatrix} I_1'(x) \\ I_2'(x) \end{pmatrix} = G^e \begin{pmatrix} I_1'(x) \\ I_2'(x) \end{pmatrix}, \quad \text{with } G^e = -g \begin{pmatrix} 1 & -1 \\ -1 & 1 \end{pmatrix}. \tag{4.74}$$

To write down the kinetic equation for the energy transport, define energy currents as

$$\partial_x J^Q_{\rho_{12}} = -\partial_t \mathcal{H}_{\rho_{12}}, \qquad \partial_x J^Q_{\tilde{\sigma}_{12}} = -\partial_t \mathcal{H}_{\tilde{\sigma}_{12}}, \tag{4.75}$$

where the energy densities are

$$\mathcal{H}_{\rho_{12}} = \frac{1}{4\pi} v_{\rho_{12}} (\partial_x \phi_{\rho_{12}})^2, \qquad \mathcal{H}_{\tilde{\sigma}_{12}} = \frac{1}{4\pi} v_{\sigma_{12}} (\partial_x \tilde{\phi}_{\sigma_{12}})^2. \tag{4.76}$$

Heat currents $J^Q_{\rho_{12}}$ and $J^Q_{\tilde{\sigma}_{12}}$ are conserved in the $S_{\Delta_{12}=1}$ theory, while they would decay if the interaction S_{int} is included. Using Eq. C.39 and Eq. 4.23 we find

$$\partial_x \begin{pmatrix} J^Q_{\rho_{12}} \\ J^Q_{\tilde{\sigma}_{12}} \end{pmatrix} = G^Q \begin{pmatrix} J^Q_{\rho_{12}} \\ J^Q_{\tilde{\sigma}_{12}} \end{pmatrix}, \quad \text{with } G^Q = -\frac{12}{5} g \begin{pmatrix} 1 & -1 \\ -1 & 1 \end{pmatrix}. \tag{4.77}$$

Therefore, the equilibration length for heat is $\ell^Q_{eq} = 5/12g$, which is in the same order of magnitude as the charge equilibration length.

4.4.1 Large equilibration length

Based on the expressions in Eq. 4.68 the conductivity coefficient is

$$g = \frac{2T^2}{3W_{12}} \left(\frac{v_1 - v_2}{v_1 + v_2 + 2v_{12}} \right)^2. \tag{4.78}$$

Therefore, if $|v_1 - v_2| \ll |v_1 + v_2 + 2v_{12}|$, $g \approx 0$ and charge equilibration is weak. We can write $v_i = v_i^{(0)} + w$ and $v_{12} = w$, where $v_i^{(0)} > 0$ parameterizes the edge confining potential

and $w > 0$ is the magnitude of the short–ranged Coulomb interaction (see the discussion following Eq. (5.5)). The above inequality translates to $|v_1^{(0)} - v_2^{(0)}| \ll |v_1^{(0)} + v_2^{(0)} + 4w|$. There are two reasons why this inequality might be satisfied. (1) Based on the measurements of the velocities of the charge $\phi_{\rho_{12}}$ and neutral $\phi_{\sigma_{12}}$ modes [113, 114], we infer that $v_i^{(0)} \ll w$. (2) If there exists approximate degeneracy between the spin–up and spin–down modes we have $v_1^{(0)} \approx v_2^{(0)}$.

We can estimate $|v_1^{(0)} - v_2^{(0)}|$ using a simple model of the confining potential $V(x)$. Assume a potential of the form $V(x) = Ax^2$ which is slowly varying on the scale of the magnetic length. Then the velocity of mode ϕ_i in the absence of the short–ranged Coulomb potential is (See Eq. 2.16)

$$v_i^{(0)} = \frac{1}{B}\partial_x V(x)|_{E_i + V(x) = E_F} = \frac{\sqrt{2A(E_F - E_i)}}{B} \tag{4.79}$$

where B is the magnetic field, E_F is the bulk Fermi energy, and E_i is the energy of the Landau level corresponding to mode ϕ_i, deep within the bulk of the sample and away from any defect. When E_F sits in the middle of Landau levels $E_F - E_i \sim \hbar\omega_c$. From an experimental study of equilibration between Landau level edge modes [98], we infer that the Zeeman gap $\Delta E_Z = E_2 - E_1$ is much smaller than the cylotron gap $\hbar\omega_c$ by about an order of magnitude. Therefore, for the difference in velocities we can write

$$\frac{v_1^{(0)} - v_2^{(0)}}{(v_1^{(0)} + v_2^{(0)})/2} \approx \frac{E_2 - E_1}{2(E_F - (E_1 + E_2)/2)} \approx \frac{\Delta E_Z}{\hbar\omega_c} \tag{4.80}$$

and so $|v_1^{(0)} - v_2^{(0)}|$ is also much smaller than the typical (average) velocity $(v_1^{(0)} + v_2^{(0)})/2$.

To summarize, these estimates show that the conductivity coefficient g between the spin–up and spin–down modes can be small even in the strong tunneling (large W_{12}) regime.

4.5 Electrical and thermal Hall conductance

The kinetic equations for the transport of charge Eq. 4.59 and heat 4.65 are linear differential equations that we can easily solve, provided we specify the appropriate boundary conditions. These boundary conditions are determined by the geometry of the transport measurement and more specifically by how each edge mode is biased at the different contacts. In this thesis, we are mostly interested in the two–terminal conductance measurements following the results carried out by Banerjee *et al.* [37, 44]. The setup is similar to Fig. 4.1.

So, we need to determine the charge/heat current of an edge mode just as it exits a contact region. Of course, this depends on how the edge modes interact with the contacts which is hard to answer in general. Kane and Fisher [103] as well as Chamon and Fradkin [97] analyzed the problem of equilibration of change between the edge modes and the contacts, when the edge modes are themselves non–interacting or weakly interacting. The summary of these studies is as follows: the measurement of the electrical Hall conductance of a state at filling fraction ν results in the universal value $G = \nu e^2/h$ only if the contacts are assumed ideal. In this case, an ideal contact means a contact that effectively equilibrates an edge mode with its own chemical potential. Specifically, a mode bosonic mode ϕ carries the charge current $I = \eta\nu\sigma_0\mu_c$ upon leaving the contact with chemical potential μ_c. These studies Ref. [97, 103] also discuss the conditions under which the assumption of ideal contacts are valid.

To our knowledge, there hasn't been a generalization of these results that look at either the equilibration of strongly–interacting modes (*e.g.* disordered fixed points) with contacts or the heat equilibration of edge modes with contacts. These are indeed the cases

that we are interested in. So, inspired by the studies mentioned above, we make similar assumptions about the equilibration of charge and heat in the contact regions. These assumptions are partly justified by the fact that they produce the correct results for the electrical and thermal conductance.

Throughout our studies, we assume the contact c in Fig. 4.1 ($c \in \{L, R\}$) is "ideal" in the following sense:

- A weakly interacting fractional mode ϕ_i carries charge current $I_i = \eta_i \nu_i \sigma_0 \mu_c$ upon leaving the $c \in \{L, R\}$ contact region (this is the assumption justified in Ref. [97, 103])

- When a fractional edge mode ϕ_i is strongly interacting with other modes and is driven to a disordered fixed point, we use the weakly interacting slow mode basis ϕ_i'' similar to Eq. 4.73. We then assume this edge mode carries charge current $I_i' = \eta_i \nu_i \sigma_0 \mu_c$ upon leaving the $c \in \{L, R\}$ contact region.

- The mode $\tilde{\phi}_\alpha$ (refer to (4.44)) carries heat current $\tilde{J}_\alpha^Q = \eta_\alpha c_\alpha \kappa_0 \frac{T_c^2}{2}$ upon leaving contact c.

Given these assumptions, we use the following procedure to calculate the electrical and thermal conductances of the edge modes. In order to solve for the electrical conductance, we first solve the linear differential equations in (4.59). Taking $\boldsymbol{\mathcal{I}}_n$ to be the eigenvectors of the matrix G^e with eigenvalue $\mathfrak{g}_n$, the general solution to the charge transport equations is

$$\boldsymbol{I}(x) = \sum_n a_n \boldsymbol{\mathcal{I}}_n \, \mathrm{e}^{\mathfrak{g}_n x} \tag{4.81}$$

for arbitrary coefficients a_n. We then impose the above "ideal contact" boundary conditions to determine the a_n for the top/bottom edges of the Hall bar. We use a similar procedure to solve the heat transport equations (4.65). From these solutions we find the total charge and heat currents moving along the top/bottom edge of the Hall bar:

$$I_{\text{total, top/bottom}} = \sum_i I_i(x), \tag{4.82a}$$

$$J^Q_{\text{total, top/bottom}} = \sum_\alpha \tilde{J}^Q_\alpha(x), \tag{4.82b}$$

where x is restricted to either the top/bottom edge of the Hall bar. In the case where some modes are strongly mixed (for example the edge modes of the $\nu = 2$ quantum Hall state near the $\Delta_{12} = 1$ fixed point, as described in section 4.4) we use the slow modes' basis to write

$$I_{\text{total, top/bottom}} = \sum_{i \notin \text{strongly mixed}} I_i(x) + \sum_{i \in \text{strongly mixed}} I'_i(x). \tag{4.83}$$

Note that this expression still represents the total charge current, since the gauge transformations that eliminate the strong–disorder tunnelings (See appendix B) only rotate the neutral currents.

The two–terminal charge and heat Hall conductances are then:

$$G = \frac{I_{\text{total, top}} + I_{\text{total, bottom}}}{\mu_L - \mu_R}, \quad K = \frac{J^Q_{\text{total, top}} + J^Q_{\text{total, bottom}}}{T_L - T_R}. \tag{4.84}$$

Depending on the degree of inter–mode equilibration along the top and bottom edges, the two–terminal conductance takes values between the fully–equilibrated and non–equilibrated values. We demonstrated in section 4.1 that the non–equilibrated value of electrical con-

ductance G and thermal conductance K are

$$G_{\text{non–eq}} = \sigma_0 \sum_i \nu_i, \qquad K_{\text{non–eq.}} = \kappa_0 T \sum_\alpha \tilde{c}_\alpha = \kappa_0 T \sum_i c_i. \tag{4.85}$$

The fully equilibrated values can be found by analyzing the kinetic equations 4.59 and 4.65. Focusing on the charge transport, if we sum Eq. 4.59 for all the modes, we find

$$\partial_x(\sum_i I_i(x)) = -\sum_j \sum_{p\in P} m_j^{(p)} I_j \left(\sum_i \eta_i \nu_i m_i^{(p)} \right) = 0. \tag{4.86}$$

The last equality follows since the tunneling processes conserve charge so that $\sum_i \eta_i \nu_i m_i^{(p)} = 0$. Therefore, the matrix G^e has at least one zero eigenvalue representing the conservation of total current. In the absence of any other symmetries and assuming that the tunneling processes tunnel electron between all the edge modes, all the other eigenvalues of G^e are finite. If the coefficients g_p are large enough so that $g_p L \gg 1$ (L is the length of the edge) then all the eigen–currents of the kinetic equation 4.59 decay quickly along the edge, and we are left, practically, with a single mode representing the total charge current $I_{\text{total}}(x)$. This current is related to the local electrical potential $\mu(x)$ as

$$I_{\text{total}}(x) = \frac{1}{2\pi}(\sum_i \eta_i \nu_i)\mu(x). \tag{4.87}$$

Using the results of section 4.1, we can simply find the electrical Hall conductance for this single mode:

$$G_{\text{fully–eq}} = \sigma_0 \left| \sum_i \eta_i \nu_i \right|. \tag{4.88}$$

Similarly we can find the fully equilibrated value of the thermal conductance under similar assumptions

$$K_{\text{fully-eq}} = \kappa_0 T \left| \sum_\alpha \tilde{\eta}_\alpha \tilde{c}_\alpha \right| = \kappa_0 T \left| \sum_i \eta_i c_i \right|. \tag{4.89}$$

4.6 Thermal Hall conductance of QHE at $\nu = 5/2$

It is generally agreed upon that the electrical Hall conductance takes its fully–equilibrated value $G_{\text{fully-eq}} = \nu e^2/h$ in all the conducted experiments on quantum Hall states. Therefore, we only look at how the different candidates for the QHE at $\nu = 5/2$ compare from the perspective of thermal Hall measurement. Throughout the rest of our discussions, we assume that the contacts are ideal in the sense defined in the previous section. In table 4.1 we list some of the candidates for the QHE at $\nu = 5/2$ along with their central charge, $K_{\text{fully-eq}}$ and $K_{\text{non-eq}}$. In section 3.3, we discussed the edge theory of the Pfaffian state, anti–Pfaffian state and the PH–Pfaffian state. See Ref. [22, 33] for the discussion of $K = 8$ state, 331 state, $SU(2)_2$ state and their particle–hole conjugates. Also

$$\text{downstream central charge} = \sum_{i:\eta_i=1} c_i \tag{4.90a}$$

$$\text{upstream central charge} = \sum_{i:\eta_i=-1} c_i. \tag{4.90b}$$

If we assume that heat is fully equilibrated along the edge, the only valid candidate is the PH–Pfaffian state with $K_{\text{fully-eq}} = \frac{5}{2}\kappa_0 T$. On the other hand, if heat is partially equilibrated, in principle, any of the candidates where

$$K_{\text{fully-eq}} \lesssim 2.5\kappa_0 T \lesssim K_{\text{non-eq}} \tag{4.91}$$

could agree with the experimental result $K \approx 2.5\kappa_0 T$. This includes the bottom four states in table 4.1. The reason why the partial equilibration in the anti–Pfaffian state has been the center of focus [43, 45–47, 115] is two–fold: first, the anti–Pfaffian state is a strong candidate based on several numerical simulations [27–29]. Second, as we demonstrate in

candidates	downstream central charge	upstream central charge	$K_{\text{fully-eq}}/\kappa_0 T$	$K_{\text{non-eq}}/\kappa_0 T$
$SU(2)_2$	9/2	0	9/2	9/2
331 state	4	0	4	4
Pfaffian	7/2	0	7/2	7/2
$K = 8$ state	3	0	3	3
PH–Pfaffian	3	1/2	5/2	7/2
Anti–$K = 8$ state	3	1	2	4
Anti–Pfaffian	3	3/2	3/2	9/2
Anti–331 state	3	2	1	5
Anti–$SU(2)_2$	3	5/2	1/2	11/2

Table 4.1: Thermal Hall conductance for some of the candidates for the QHE at $\nu = 5/2$. Depending on the degree of heat equilibration along the edge the thermal conductance K of a state takes values in $K_{\text{fully–eq}} \leq K \leq K_{\text{non–eq}}$.

the next two chapters, partial equilibration in the anti–Pfaffian state could be explained based on the physical characteristics of the edge. In particular, strong short–range Coulomb interaction and an approximate spin symmetry play crucial roles in explaining this partial equilibration. This is in contrast to the other states (anti–$SU(2)_2$ state, anti–331 state and anti–$K = 8$ state) where we don't have any physical arguments for the partial equilibrated of heat.

Chapter 5

Theory of anti–Pfaffian edge states at $\nu = 5/2$

In section 3.3 we introduced the edge theory of the anti–Pfaffian state. In this chapter we study the edge theory of this state in details borrowing the methods introduced in chapter 3. We consider the interactions between the modes and identify the possible low–energy theories of this state. In sections 5.2 and 5.3 we describe two of the fixed point theories that we suspect can explain the thermal conductance measurements of Banerjee *et al.* [37].

5.1 Setup and assumptions

In the absence of edge reconstruction, the anti–Pfaffian state at $\nu = 5/2$ hosts a total of five edge modes (Fig. 5.1) [20, 21](section 3.3). The lowest Landau level contributes (1) a spin–up integer mode and (2) a spin–down integer mode, both moving downstream.

From the first Landau level we have (3) a downstream spin–up integer mode, (4) an upstream spin–up $\nu = \frac{1}{2}$ bosonic mode, and an upstream Majorana mode ψ.

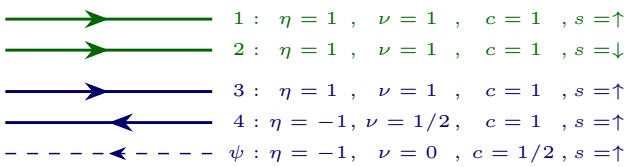

Figure 5.1: Edge modes of the anti–Pfaffian state at $\nu = 5/2$ in the absence of edge reconstruction: $\eta_i = \pm 1$ denotes the chirality of the edge mode; ν_i is the charge carried by the edge mode; c_i is the central charge of the edge mode; and s_i is the spin of the Landau level associated to a particular edge mode. Subscripts labeling the different edge modes are suppressed in the figure.

Similar to section 3.4.3 we assume the quenched disorder along the edge is effective in tunneling electrons. With these considerations, the low–energy effective theory for the anti–Pfaffian edge state at $\nu = 5/2$ takes the form $S = \sum_{i=1}^{4} S_i + S_\psi + \sum_{i \neq j} S_{ij} + S_{\text{tunneling}}$ [20, 21]:

$$S_i = -\frac{1}{4\pi\nu_i} \int_{t,x} \left[\partial_x \phi_i (\eta_i \partial_t \phi_i + v_i \partial_x \phi_i)\right], \tag{5.1a}$$

$$S_\psi = \frac{1}{4} \int_{t,x} i\psi(\partial_t \psi - u \partial_x \psi), \tag{5.1b}$$

$$\sum_{i \neq j} S_{ij} = -\sum_{i \neq j} \frac{v_{ij}}{4\pi} \int_{t,x} \partial_x \phi_i \partial_x \phi_j, \tag{5.1c}$$

$$S_{\text{tunneling}} = -\int_{t,x} \sum_{p \in P} \left[\xi_p(x)\, \mathrm{e}^{i \sum_j m_j^{(p)} \phi_j}\, \psi^{m_\psi^{(p)}} + \text{h.c.}\right]. \tag{5.1d}$$

Similar to before, P is the set of charge–conserving processes defined by the integers $(m_j^{(p)}, m_\psi^{(p)})$ that tunnel electrons between the edge modes, and ξ_p is a Gaussian random

field with statistical average $\overline{\xi_p(x)\xi^*_{p'}(x')} = \delta_{pp'} W_p \delta(x - x')$.

Unless the Coulomb interaction between edge modes of the different Landau levels can be ignored, it's not obvious what tunneling operators are most relevant. In principle, multi–electron tunneling operators can be more relevant than those that only involve a single–electron tunneling process. However, the largeness of the Landau gap compared to the electrochemical potential difference between the edge modes, present in the experiments [37, 116], and the large equilibration lengths reported for modes in different Landau levels [98, 117] suggest that tunneling between edge channels belonging to different Landau levels is generally suppressed.

Experiments also report a large equilibration length between spin–up and spin–down modes [100, 117]. This has been attributed to suppressed tunneling between these modes due to weak spin–orbit coupling. This is the assumption made in Ref. [46]; we relax this assumption in this paper. Following the analysis in Section 4.4, where we provided an alternative explanation for the large equilibration length between spin–up and spin–down integer modes, we assume strong tunneling between spin–up and spin–down electrons of the lowest Landau level. Therefore, the most relevant tunnelings to include in $S_{\text{tunneling}}$ are

$$S_{\text{tunneling},12} = -\int_{t,x} \left[\xi_{12}(x)\, \mathrm{e}^{i(\phi_1 - \phi_2)} + \text{h.c.}\right], \tag{5.2a}$$

$$S_{\text{tunneling},34\psi} = -\int_{t,x} \left[\xi_{34}(x)\, \mathrm{e}^{i(\phi_3 + 2\phi_4)}\, \psi + \text{h.c.}\right]. \tag{5.2b}$$

If the Coulomb interaction between edge modes of different Landau levels is ignored the term $S_{\text{tunneling},12}$ is always relevant; $S_{\text{tunneling},34\psi}$ is relevant if the Coulomb interaction between edge modes of the first Landau level interaction is sufficiently strong. If the modes in the lowest Landau level are decoupled from the modes in the first Landau level (and

if equilibration of the first Landau level edge modes occurs via $S_{\text{tunneling},34\psi}$), the low–temperature thermal Hall conductance is the sum of the contributions from the lowest Landau level and the first Landau level $K = K_{\text{LLL}} + K_{1\text{LL}} = \frac{5}{2}\kappa_0 T$.

However, we aren't aware of any reason that the Coulomb interaction between the Landau levels is suppressed. Consequently, either of the two tunneling terms in 5.2 can be relevant or irrelevant, depending on the specific nature of the Coulomb interaction, i.e., the values of the v_{ij} in Eq. (5.1c); even strong Coulomb repulsion between all the modes doesn't uniquely specify an IR fixed point. We identify four possible IR fixed points:

1. $W_{12} = 0$ and $W_{34} = 0$ while $\Delta_{12} > \frac{3}{2}$ and $\Delta_{34} > \frac{3}{2}$
2. $W_{12} = 0$ ($\Delta_{12} > \frac{3}{2}$) and $\Delta_{34} = 1$
3. $\Delta_{12} = 1$ and $W_{34} = 0$ ($\Delta_{34} > \frac{3}{2}$)
4. $\Delta_{12} = 1$ and $\Delta_{34} = 1$.

Above, Δ_{12} and Δ_{34} are the scaling dimensions of $\mathrm{e}^{i(\phi_1-\phi_2)}$ and $\mathrm{e}^{i(\phi_3+2\phi_4)}\,\psi$. The second case was analyzed in [46], where it was argued that $K = 2.5\kappa_0 T$ requires fine–tuning. The first case is similar to the second one in this regard so we won't discuss it. In this paper, we investigate the third and the fourth low–temperature fixed points. In chapter 6, we describe the conditions under which $K = 2.5\kappa_0 T$ is consistent with either of these fixed points.

5.2 $\Delta_{12} = 1, W_{34} = 0$ disordered fixed point

In order to study this fixed point we change variables to charge $\phi_{\rho_{12}} = \frac{1}{\sqrt{2}}(\phi_1 + \phi_2)$ and spin $\phi_{\sigma_{12}} = \frac{1}{\sqrt{2}}(\phi_1 - \phi_2)$ modes [92]. For v_{ij} such that there is no coupling between

$\partial_x\phi_{\sigma_{12}}$ and $\partial_x\phi_4$ the theory has an emergent $SO(3)$ symmetry [92, 93, 95] that acts on the $\phi_{\sigma_{12}}$ sector. In Appendix B we show how this symmetry can be used to eliminate $S_{\text{tunneling},12}$, after which an $SO(3)$ transformed spin mode $\tilde{\phi}_{12}$ is introduced. The resulting action becomes $S = S_{\Delta_{12}=1} + S_{\text{int}}$ where

$$S_{\Delta_{12}=1} = S_{\rho_{12}} + S_{\sigma_{12}} + S_3 + S_4 + S_\psi + \sum_{i\neq j\in\{\rho_{12},3,4\}} S_{ij}, \tag{5.3a}$$

$$S_{\rho_{12}} = -\frac{1}{4\pi}\int_{t,x}\left[\partial_x\phi_{\rho_{12}}(\partial_t\phi_{\rho_{12}} + v_{\rho_{12}}\partial_x\phi_{\rho_{12}})\right], \tag{5.3b}$$

$$S_{\sigma_{12}} = -\frac{1}{4\pi}\int_{t,x}\left[\partial_x\tilde{\phi}_{\sigma_{12}}(\partial_t\tilde{\phi}_{\sigma_{12}} + v_{\sigma_{12}}\partial_x\tilde{\phi}_{\sigma_{12}}\right], \tag{5.3c}$$

and

$$S_{\text{int}} = \sum_{i\in\{3,4,\rho_{12}\}} S_{\sigma_{12},i} + S_{\text{tunneling},34\psi}, \tag{5.4a}$$

$$S_{\sigma_{12},i} = -\frac{2v_{\sigma_{12},i}}{4\pi}\int_{t,x}\partial_x\phi_i\left(\frac{\sqrt{2}}{a}O^{zx}\cos(\sqrt{2}\tilde{\phi}_{\sigma_{12}}) + \frac{\sqrt{2}}{a}O^{zy}\sin(\sqrt{2}\tilde{\phi}_{\sigma_{12}}) + O^{zz}\partial_x\tilde{\phi}_{\sigma_{12}}\right). \tag{5.4b}$$

$O^{ab}(x)$ are matrix elements of the $SO(3)$ rotation that we employed in order to eliminate the $\xi_{12}(x)$ tunneling term. The S_{ij} and v_{ij} with $i,j \in \{\rho_{12},\sigma_{12},3,4\}$ obtain from the S_{ij} and v_{ij} with $i,j\in\{1,2,3,4\}$ after the above field redefinition. $S_{\Delta_{12}=1}$ describes the $\Delta_{12}=1$ fixed point at which the terms in S_{int} vanish: $v_{\sigma_{12},\rho_{12}} = v_{\sigma_{12},3} = v_{\sigma_{12},4} = W_{34} = 0$. The density–density interactions in $S_{\sigma_{12},i}$ are irrelevant near the $\Delta_{12}=1$ fixed point. We assume $S_{\text{tunneling},34\psi}$ is irrelevant at this fixed point, *i.e.* $\Delta_{34} > \frac{3}{2}$, so that $S_{\Delta_{12}=1}$ describes the low energy behavior of the anti–Pfaffian edge. When $S_{\text{tunneling},34\psi}$ is relevant, the low–energy theory might be described by one of the other fixed points in 5.1. In section 6.4 we discuss the domain of validity of describing the low–temperature physics using perturbation theory around the fixed point action 5.3a.

In order to analyze the finite–temperature transport in the vicinity of the $\Delta_{12} = 1$ fixed point, the terms in $S_{\rm int}$ must be included. Consequently, we need to make a choice for the short–ranged Coulomb interaction v_{ij} and diagonalize $S_{\Delta_{12}=1}$. The choice of the Coulomb interaction is non–universal.

Denote by $S_B = \sum_i S_i + \sum_{i\neq j} S_{ij}$, the quadratic part of (5.1) that describes the chiral bosons, and write it as

$$S_B = -\frac{1}{4\pi}\int_{t,x}\left[\sum_i \frac{\eta_i}{\nu_i}\partial_x\phi_i\partial_t\phi_i + \sum_{i,j} V_{ij}\partial_x\phi_i\partial_x\phi_j\right]. \tag{5.5}$$

We model the "velocity matrix" V_{ij} following [118]. In the absence of a short–ranged Coulomb interaction, the action for the bosonic modes is

$$S_{0,B} = -\frac{1}{4\pi}\sum_i \int_{t,x}\frac{1}{\nu_i}\left[\partial_x\phi_i(\eta_i\partial_t\phi_i + v_i^{(0)}\partial_x\phi_i)\right]. \tag{5.6}$$

Thus, $v_i^{(0)}$ is the velocity of ϕ_i when the Coulomb interaction is ignored. We include the short–ranged Coulomb interaction via the ansatz,

$$S_{\rm Coulomb} = -\pi w\int_{t,x} n_{\rm tot}(x)^2 = -\frac{w}{4\pi}\int_{t,x}(\sum_i \partial_x\phi_i)^2, \tag{5.7}$$

where $n_{\rm tot} = \frac{1}{2\pi}\sum_i \partial_x\phi_i$ is the total charge density and w is the strength of the Coulomb interaction. The Hamiltonian for the bosonic modes is

$$H_B = H_{0,B} + H_{\rm Coulomb} = \frac{1}{4\pi}\int {\rm d}x \sum_{ij} V_{ij}\partial_x\phi_i\partial_x\phi_j, \tag{5.8}$$

where the "velocity matrix" is

$$V_{ij} = \begin{cases} \frac{1}{\nu_i}v_i^{(0)} + w & i = j, \\ w & i \neq j. \end{cases} \tag{5.9}$$

First consider the limit $v_i^{(0)} = 0$ for all i at which the total Hamiltonian is given by the Coulomb term only. Here, the action is diagonalized using a charge–neutral basis. One such basis choice, that is consistent with our earlier treatment of the relevant $e^{i(\phi_1-\phi_2)}$ term, is

$$\begin{pmatrix} \phi_\rho \\ \phi_{\sigma_1} \\ \phi_{\sigma_2} \\ \phi_{\sigma_3} \end{pmatrix} = \begin{pmatrix} \sqrt{\frac{2}{5}} & \sqrt{\frac{2}{5}} & \sqrt{\frac{2}{5}} & \sqrt{\frac{2}{5}} \\ \frac{1}{\sqrt{2}} & -\frac{1}{\sqrt{2}} & 0 & 0 \\ \frac{1}{\sqrt{6}} & \frac{1}{\sqrt{6}} & -\frac{2}{\sqrt{6}} & 0 \\ \frac{1}{\sqrt{15}} & \frac{1}{\sqrt{15}} & \frac{1}{\sqrt{15}} & \frac{6}{\sqrt{15}} \end{pmatrix} \begin{pmatrix} \phi_1 \\ \phi_2 \\ \phi_3 \\ \phi_4 \end{pmatrix}. \tag{5.10}$$

Notice that $\phi_{\sigma_1} = \phi_{\sigma_{12}}$. When $v_i^{(0)} = 0$, the velocity of the charge mode ϕ_ρ is νw ($\nu = \frac{5}{2}$), while the velocities of the neutral modes ϕ_{σ_α} are zero. This three–fold degeneracy in the velocity matrix exists because there is freedom in choosing the neutral basis given by $\phi_{\sigma_i} = \Lambda^\sigma_{ij}\phi_{\tilde{\sigma}_j}$ where Λ^σ is an arbitrary $SO(2,1)$ rotation.

Experiments [113, 114] suggest the velocity of the charge mode is generally about an order of magnitude larger than the velocity of a neutral mode. This was predicted earlier in [119]. Thus, we assume small, but finite $v_i^{(0)} \ll w$. The modes that diagonalize $S_{\Delta_{12}=1}$ when $v_i^{(0)} \neq 0$ are not exactly the charge and neutral basis in Eq. (5.10). We denote the diagonal modes as $\phi_r, \phi_{\sigma_{12}}, \phi_{s_2}, \phi_{s_3}$; in the small $v_i^{(0)}$ limit, the ϕ_r mode is "close" to the total charge mode while ϕ_{s_2} and ϕ_{s_3} are "almost neutral" modes. Based on (4.79), we expect all the $v_i^{(0)}$ as well as the Majorana velocity u, to have the same order of magnitude, which we denote by $v^{(0)}$. Therefore, to leading order in $v^{(0)}/w$, the velocities for the modes $\phi_r, \phi_{\sigma_{12}}, \phi_{s_2}, \phi_{s_3}$ are

$$v_r = \nu w + O(v^{(0)}), \quad v_\beta = O(v^{(0)}) \text{ for } \beta = \sigma_{12}, s_2, s_3. \tag{5.11}$$

The density–density interactions between the $\phi_{\sigma_{12}}$ mode and the other modes (the

first term in (5.4a)) become irrelevant on scales larger than $v_{\sigma_{12}}^2/W_{12}$. In Section 6 we include the effects of such interactions on charge and heat transport near the $\Delta_{12} = 1$ fixed point. The couplings for these interactions, $v_{\sigma_{12},r}, v_{\sigma_{12},s_2}$, and v_{σ_{12},s_3}, vanish in the limit where there's a degeneracy between the up and down spin electrons in the lowest Landau level. To see this, consider a general $SO(3,1)$ transformation $\Lambda_{i\alpha}$ from the fractional modes $\phi_i, i = 1,2,3,4$ to some new modes ϕ_α with $\alpha = \sigma_{12}, \tilde{2}, \tilde{3}, \tilde{4}$, such that one of the modes is the spin mode $\phi_{\sigma_{12}}$. From the definition of the spin mode we see that

$$\phi_1 = \frac{1}{\sqrt{2}}\phi_{\sigma_{12}} + \sum_{\alpha \neq \sigma_{12}} \Lambda_{1\alpha}\phi_\alpha \tag{5.12a}$$

$$\phi_2 = -\frac{1}{\sqrt{2}}\phi_{\sigma_{12}} + \sum_{\alpha \neq \sigma_{12}} \Lambda_{2\alpha}\phi_\alpha \tag{5.12b}$$

with $\Lambda_{1\alpha} = \Lambda_{2\alpha}$ for $\alpha \neq \sigma_{12}$ while $\Lambda_{3,\sigma_{12}} = \Lambda_{4,\sigma_{12}} = 0$. The velocity matrix tranforms as $v_{\alpha\beta} = \sum_{ij} V_{ij}\Lambda_{i\alpha}\Lambda_{j\beta}$. So for $v_{\sigma_{12},\alpha}$ we have

$$\begin{aligned}
\beta \neq \sigma_{12} : v_{\sigma_{12},\beta} =& \sum_{ij} V_{ij}\Lambda_{i\sigma_{12}}\Lambda_{j\beta} \\
=& V_{11}\Lambda_{1,\sigma_{12}}\Lambda_{1,\beta} + V_{22}\Lambda_{2,\sigma_{12}}\Lambda_{2,\beta} + V_{12}\left(\Lambda_{1,\sigma_{12}}\Lambda_{2,\beta} + \Lambda_{2,\sigma_{12}}\Lambda_{1,\beta}\right) \\
&+ \sum_{j\neq 1,2} V_{1j}(\Lambda_{1,\sigma_{12}}\Lambda_{j,\beta} + \Lambda_{j,\sigma_{12}}\Lambda_{1,\beta}) + V_{2j}(\Lambda_{2,\sigma_{12}}\Lambda_{j,\beta} + \Lambda_{j,\sigma_{12}}\Lambda_{2,\beta}) \\
&+ \sum_{i,j\neq 1,2} V_{ij}\Lambda_{i,\sigma_{12}}\Lambda_{j,\beta}.
\end{aligned} \tag{5.13}$$

Using (5.12) we get

$$\beta \neq \sigma_{12} : v_{\sigma_{12},\beta} = \frac{1}{\sqrt{2}}\Lambda_{1,\beta}(V_{11} - V_{22}) + \frac{1}{\sqrt{2}}\sum_{j\neq 1,2} \Lambda_{j,\beta}(V_{1j} - V_{2j}) \tag{5.14}$$

which vanishes when $V_{11} = V_{22}$ and $V_{1i} = V_{2i}, i = 3,4$, i.e., when there exists symmetry between the spin–up and spin–down modes. Note that this result is independent of our specific modeling of the velocity matrix.

5.3 $\Delta_{12} = \Delta_{34} = 1$ disordered fixed point

Here, in addition to the field redefinition of the edge modes arising from the lowest Landau level considered in the previous section, we introduce the charge $\phi_{\rho_{34}} = \sqrt{2}(\phi_3+\phi_4)$ and neutral $\phi_{\sigma_{34}} = \phi_3 + 2\phi_4$ fields [20, 21]. We also define the Majorana vector $\boldsymbol{\psi}^T = (\psi_1, \psi_2, \psi_3)$ with Majorana fermions $\psi_1 = \mathrm{e}^{i\phi_{\sigma_{34}}} + \mathrm{e}^{-i\phi_{\sigma_{34}}}, \psi_2 = i(\mathrm{e}^{i\phi_{\sigma_{34}}} - \mathrm{e}^{-i\phi_{\sigma_{34}}}), \psi_3 = \psi$. In terms of these fields the action is

$$S = \sum_{i\in\{\sigma_{12},\rho_{12},\rho_{34}\}} S_i + \sum_{i\neq j\in\{\sigma_{12},\rho_{12},\sigma_{34},\rho_{34}\}} S_{ij} + S_{\text{neutral}}, \tag{5.15a}$$

$$S_{\rho_{34}} = -\frac{1}{4\pi}\int_{t,x} \partial_x\phi_{\rho_{34}}(\partial_t\phi_{\rho_{34}} + v_{\rho_{34}}\partial_x\phi_{\rho_{34}}), \tag{5.15b}$$

$$S_{\text{neutral}} = S_{\text{sym}} + S_{\text{anis}}, \tag{5.15c}$$

$$S_{\text{sym.}} = \frac{1}{4}\int_{t,x} i\boldsymbol{\psi}^T(\partial_t\boldsymbol{\psi} - \overline{v}\partial_x\boldsymbol{\psi} - \frac{\boldsymbol{\xi}_{34}.\boldsymbol{L}}{2}\boldsymbol{\psi}), \quad \boldsymbol{\xi}_{34} = \Big(\frac{\xi_{34}+\xi_{34}^*}{2}, \frac{\xi_{34}-\xi_{34}^*}{2i}, 0\Big), \tag{5.15d}$$

$$S_{\text{anis.}} = -\frac{1}{4}\int_{t,x} i\boldsymbol{\psi}^T\delta v\partial_x\boldsymbol{\psi}, \tag{5.15e}$$

$$S_{ij} = -\frac{2v_{ij}}{4\pi}\int_{t,x} \partial_x\phi_i\partial_x\phi_j, \tag{5.15f}$$

where the average velocity $\overline{v} \equiv \frac{2v_{\sigma_{34}}+u}{3}$ and the anisotropic velocity matrix $\delta v \equiv \mathrm{diag}(v_{\sigma_{34}} - \overline{v}, v_{\sigma_{34}} - \overline{v}, u - \overline{v})$. $\boldsymbol{L} = (L^x, L^y, L^z)$ is the vector composed of the three generators of $SO(3)$. S_{sym} has an $SO(3)$ gauge symmetry $\boldsymbol{\psi}(x,t) = O(x)\tilde{\boldsymbol{\psi}}(x,t)$ provided the disorder vector also transforms as

$$\tilde{\xi}_{34}^a = \frac{1}{2}\epsilon^{abc}\left(O^T(\boldsymbol{\xi}_{34}.\boldsymbol{L})O\right)^{bc} + \overline{v}\epsilon^{abc}(O^T\partial_x O)^{bc}. \tag{5.16}$$

However under this transformation, the term $\tilde{\boldsymbol{\psi}}^T(O^T\delta v\partial_x O)\tilde{\boldsymbol{\psi}}$ shows up in S_{anis}. In order to get rid of such a term we instead require ξ_{34} to transform as

$$\tilde{\xi}^a_{34} = \frac{1}{2}\epsilon^{abc}\left(O^T(\boldsymbol{\xi}_{34}.\boldsymbol{L})O\right)^{bc} + \epsilon^{abc}(O^T v\partial_x O)^{bc}, \tag{5.17}$$

with velocity matrix $v = \text{diag}(v_{\sigma_{34}}, v_{\sigma_{34}}, u)$. Requiring $\tilde{\boldsymbol{\xi}}_{34} = 0$, the transformed action becomes $S = S_{\Delta_{12}=\Delta_{34}=1} + S_{\text{int}}$ where

$$S_{\Delta_{12}=\Delta_{34}=1} = \sum_{i\in\{\sigma_{12},\rho_{12},\rho_{34}\}} S_i + S_{\text{neutral sym}} + S_{\rho_{12},\rho_{34}}, \tag{5.18a}$$

$$S_{\text{neutral sym}} = \frac{1}{4}\int_{t,x} i\tilde{\boldsymbol{\psi}}^T(\partial_t\tilde{\boldsymbol{\psi}} - \overline{v}\partial_x\tilde{\boldsymbol{\psi}}), \tag{5.18b}$$

$$S_{\rho_{12},\rho_{34}} = -\frac{v_{\rho_{12},\rho_{34}}}{8\pi}\int_{t,x} \partial_x\phi_{\rho_{12}}\partial_x\phi_{\rho_{34}}, \tag{5.18c}$$

and

$$S_{\text{int}} = \sum_{i\in\{\rho_{12},\rho_{34}\}} (S_{\sigma_{34},i} + S_{\sigma_{12},i}) + S_{\sigma_{12},\sigma_{34}} + S_{\text{neutral int}}, \tag{5.19a}$$

$$S_{\text{neutral int}} = -\int_{t,x} i\tilde{\boldsymbol{\psi}}^T\widetilde{\delta v}\partial_x\tilde{\boldsymbol{\psi}}, \tag{5.19b}$$

$$S_{\sigma_{34},i} = -\frac{v_{i.\sigma_{34}}}{8\pi}\int_{t,x} \partial_x\phi_{\sigma_{34}}\left(i\tilde{\boldsymbol{\psi}}^T L^z(x)\tilde{\boldsymbol{\psi}}\right), \tag{5.19c}$$

$$\begin{aligned} S_{\sigma_{12},\sigma_{34}} = -\frac{2v_{\sigma_{12},\sigma_{34}}}{4\pi}\int_{t,x}&\left(i\tilde{\boldsymbol{\psi}}^T L^z(x)\tilde{\boldsymbol{\psi}}\right) \\ &\times\left(\frac{\sqrt{2}}{a}O^{zx}\cos(\sqrt{2}\tilde{\phi}_{\sigma_{12}}) + \frac{\sqrt{2}}{a}O^{zy}\sin(\sqrt{2}\tilde{\phi}_{\sigma_{12}}) + O^{zz}\partial_x\tilde{\phi}_{\sigma_{12}}\right), \end{aligned} \tag{5.19d}$$

with $\widetilde{\delta v}(x) \equiv O^T(x)\delta v O(x)$ and $L^z(x) \equiv O^T(x)L^z O(x)$. The $\Delta_{12} = \Delta_{34} = 1$ fixed point is described by $S_{\Delta_{12}=\Delta_{34}=1}$ about which the terms in $S_{\sigma_{34},i}$ and $S_{\sigma_{34},i}$ are irrelevant. Here, the auto–correlation of elements of matrices $L^z(x)$ and $\widetilde{\delta v}(x)$ decay on length scales $\sim \overline{v}^2/W_{34}$.

We model the short–ranged Coulomb interaction as in the previous section. Here, the diagonal modes are $\phi_r, \phi_{\sigma_{12}}, \phi_{s_2}, \phi_{\sigma_{34}}$, where ϕ_{s_2} is some "almost neutral" mode. To

leading order in $v^{(0)}/w$ the velocities for these modes are

$$v_r = \nu w + O(v^{(0)}), \quad v_\beta = O(v^{(0)}) \text{ for } \beta = \sigma_{12}, s_2, \sigma_{34}. \tag{5.20}$$

Since $u = O(v^{(0)})$, we can write $\overline{v} \approx O(v^{(0)})$. As for the magnitude of couplings in (5.19), we have $v_{\sigma_{34},\beta} = O(v^{(0)})$ for $\beta = r, s_2$ while $v_{\sigma_{12},\beta}$ vanish for $\beta = r, \sigma_{12}, s_2$ in the spin–degenerate limit as demonstrated in the previous section.

Chapter 6

Transport and equilibration along the anti–Pfaffian edge

In this section, we analyze the low–temperature transport properties of the effective theories of the $\nu = 5/2$ anti–Pfaffian state described in Sections 5.2 and 5.3. We will apply charge and heat kinetic equations introduced in chapter 4 to each of these fixed points, calculate the expressions for conductivity coefficients, and eventually solve for the electrical and thermal Hall conductances. We estimate the parameter regime that describes the experimental observation of $\kappa = 2.5\kappa_0 T$ in order to determine the experimental relevance of each fixed point. In Section 6.3 we examine quantum point contact tunneling in the anti–Pfaffian state in the vicinity of these low–energy edge states. Finally, in section 6.4 we discuss the domain of edge parameters that each of discussed fixed point theories can reasonably explain.

6.1 $\Delta_{12} = 1$ fixed point

6.1.1 Charge transport

At this fixed point, the processes that cause equilibration are the irrelevant terms in (5.4a). Using (4.59) (see appendix C.1 for details) we write down the equations describing charge transport resulting from such interactions. In the basis (I_1', I_2', I_3, I_4) the matrix G^e is

$$G^e = -\Big(\sum_{\beta=r,s_2,s_3} g_{V_{\sigma_{12},\beta}}\Big)\begin{pmatrix} 1 & -1 & 0 & 0 \\ -1 & 1 & 0 & 0 \\ 0 & 0 & 0 & 0 \\ 0 & 0 & 0 & 0 \end{pmatrix} - g_{V_{34}}\begin{pmatrix} 0 & 0 & 0 & 0 \\ 0 & 0 & 0 & 0 \\ 0 & 0 & 1 & 2 \\ 0 & 0 & -1 & -2 \end{pmatrix} \tag{6.1}$$

with

$$\beta = r, s_2, s_3 : g_{V_{\sigma_{12},\beta}} = \frac{2\pi^2 v_{\sigma_{12},\beta}^2 T^2}{3 v_\beta^2 W_{12}} \tag{6.2a}$$

$$g_{V_{34}} = \frac{\Gamma(\Delta_{34})^2}{\Gamma(2\Delta_{34})}\frac{W_{34}}{\overline{v}_{V_{34}}^{2\Delta_{34}}}\left(2\pi a T\right)^{2\Delta_{34}-2}, \quad \overline{v}_{V_{34}} = O(v^{(0)}). \tag{6.2b}$$

The velocities are defined in (5.11), and a is the short–distance cutoff [102].

The last term in G^e couples the downstream and upstream charge modes. Therefore, largeness of $g_{V_{34}}$ (see below) is required for the proper quantization of the electrical conductance at $G = 2.5\sigma_0$. To quantify this we solve for the electrical conductance using (6.1) and boundary conditions specified in Section 4.5. We find

$$G = \sigma_0\left(2 + \frac{2 + \mathrm{e}^{-g_{V_{34}}L}}{2(2 - \mathrm{e}^{-g_{V_{34}}L})}\right), \tag{6.3}$$

where L is the effective length on the sample's top/bottom edge along which equilibration takes place. If the electrical conductance is measured to be $G = 2.50\sigma_0$ within the

uncertainty $\Delta G = 0.01\sigma_0$ we find the bound $g_{V_{34}} L \gtrsim 4$.

6.1.2 Heat transport

Based on (4.65), the heat transport matrix G^Q in the basis $(r, \phi_{\sigma_{12}}, \phi_{s_2}, \phi_{s_3}, \psi)$ is

$$G^Q = \frac{12 g_{V_{\sigma_{12},r}}}{5} \begin{pmatrix} -1 & 1 & 0 & 0 & 0 \\ 1 & -1 & 0 & 0 & 0 \\ 0 & 0 & 0 & 0 & 0 \\ 0 & 0 & 0 & 0 & 0 \\ 0 & 0 & 0 & 0 & 0 \end{pmatrix} + \frac{12 g_{V_{\sigma_{12},s_2}}}{5} \begin{pmatrix} 0 & 0 & 0 & 0 & 0 \\ 0 & -1 & 1 & 0 & 0 \\ 0 & 1 & -1 & 0 & 0 \\ 0 & 0 & 0 & 0 & 0 \\ 0 & 0 & 0 & 0 & 0 \end{pmatrix} + \frac{12 g_{V_{\sigma_{12},s_3}}}{5} \begin{pmatrix} 0 & 0 & 0 & 0 & 0 \\ 0 & -1 & 0 & -1 & 0 \\ 0 & 0 & 0 & 0 & 0 \\ 0 & 1 & 0 & 1 & 0 \\ 0 & 0 & 0 & 0 & 0 \end{pmatrix}$$
$$+ \frac{12 g_{V_{34}}}{1 + 2\Delta_{34}} \begin{pmatrix} -d_r(d_{s_2} + d_{s_3} + d_\psi) & 0 & d_r d_{s_2} & -d_r d_{s_3} & -2 d_r d_\psi \\ 0 & 0 & 0 & 0 & 0 \\ d_r d_{s_2} & 0 & -d_{s_2}(d_r + d_{s_3} + d_\psi) & -d_{s_2} d_{s_3} & -2 d_{s_2} d_\psi \\ d_r d_{s_3} & 0 & d_{s_2} d_{s_3} & d_{s_3}(d_r + d_{s_2} + d_\psi) & -2 d_{s_3} d_\psi \\ d_r d_\psi & 0 & d_{s_2} d_\psi & -d_{s_3} d_\psi & 2 d_\psi (d_r + d_{s_2} + d_{s_2}) \end{pmatrix} \tag{6.4}$$

where $d_\psi = \frac{1}{2}$ and $d_\alpha = (\Lambda_{3\alpha} + 2\Lambda_{4\alpha})^2 / 2$. Also we have $\sum_{\alpha = r, s_2, s_3, \psi} d_\alpha = \Delta_{34}$. See C.2 for the definition of d_α. Λ is the $SO(3,1)$ transformation expressing the fractional modes ϕ_i in terms of $(\phi_r, \phi_{\sigma_{12}}, \phi_{s_2}, \phi_{s_3})$, i.e., the diagonal modes of $S_{\Delta_{12}=1}$.

This transformation depends on the velocity matrix in (5.3a). We use the velocity matrix in Eq. (5.9) in order to estimate the d_α. In the $v_i^{(0)}/w = 0$ limit, ϕ_r is the total charge mode, and, consequently, it commutes with the neutral mode $\phi_3 + 2\phi_4$. Therefore, in this limit, $d_r = (\Lambda_{3,r} + 2\Lambda_{4,r})^2 / 2 = 0$. For finite but small $v^{(0)}/w$, we have $d_r = O\left((\frac{v^{(0)}}{w})^2\right)$ to leading order.

In order to estimate d_{s_2} and d_{s_3}, we look at the spin of the operator $\mathrm{e}^{i\phi_3 + 2i\phi_4}$. Generally, for a set of chiral bosons ϕ_i with commutation relation $[\phi_i(x), \phi_j(x')] = \pi i K^{-1}_{ij} \operatorname{sign}(x -$

x'), the spin of the vertex operator $\mathrm{e}^{i\sum_i n_i\phi_i}$ is

$$h_- = \frac{1}{2} n_i K^{-1}_{ij} n_j = \Delta_R - \Delta_L, \tag{6.5}$$

where Δ_R (Δ_L) is the scaling dimension of the right–moving (left–moving) part of $\mathrm{e}^{i\sum_i n_i\phi_i}$. Therefore, the spin of the tunneling operator $\mathrm{e}^{i\phi_3+2i\phi_4}$ is $h_- = -\frac{1}{2} = \Delta_R - \Delta_L$. Also, we have $\Delta_R = d_r + d_{s_2}$ and $\Delta_L = d_{s_3}$. Along with $d_r + d_{s_2} + d_{s_3} + d_\psi = \Delta_{34}$, to leading order in $v_i^{(0)}/w$ we find

$$d_{s_2} = \frac{\Delta_{34}-1}{2} - d_r = \frac{\Delta_{34}-1}{2} - O\left((\frac{v^{(0)}}{w})^2\right) \tag{6.6a}$$

$$d_{s_3} = \frac{\Delta_{34}}{2}. \tag{6.6b}$$

As we mentioned in Section 5.2, we take $\Delta_{34} \geq \frac{3}{2}$ so that $S_{\Delta_{12}} = 1$ describes the low–energy physics of the $\Delta_{12} = 1$ fixed point. On the other hand, since $g_{V_{34}} L$ is large, based on Eq. (6.2), we don't expect Δ_{34} to be very large. This is due to the fact that *i*) the prefactor $\Gamma(\Delta_{34})^2/\Gamma(2\Delta_{34})$ vanishes rapidly for large Δ_{34} and *ii*) $g_{V_{34}} \sim T^{2(\Delta_{34}-1)}$ and so the equilibration process corresponding to $g_{V_{34}}$ would have subleading contribution at small temperatures, if Δ_{34} was large.

We can estimate Δ_{34} for $v_i^{(0)} = v^{(0)}$. In this case, using (5.10) we can write

$$\begin{aligned} H &= \frac{1}{4\pi}\int_x V_{ij}\partial_x\phi_i\partial_x\phi_j \\ &= \frac{1}{4\pi}\int_x \Big[(w+\frac{7}{5}v^{(0)})(\partial_x\phi_\rho)^2 + v^{(0)}(\partial_x\phi_{\sigma_1})^2 \\ &\qquad + v^{(0)}(\partial_x\phi_{\sigma_2})^2 + \frac{7}{5}v^{(0)}(\partial_x\phi_{\sigma_3})^2 - \frac{4\sqrt{6}}{5}v^{(0)}\partial_x\phi_\rho\partial_x\phi_{\sigma_3}\Big]. \end{aligned} \tag{6.7}$$

Therefore, for small $v^{(0)}/w$ a small rotation in the $(\phi_\rho, \phi_{\sigma_3})$ plane would diagonalize the Hamiltonian. So, using (5.10) we find $\Delta_{34} = \frac{5}{3}$ in the vanishing $v^{(0)}/w$ limit.

We are interested in determining the regime for which this matrix G^Q leads to a thermal Hall conductance $K = 2.5\kappa_0 T$ within the uncertainties of the experiment. Quantization of electrical conductance $G = 2.5\sigma_0$ implies that $g_{V_{23}}$ is large. Looking at the last term in (6.4), more specifically, the $(\phi_{s_2}, \phi_{s_3}, \psi)$ block, it appears that the ϕ_{s_2},ϕ_{s_3} and ψ modes equilibrate with each other. For the moment, let's assume they are completely equilibrated; we will relax this assumption later. In this case, we can think of these modes as a single upstream mode with central charge $c = \frac{1}{2}$. We call this mode $\tilde{s}$.

If equilibration between the first two modes in (6.4) and the $\tilde{s}$ mode is suppressed, the thermal conductance theis sum of the contributions from the first two modes $K_{r+\sigma_{12}}$ and from the $\tilde{s}$ mode $K_{\tilde{s}}$. That is $K = K_{r+\sigma_{12}} + K_{\tilde{s}} = (2 + |-0.5|)\,\kappa_0 T = 2.5\kappa_0 T$. This requires

$$g_{V_{\sigma_{12},s_2}} L \ll 1, \quad g_{V_{\sigma_{12},s_3}} L \ll 1, \quad g_{r,\tilde{s}} L \ll 1, \tag{6.8}$$

where we defined $g_{r,\tilde{s}} = d_r(\Delta_{34} - d_r) g_{V_{34}}$. Therefore, we see that there exists a regime of parameters where the fixed point $\Delta_{12} = 1$ can be consistent with experiments. Using the details of the experimental measurements, we can gain a more quantitative estimation of this regime.

We use the above G^Q matrix and boundary conditions given in Section 4.5 to solve for the thermal conductance. Following our earlier discussion we will take $\Delta_{34} = \frac{5}{3}$, and consequently $d_{s_2} = \frac{1}{3}, d_{s_3} = \frac{5}{6}$. Later, we will discuss how our results depend on these values.

We also ignore the first term in (6.4) in the remainder. This follows from our discussion in Section 4.4: we expect $g_{\sigma_{12},r} L$ to be suppressed both due to the strong Coulomb inter-

action and small spin gap. Also, since $g_{\sigma_{12},r}$ quantifies equilibration between co-propagating modes, its magnitude does not have much effect on the thermal conductance.

The contour plot of $K(g_{V_{\sigma_{12},s_2}}L, g_{V_{\sigma_{12},s_2}}L, g_{r,\tilde{s}}L, g_{V_{34}}L)$ along several surfaces is given in Fig. 6.1. The thermal conductance observed in the experiments ([37]) at temperatures ($T \approx 18$ - $25\ mK$) $2.49\kappa_0 T < K < 2.57\kappa_0 T$ is enclosed within the white contours. The hatched region represents the regime where the electrical conductance $G = (2.50 \pm 0.01)\sigma_0$.

We observe that not all the region observed in the experiment $2.49\kappa_0 T < K < 2.75\kappa_0 T$ is consistent with the electrical conductance $G = (2.50 \pm 0.01)\sigma_0$: we find that when $K \gtrsim 2.65\kappa_0 T$, the electrical conductance deviates from $G = (2.50 \pm 0.01)\sigma_0$. In addition, we can deduce some information about which point of the region $2.49\kappa_0 T < K < 2.75\kappa_0 T$ we are at by examining how the thermal conductance varies as a function of temperature.

The conductivity coefficients have power law dependence on temperature as Eq. (6.2). Therefore, the thermal conductance moves along straight lines in Fig. 6.1, as the temperature is varied. From the experimental data, as the temperature is lowered from $T \approx 18$ - $25\ mK$ to $T \approx 12\ mK$, i.e., by a factor of about 2, the thermal conductance increases from $K \approx 2.53\kappa_0 T$ to $K \approx 2.75\kappa_0 T$. It follows that g_{34} would vary by a factor of $2^{(2\Delta_{34}-2)}$ while g_{σ_{12},s_2} and g_{σ_{12},s_3} would vary by a factor of 4. We can look for lines in the space of conductivity coefficients where such a variation occurs.

First, we look at how the thermal conductance varies along the surface $g_{\sigma_{12},s_2} = g_{\sigma_{12},s_3}$ when $g_{r,\tilde{s}} = 0$. This is demonstrated in Fig. 6.2. The red line showcases a variation of conductivity coefficients with temperature that is consistent with the experiments: as the temperature is lowered by a factor of ~ 2, between the cross marks, the thermal conductance

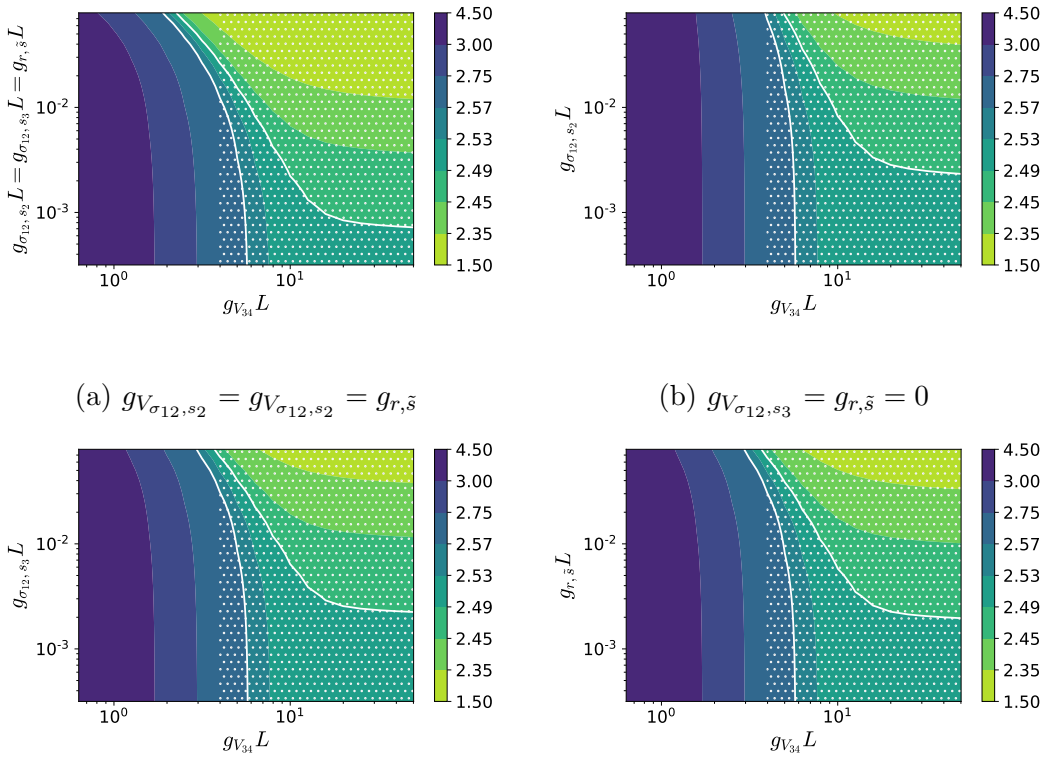

(a) $g_{V_{\sigma_{12},s_2}} = g_{V_{\sigma_{12},s_2}} = g_{r,\tilde{s}}$

(b) $g_{V_{\sigma_{12},s_3}} = g_{r,\tilde{s}} = 0$

(c) $g_{V_{\sigma_{12},s_2}} = g_{r,\tilde{s}} = 0$

(d) $g_{V_{\sigma_{12},s_2}} = g_{V_{\sigma_{12},s_3}} = 0$

Figure 6.1: Contour plot of thermal conductance about the $\Delta_{12} = 1$ fixed point, $K(g_{V_{\sigma_{12},s_2}}L, g_{V_{\sigma_{12},s_3}}L, g_{r,\tilde{s}}L, g_{V_{34}}L)/\kappa_0 T$ along several surfaces. $\Delta_{34} = 5/3$ for all the sub-plots. The regions within the white contour represent the measured thermal conductance $K = (2.53 \pm 0.04)\kappa_0 T$, while the hatched regions represent the regime where $G = (2.50 \pm 0.01)\sigma_0$.

increases from $K \approx 2.53\kappa_0 T$ to $K \approx 2.75\kappa_0 T$. This gives us a rough estimate for the value of the conductivity coefficients at these temperatures. Examining the red line in Fig. 6.2 for $T = 18\text{-}25\ mK$, we find

$$g_{V_{34}}L \approx 7, \quad g_{\sigma_{12},s_2/s_3}L \approx 0.005. \tag{6.9}$$

A similar picture also shows $g_{r,\tilde{s}}L \approx 0.005$. Here, the thermal conductance does not vary much as a function of $g_{\sigma_{12},s_2/s_3}$ and $g_{r,\tilde{s}}$ when these coefficients are small. Consequently, the error in the estimate of $g_{\sigma_{12},s_2/s_3}$ and $g_{r,\tilde{s}}$ is large and the above estimates for $g_{\sigma_{12},s_2/s_3}$ and $g_{r,\tilde{s}}$ should be interpreted as upper bounds.

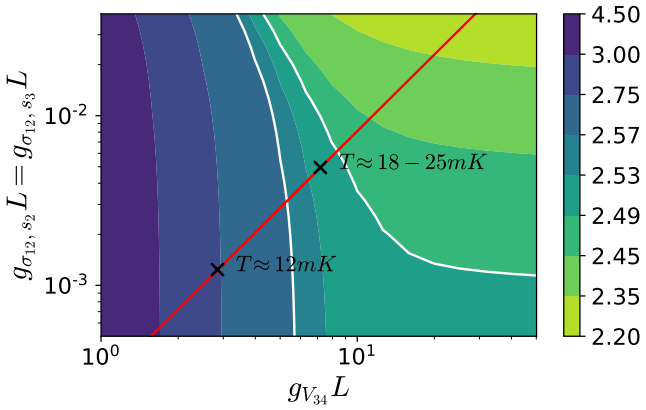

Figure 6.2: Thermal conductance about the $\Delta_{12} = 1$ fixed point on the surface $g_{V_{\sigma_{12},s_2}} = g_{V_{\sigma_{12},s_3}}$ and $g_{r,\tilde{s}} = 0$. $\Delta_{34} = 5/3$. The red line represents a typical line along which the thermal conductance varies as a function of temperature. This specific red line passes through points that are consistent with measurements of thermal conductance.

Based on these estimates, we infer

$$\frac{g_{r,\tilde{s}}}{g_{V_{34}}} = (\Delta_{34} - d_r)d_r \sim (\frac{v^{(0)}}{w})^2 \lesssim 0.001. \tag{6.10}$$

Since $d_r \sim (\frac{v^{(0)}}{w})^2$ the above bound is not unexpected for strong short-ranged Coulomb interactions. Our numerical estimates for d_r based on the velocity matrix in Eq. 5.9 and sensible choice of $v_i^{(0)}$'s, do satisfy this bound for $v_i^{(0)}$'s as large as $w/5$.

On the other hand, the coefficients g_{σ_{12},s_2} and g_{σ_{12},s_3} in (6.2) are proportional to the

square of v_{σ_{12},s_2} and v_{σ_{12},s_3}. As we demonstrated in Eq. (5.14), these velocity entries vanish in the spin-degenerate limit. Therefore, it is not unexpected that the bound $g_{\sigma_{12},s_2/s_3}L \lesssim 0.01$ is satisfied when the spin gap is small. However, we don't have any estimate for these conductivity coefficients based on the experimental data.

In order to find these results, we used the estimate $\Delta_{34} = 5/3$. In order to see how much our results depend on this estimate, we look at two other cases: *i)* $\Delta_{34} = 3/2$ and *ii)* $\Delta_{34} = 2$. For these two values, we plot $K(g_{V_{\sigma_{12},s_2}}L, g_{V_{\sigma_{12},s_2}}L, g_{r,\tilde{s}}L = 0, g_{V_{34}}L)$ along the $g_{V_{\sigma_{12},s_2}} = g_{V_{\sigma_{12},s_3}}$ surface in Fig. 6.3. First, we see that while the observation of $G = (2.50 \pm 0.01)\sigma_0$ is mostly consistent with $2.49\kappa_0 T \leq K \leq 2.75\kappa_0 T$ for $\Delta_{34} = 3/2$, this is not the case for $\Delta_{34} = 2$: in the region $2.57\kappa_0 T \leq K \leq 2.75\kappa_0 T$, the electrical conductance deviates from $G = (2.50 \pm 0.01)\sigma_0$. In addition, while for $\Delta_{34} = 3/2$ the bounds on the

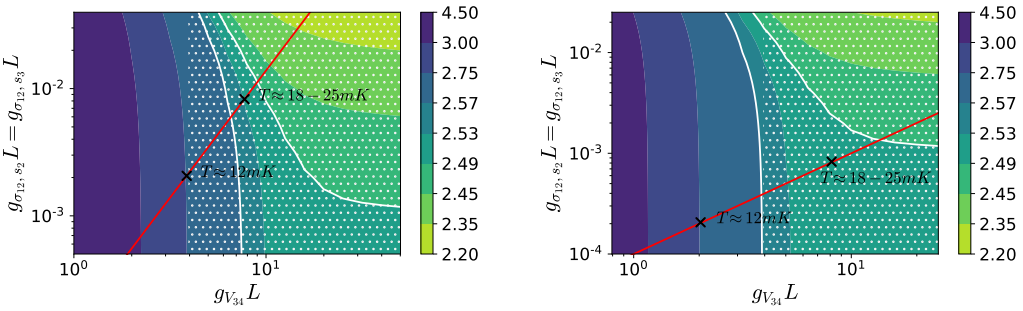

(a) $\Delta_{34} = 3/2$ (b) $\Delta_{34} = 2$

Figure 6.3: Contour plot of thermal conductance about the $\Delta_{12} = 1$ fixed point, $K(g_{V_{\sigma_{12},s_2}}L, g_{V_{\sigma_{12},s_3}}L, g_{r,\tilde{s}}L, g_{V_{34}}L)/\kappa_0 T$ along the surface $g_{V_{\sigma_{12},s_2}} = g_{V_{\sigma_{12},s_2}}, g_{r,\tilde{s}} = 0$. The hatched regions represent the regime where $G = (2.50 \pm 0.01)\sigma_0$.

conductivity coefficients are close to the $\Delta_{34} = 5/3$ case, for $\Delta_{34} = 2$ we get

$$g_{V_{34}} L \approx 10, \quad g_{\sigma_{12}, s_2/s_3} L \lesssim 0.001, \tag{6.11}$$

which are much stronger bounds.

We conclude that there exists a regime of parameters about the $\Delta_{12} = 1$ fixed point of the anti–Pfaffian edge state where $K \approx 2.5\kappa_0 T$ is observed in a range of temperatures ($T \approx 18$ - $25\ mK$). Our estimates demonstrate that this regime is possible for realistic parameters only when $\Delta_{34} \lesssim 5/3$.

6.2 $\Delta_{12} = \Delta_{34} = 1$ fixed point

6.2.1 Charge transport

At this fixed point, the processes that cause equilibration are the irrelevant terms in (5.19). To find the kinetic equations involving the second Landau level modes, we first introduce the neutral currents operators

$$J^a_{34} \equiv \frac{i}{8\pi} \boldsymbol{\psi}^T L^a \boldsymbol{\psi} \tag{6.12}$$

where $L^a, a = x, y, z$ are the generators of $SO(3)$. In terms of these operators we have $\frac{1}{2\pi}\partial_x \phi_{\sigma_{34}} = J^z_{34}$. Using a similar set of calculations as in section C.1.2, we derive the kinetic equation for the gauge-transformed density

$$\tilde{n}_{\sigma_{34}} \equiv \frac{1}{2\pi}\partial_x \tilde{\phi}_{\sigma_{34}} \equiv \tilde{J}^z_{34} = \frac{i}{8\pi} \tilde{\boldsymbol{\psi}}^T L^z \tilde{\boldsymbol{\psi}}. \tag{6.13}$$

We also define the "slow modes" basis as

$$I_3' = \sqrt{2} I_{\rho_{34}} - \tilde{I}_{\sigma_{34}} \tag{6.14a}$$

$$I_4' = -\frac{1}{\sqrt{2}} I_{\rho_{34}} + \tilde{I}_{\sigma_{34}} \tag{6.14b}$$

where $I_{\rho_{34}}$ is the charge current carried by the mode $\phi_{\rho_{34}}$ and the current neutral current $\tilde{I}_{\sigma_{34}}$ is defined by the conservation equation

$$\partial_x \tilde{I}_{\sigma_{34}} + \partial_t \tilde{n}_{\sigma_{34}} = 0. \tag{6.15}$$

It follows that for charge equilibration in the basis (I_1', I_2', I_3', I_4') we have

$$G^e = -\Big(\sum_{\beta=r,s_2,\sigma_{34}} g_{V_{\sigma_{12},\beta}}\Big) \begin{pmatrix} 1 & -1 & 0 & 0 \\ -1 & 1 & 0 & 0 \\ 0 & 0 & 0 & 0 \\ 0 & 0 & 0 & 0 \end{pmatrix} - \Big(\sum_{\beta=r,\sigma_{12},s_2} g_{V_{\sigma_{34},\beta}}\Big) \begin{pmatrix} 0 & 0 & 0 & 0 \\ 0 & 0 & 0 & 0 \\ 0 & 0 & 1 & 2 \\ 0 & 0 & -1 & -2 \end{pmatrix} \tag{6.16}$$

with

$$g_{V_{\sigma_{12},\sigma_{34}}} = \frac{2\pi^2 v_{\sigma_{12},\sigma_{34}}^2}{3(v_{\sigma_{12}}^2 W_{34} + v_{\sigma_{34}}^2 W_{12})} T^2 \tag{6.17a}$$

$$\beta = r, s_2 : g_{V_{\sigma_{12},\beta}} = \frac{2\pi^2 v_{\sigma_{12},\beta}^2}{3 v_\beta^2 W_{12}} T^2 \tag{6.17b}$$

$$\beta = r, s_2 : g_{V_{\sigma_{34},\beta}} = \frac{2\pi^2 v_{\sigma_{34},\beta}^2 T^2}{3 v_\beta^2 W_{34}}. \tag{6.17c}$$

We can calculate the electrical conductance as in the previous section. The solution is similar to Eq. (6.3) with $g_{V_{34}}$ replaced by $\sum_{\beta=r,\sigma_{12},s_2} g_{V_{\sigma_{34},\beta}}$. An electrical conductance of $G = (2.50 \pm 0.01)\sigma_0$ implies $\sum_{\beta=r,\sigma_{12},s_2} g_{V_{\sigma_{34},\beta}} L \gtrsim 4$. Looking at Eq. (6.17) we can estimate

the relative magnitude of the terms in $\sum_{\beta=r,\sigma_{12},s_2} g_{V_{\sigma_{34},\beta}}$. We find

$$\frac{g_{V_{\sigma_{34},r}}}{g_{V_{\sigma_{34},s_2}}} = (\frac{v_{\sigma_{34},r} v_{s_2}}{v_{\sigma_{34},s_2} v_r})^2 \sim (\frac{v^{(0)}}{\nu w})^2, \tag{6.18a}$$

$$\frac{g_{V_{\sigma_{34},\sigma_{12}}}}{g_{V_{\sigma_{34},s_2}}} \approx \frac{W_{34}}{W_{12}+W_{34}} . (\frac{v_{\sigma_{34},\sigma_{12}} v_{s_2}}{v_{\sigma_{34},s_2} v_{\sigma_{12}}})^2 \sim \frac{W_{34}}{W_{12}+W_{34}} . (\frac{v_{\sigma_{34},\sigma_{12}}}{v^{(0)}})^2. \tag{6.18b}$$

Therefore, both $g_{V_{\sigma_{34},\sigma_{12}}}$ and $g_{V_{\sigma_{34},r}}$ are much smaller than $g_{V_{\sigma_{34},s_2}}$ for strong Coulomb interactions and small spin gap, and so we have $g_{V_{\sigma_{34},s_2}} L \gtrsim 1$ based on quantization of the electrical conductance. In the above we used the estimate that $v_{s_2}, v_{\sigma_{12}}, v_{\sigma_{34},r}, v_{\sigma_{34},s_2}$ all have the same order of magnitude $v^{(0)}$. Also, based on the velocity matrix of Eq. 5.9 and using Eq. 5.14 we should have $v_{\sigma_{34},\sigma_{12}} = 0$. However, since we only take this velocity matrix as an estimation, we allow for finite $v_{\sigma_{34},\sigma_{12}}$ which vanishes in the spin-symmetric limit.

6.2.2 Heat transport

At this fixed point, since there exists an $SO(3)$ symmetry between the three Majorana modes, we take their contribution as one upstream mode with central charge $c = \frac{3}{2}$. We call this mode Ψ. Therefore, in the basis $(r, \sigma_{12}, s_2, \Psi)$ we have

$$\begin{aligned} G^Q =& \frac{12}{5} g_{V_{\sigma_{12},r}} \begin{pmatrix} -1 & 1 & 0 & 0 \\ 1 & -1 & 0 & 0 \\ 0 & 0 & 0 & 0 \\ 0 & 0 & 0 & 0 \end{pmatrix} + \frac{12}{5} g_{V_{\sigma_{12},s_2}} \begin{pmatrix} 0 & 0 & 0 & 0 \\ 0 & -1 & 1 & 0 \\ 0 & 1 & -1 & 0 \\ 0 & 0 & 0 & 0 \end{pmatrix} + \frac{12}{5} g_{V_{\sigma_{12},\sigma_{34}}} \begin{pmatrix} 0 & 0 & 0 & 0 \\ 0 & -1 & 0 & -2/3 \\ 0 & 0 & 0 & 0 \\ 0 & 1 & 0 & 2/3 \end{pmatrix} \\ &+ \frac{12}{5} g_{V_{\sigma_{34},r}} \begin{pmatrix} -1 & 0 & 0 & -2/3 \\ 0 & 0 & 0 & 0 \\ 0 & 0 & 0 & 0 \\ 1 & 0 & 0 & 2/3 \end{pmatrix} + \frac{12}{5} g_{V_{\sigma_{34},s_2}} \begin{pmatrix} 0 & 0 & 0 & 0 \\ 0 & 0 & 0 & 0 \\ 0 & 0 & -1 & -2/3 \\ 0 & 0 & 1 & 2/3 \end{pmatrix}. \end{aligned} \tag{6.19}$$

Since $g_{V_{\sigma_{34},s_2}} L \gtrsim 1$, the modes s_2 and Ψ are expected to be well equilibrated. Therefore, similar to the $\Delta_{12} = 1$ fixed point, the thermal conductance $K \approx 2.5\kappa_0 T$ is only possible when equilibration between the modes $\{r, \sigma_{12}\}$ and $\{s_2, \Psi\}$ is suppressed. In order to look for such a regime, we solve the heat transport equation using the above G^Q matrix, and calculate the thermal conductance as a function of $g_{V_{\sigma_{12},s_2}}, g_{V_{\sigma_{12},\sigma_{34}}}, g_{V_{\sigma_{34},r}}$ and $g_{V_{\sigma_{34},r}}$. As before, we ignore the first term in G^Q. Fig. 6.4 shows the contour plot of the thermal conductance along the surface $g_{V_{\sigma_{12},s_2}} = g_{V_{\sigma_{12},\sigma_{34}}} = g_{V_{\sigma_{34},r}}$. The region within the white contour has $2.49\kappa_0 T < K < 2.57\kappa_0 T$, while the hatched region has electrical conductance $G = (2.50 \pm 0.01)\sigma_0$.

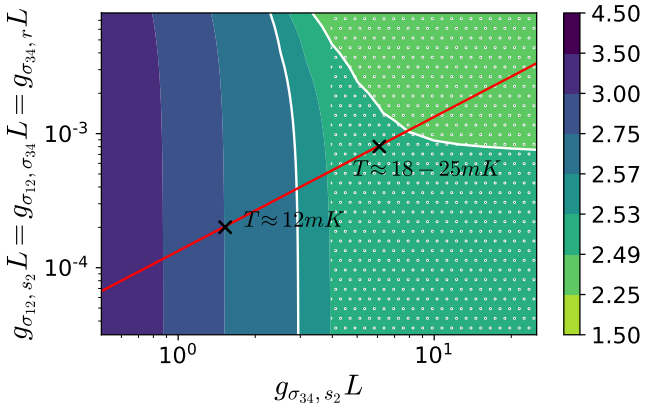

Figure 6.4: Thermal conductance about the $\Delta_{12} = \Delta_{34} = 1$ fixed point, along the surface $g_{V_{\sigma_{12},s_2}} = g_{V_{\sigma_{12},\sigma_{34}}} = g_{V_{\sigma_{34},r}}$. The region within the white contour has $2.49\kappa_0 T < K < 2.57\kappa_0 T$, while the hatched region has electrical conductance $G = (2.50 \pm 0.01)\sigma_0$. The thermal conductance varies along lines parallel to the red line as the temperature is varied.

Here, unlike the $\Delta_{12} = 1$ fixed point, there exists a region where $2.49\kappa_0 T < K < 2.75\kappa_0 T$ while the electrical conductance deviates from $G = (2.50 \pm 0.01)\sigma_0$. If, the electrical

conductance is indeed measured to be $G = (2.50 \pm 0.01)\sigma_0$, even at lowest temperatures $\sim 12mK$, then this fixed point is not consistent with the experiments.

We proceed to find estimates for the conductivity coefficients based on how the thermal conductance varies with temperature. Based on Fig. 6.4 and following an analysis similar to the $\Delta_{12} = 1$ fixed point, we estimate

$$g_{V_{\sigma_{34},s_2}} L \approx 6, \quad g_{V_{\sigma_{12},s_2}} L, g_{V_{\sigma_{12},\sigma_{34}}} L, g_{V_{\sigma_{34},r}} L \lesssim 10^{-3} \tag{6.20}$$

for $T = 18\text{-}25\ mK$. Therefore, using Eq. (6.18), we require

$$\frac{g_{V_{\sigma_{34},r}}}{g_{V_{\sigma_{34},s_2}}} \sim (\frac{v^{(0)}}{\nu w})^2 \lesssim 2 \times 10^{-4}, \tag{6.21a}$$

$$\frac{g_{V_{\sigma_{34},\sigma_{12}}}}{g_{V_{\sigma_{34},s_2}}} \sim \frac{W_{34}}{W_{12}+W_{34}}.(\frac{v_{\sigma_{34},\sigma_{12}}}{v^{(0)}})^2 \lesssim 2 \times 10^{-4}, \tag{6.21b}$$

$$\frac{g_{V_{\sigma_{12},s_2}}}{g_{V_{\sigma_{34},s_2}}} \sim \frac{W_{34}}{W_{12}}.(\frac{v_1^{(0)} - v_2^{(0)}}{v^{(0)}})^2 \lesssim 2 \times 10^{-4}. \tag{6.21c}$$

Generally, we expect the conductivity coefficients $g_{\sigma_{34},r}, g_{V_{\sigma_{12},s_2}}$ and $g_{V_{\sigma_{12},\sigma_{34}}}$ to be much smaller than g_{σ_{34},s_2} for strong short-ranged Coulomb interaction ($w \gg v^{(0)}$) and small spin gap ($v_1^{(0)} - v_2^{(0)} \ll v^{(0)}, v_{\sigma_{34},\sigma_{12}} \ll v^{(0)}$). However, our estimates for $v^{(0)}/w$ (see Section 5.2) and $(v_1^{(0)} - v_2^{(0)})/v^{(0)}$ in Eq. (4.80)) only show ratios of about 10^{-1}. Therefore, we are not aware of any reason why the bounds in Eq. 6.21a might be satisfied.

We conclude that the $\Delta_{12} = \Delta_{34} = 1$ fixed point of the anti–Pfaffian state is not consistent with the transport measurements. This theory predicts that the electrical conductance would deviate from its quantized value $G = 2.5\sigma_0$ at temperatures $T \approx 12\ mK$, a feature that does not appear to be observed in the experiments of Banerjee *et al.*[37]. Furthermore, observation of thermal conductance $K \approx 2.5\kappa_0 T$ requires some parameters in this theory ($v^{(0)}/w$ and $(v_1^{(0)} - v_2^{(0)})/v^{(0)}$) to be fine–tuned; we don't believe such a regime

to be realistic.

6.3 Quantum point contact tunneling

Tunneling conductance at quantum point contacts (QPC) in the ohmic regime ($eV \ll k_B T$) scales as $G_{\rm tun} \sim T^{2g-2}$. Here, g is the scaling dimension of the tunneling operator that transfers charge across the Hall bar. Therefore, at low temperatures, charge tunneling is dominated by the operator with the smallest scaling dimension. In the case of the anti–Pfaffian state, due to the physical separation between the lowest and the first Landau level edge modes, this tunneling is dominated by the tunneling of electrons/quasi–particles belonging to the first Landau level. The most general tunneling operator is then $\mathrm{e}^{i(n_3\phi_3+n_4\phi_4/2)}\,\chi$ where n_3 and n_4 are integers and $\chi = 1, \psi, \sigma$ [20, 21]. This tunneling operator creates an excitation of charge $q = (n_4/4 - n_3)e$. The operator σ changes the boundary condition for the Majorana mode ψ and has scaling dimension $\Delta_\sigma = 1/16$. In addition, n_4 is an odd integer when $\chi = \sigma$.

At the $\Delta_{12} = \Delta_{34} = 1$ fixed point, the charge creation operator with the smallest scaling dimension is $\sigma e^{i\phi_4/2}$ [20, 21], which creates a quasi–particle of charge $e/4$. A similar operator annihilates this quasi–particle across the quantum Hall bar. So

$$g = 2\Delta(\sigma e^{i\phi_4/2}) = 2\Delta_\sigma + 2\Delta(\mathrm{e}^{i\phi_4/2}) = 1/2 \tag{6.22}$$

where we denote by $\Delta(\mathcal{O})$ the scaling dimension of operator $\mathcal{O}$.

For the $\Delta_{12} = 1$ fixed point, the scaling dimension of the operator $\mathrm{e}^{i(n_3\phi_3+n_4\phi_4/2)}$ depends on the velocity matrix in $S_{\Delta_{12}=1}$ 5.3a, and therefore is non–universal. In general, the minimum scaling dimension of a vertex operator is the absolute value of its spin, i.e.,

$\Delta_R + \Delta_L \geq |\Delta_R - \Delta_L|$. See Eq. (6.5). Therefore, one can check that among all excitation operators, $\sigma\, \mathrm{e}^{i\phi_4/2}$ has the minimum scaling dimension of 1/8. Therefore, we always have $g \geq 1/4$ for the anti–Pfaffian state.

We can get a better bound in the limit of strong short–ranged Coulomb interaction. Using (5.10) we can write

$$\mathrm{e}^{i(n_3\phi_3+n_4\phi_4/2)} = \mathrm{e}^{i\sqrt{\frac{2}{5}}(n_3-n_4/4)\phi_\rho}\, \mathrm{e}^{-in_3\sqrt{\frac{2}{3}}\phi_{\sigma_2}-\frac{i}{\sqrt{15}}(n_3+3n_4/2)\phi_{\sigma_3}}\,. \tag{6.23}$$

Similar to Eq. (6.7), in the vanishing $v^{(0)}/w$ limit, ϕ_ρ is a diagonal mode of $S_{\Delta_{12}=1}$. Therefore, in this limit:

$$\Delta(\mathrm{e}^{i(n_3\phi_3+n_4\phi_4/2)}) = \Delta(\mathrm{e}^{i\sqrt{\frac{2}{5}}(n_3-n_4/4)\phi_\rho}) + \Delta(\mathrm{e}^{-in_3\sqrt{\frac{2}{3}}\phi_{\sigma_2}-\frac{i}{\sqrt{15}}(n_3+3n_4/2)\phi_{\sigma_3}}) \tag{6.24}$$

$$\leq \frac{1}{5}(n_3 - n_4/4)^2 + \left|\frac{1}{3}n_3^2 - \frac{1}{30}(n_3+3n_4/2)^2\right|. \tag{6.25}$$

Using this inequality, we can check that the minimum scaling dimension is 3/20 for the operator $\sigma e^{i\phi_4/2}$. The next smallest scaling dimension is 7/20 for the operator $e^{i\phi_4}$ which creates an excitation of charge $e/2$. Therefore, for strong Coulomb interactions we have $g \geq 3/10$ with the minimum happening for the operator $\sigma e^{i\phi_4/2}$. Note that this estimate is independent of the fact that $\Delta_{12} = 1$. Therefore, this bound is also valid for the clean fixed point description of the anti–Pfaffian edge theory.

Experimental measurements of g give values $g = 0.34 - 0.42$ [30, 31], depending on the geometry of the quantum point contact. So, the fixed points about which the tunneling term $\mathrm{e}^{i(\phi_3+2\phi_4)}\,\psi$ is irrelevant can be consistent with the measured tunneling exponents. These fixed points are realized only when the short–ranged Coulomb interactions between the Landau levels is included. This is because, if such interactions are ignored, the tunneling

term $e^{i(\phi_3+2\phi_4)}\,\psi$ is always relevant due to the strong Coulomb interaction within the second Landau level.

6.4 Domain of validity of descriptions at weak/strong disorder

Weak disorder

In section 5, we observed that the $\Delta_{12} = 1$ fixed point description of the anti–Pfaffian state is in agreement with experiments only if $\Delta_{34} \approx 3/2$. Since for $\Delta_{34} < 3/2$ the system flows to the $\Delta_{34} = 1$ fixed point [93] we might wonder if treating the W_{34} tunneling term perturbatively is a good description of the anti–Pfaffian edge. To answer this question we first look at the RG equation for W_{34}. To leading order we have

$$\frac{dW_{34}}{dl} = (3 - 2\Delta_{34})W_{34}. \tag{6.26}$$

So, the effective strength of this tunneling term at temperature T is

$$W_{34,\text{eff.}}(T) = W_{34}(\frac{T}{T_0})^{2\Delta_{34}-3} \tag{6.27}$$

where T_0 is the cutoff temperature, and is related to the short–distance cutoff a as

$$T_0 = \frac{v_\sigma}{2\pi a}. \tag{6.28}$$

Here v_σ is the typical velocity of the neutral modes. The reason that we chose the neutral velocity in defining T_0 is that for strong short–ranged Coulomb interactions, tunneling terms only couple the ("almost") neutral modes. This can be seen from the expressions for the

conductivity coefficients such as $g_{V_{34}}$ is Eq. 6.2. We can write $g_{V_{34}}$ as

$$g_{V_{34}} = \frac{\Gamma(\Delta_{34})^2}{\Gamma(2\Delta_{34})} \frac{W_{34}}{\overline{v}_{V_{34}}^2} \left(\frac{T}{T_0}\right)^{2\Delta_{34}-2} \tag{6.29}$$

with the above definition of T_0 with $v_\sigma = \overline{v}_{V_{34}} \approx v^{(0)}$.

When $\Delta_{34} > 3/2$ but is close to $3/2$ and for finite temperatures, the W_{34} tunneling term might still be strong. A rough estimate for the range of validity of perturbation in W_{34} can be obtained if we require the length scale associated with the effective tunneling strength $W_{34,\text{eff}}(T)$ to be larger than the short–distance cutoff a. The length scale associated with $W_{34,\text{eff.}}$ is $\ell_{W_{34}}(T) = v_\sigma^2/W_{34,\text{eff}}(T)$. So the condition for the validity of perturbation theory is

$$a \ll \ell_{W_{34}}(T) = \frac{v_\sigma^2}{W_{34}} \left(\frac{v_\sigma}{2\pi a T}\right)^{2\Delta_{34}-3}. \tag{6.30}$$

Along with Eq. 6.29 we can write this condition as (ignoring numerical factors)

$$g_{V_{34}}^{-1} = \ell_{\text{eq.},V_{34}} \gg L_T. \tag{6.31}$$

where $\ell_{\text{eq.},V_{34}}$ is the charge equilibration length between the modes ϕ_3 and ϕ_4 (See Eq. 6.3), and $L_T = v_\sigma/2\pi T$ is the thermal length. The last inequality illustrates a more practical check for the domain of validity of the incoherent regime.

Strong disorder

Another question is whether $S_{\Delta_{12}=1}$ is a good description of modes ϕ_1 and ϕ_2 at low temperatures, when the tunnelings between these two modes are weak. The tunnelings between the ϕ_1 and ϕ_2 modes require spin–flipping, and so they are expected to be weaker than the corresponding spin–conserving tunnelings. Therefore even for $\Delta_{12} < 3/2$ and

at finite temperatures, the tunneling term might not drive the system all the way to the $\Delta_{12} = 1$ fixed point. In order to address such concerns we first start from the RG equation for W_{12} near the clean fixed point $W_{12} = 1$ (this section follows similar estimations as Ref. [95]). Solving the RG equation, the effective tunneling strength at length scale L is

$$W_{12,\text{eff.}}(L) = W_{12}(\frac{L}{a})^{3-2\Delta_{12}} \tag{6.32}$$

For weak W_{12} and small enough lengths L (high enough temperatures) such that

$$\ell_{W_{12},\text{eff.}}(L) \equiv \frac{v_\sigma^2}{W_{12,\text{eff.}}(L)} \gg a \tag{6.33}$$

we can still treat this tunneling term in perturbation theory. However, for larger length scales the two modes ϕ_1 and ϕ_2 are strongly mixed and the clean fixed point description is no longer valid. We can obtain an estimate for the length scale L_{mix} where such a transition happens by solving

$$\ell_{W_{12},\text{eff.}}(L_{\text{mix}}) = a. \tag{6.34}$$

When the velocity of the two modes ϕ_1 and ϕ_2 are close to each other, the mode $\phi_{\sigma_{12}}$ decouples from other modes (See section 5.2) and we have $\Delta_{12} \approx 1$. So we find

$$L_{\text{mix}} \approx \frac{v_\sigma^2}{W_{12}}. \tag{6.35}$$

This length also serves as the short–distance cutoff for the $\tilde{\phi}_{\sigma_{12}}$ mode (See Appendix B). For length scales larger than L_{mix}, i.e. $L_T > L_{\text{mix}}$, we follow the same line of arguments as before, in order to estimate the domain of validity of perturbation theory in the disordered density–density interactions $S_{\sigma_{12},i}$ in Eq. 5.4a. We find

$$\beta = r, s_2, s_3 : \ell_{\text{eq.},V_{\sigma_{12},\beta}} \equiv g^{-1}_{V_{\sigma_{12},\beta}} \gg L_T = \frac{v_\sigma}{2\pi T} \tag{6.36}$$

or

$$W_{12} \gg \frac{v_{\sigma_{12},\beta}^2 v_\sigma}{v_\beta^2} T. \tag{6.37}$$

As we demonstrated in section 5.2, $v_{\sigma_{12},\beta}$ goes to zero as the Zeeman gap vanishes. Therefore, we expect this inequality to be more valid as we approach the regimes where we expect the thermal conductance $K = 2.5\kappa_0 T$.

Chapter 7

Conclusions

7.1 Results and predictions

In this thesis, we considered equilibration of charge and heat along the edge of the anti–Pfaffian state realized in the first Landau level at $\nu = 5/2$. We assumed that the dominant cause of equilibration is due to short–ranged disorder that allows tunneling of charge between the different edge modes. While tunneling between edge modes belonging to different Landau levels is ignored in our analysis, a strong short–ranged Coulomb interaction is assumed. Under these assumptions, we analyzed the conditions under which the edge modes are not fully in equilibrium.

In the limit of a strong short–ranged Coulomb interaction, equilibration between the total charge mode and the rest of the edge modes is suppressed due to the high velocity of the charge mode relative to the neutral modes. This picture was also considered by Ma and Feldman in [46].

In addition, in the absence of Zeeman splitting between the two modes in the lowest

Landau level, their total spin is independently conserved. Consequently, heat equilibration between the spin mode and other modes is suppressed. For finite Zeeman splitting, electron tunneling between these two modes can drive the edge into the spin–symmetric fixed point where the spin mode is conserved. At finite temperature, the irrelevant interactions present due to the spin asymmetry can bring this spin mode to equilibrium with the other edge modes. For small enough spin asymmetry, this equilibration processes can be slow on the length scales of the system size.

Due to these weak equilibration processes, the thermal conductance is given by $K = K_{\text{total charge mode}} + K_{\text{LLL spin mode}} + K_{\text{other modes}}$, where the nature of the "other modes" depends on the specific fixed point. Based on the quantization of electrical conductance, we infer that the "other modes" should be in equilibrium with each other. So $K = (1 + 1 + |-1.5|)\kappa_0 T = 2.5\kappa_0 T$. This picture relies on the partial equilibration of the fixed points $\Delta_{12} = 1$ and $\Delta_{12} = \Delta_{34} = 1$ studied here. For both of these fixed points, electron tunneling between the spin–up and spin–down modes (*i.e.* $e^{i(\phi_1 - \phi_2)}$) drives the edge into a spin–symmetric fixed point. In contrast, other fixed point theories where such electron tunnelings are weak do not have such an emergent symmetry. However, if the spin asymmetry is small, the spin density $\partial_x \phi_{\sigma_{12}}$ is almost conserved and its equilibration with other modes is suppressed. This situation was discussed in [46] for the $\Delta_{34} = 1$ fixed point.

Therefore, suppressed equilibration of the total charge mode ϕ_ρ and the spin mode $\phi_{\sigma_{12}}$ can be realized for all the four fixed points mentioned in Ssection 5.1. The difference is in the details of the equilibration process, e.g., the parametric dependence of the conductivity coefficients and their temperature dependence. We demonstrated this for the two

fixed points: $\Delta_{12} = 1$ and $\Delta_{12} = \Delta_{34} = 1$. In light of the existing experimental data, these two fixed point theories differ in two important ways:

- About the $\Delta_{12} = \Delta_{34} = 1$ fixed point, the electrical conductance $G = (2.50 \pm 0.01)\sigma_0$ and the thermal conductance $2.49\kappa_0 T < K < 2.75\kappa_0 T$ cannot be observed simultaneously. In contrast, these measurements can be consistent with the $\Delta_{12} = 1$ fixed point when $\Delta_{34} \approx 3/2$.

- About the $\Delta_{12} = \Delta_{34} = 1$ fixed point, the range of parameters required to have $K \approx 2.5\kappa_0 T$ is not compatible with our estimate of these parameters. On the other hand, at the $\Delta_{12} = 1$ fixed point, there exists a realistic regime of parameters (as far as our estimates permit) that results in $K \approx 2.5\kappa_0 T$. This regime is possible only when Δ_{34} is small enough $\Delta_{34} \lesssim 5/3$.

Therefore, the $\Delta_{12} = 1$ fixed point theory of the anti–Pfaffian state better describes the recent transport measurements [37]. About this fixed point the quantum point contact tunnelings exponents depend on the inter–mode Coulomb interactions and are, therefore, non–universal. Nevertheless, the predictions of this fixed point appear to be consistent with the existing experimental quantum point contact measurements. From our analysis of the $\Delta_{12} = 1$ fixed point, we make the following predictions for temperatures not reported in [37]:

- Based on Fig. 6.3, even for the lowest value of $\Delta_{34} = 3/2$, the electrical conductance would deviate from $G = (2.50 \pm 0.01)\kappa_0 T$ for temperatures lower than $T \approx 12mK$.

- Generally at higher temperatures, equilibration between the edge modes is improved.

Therefore, if the state observed in the experiments by Banerjee *et al.* [37] is indeed the anti–Pfaffian state, the thermal Hall conductance would decrease below $K \approx 2.5\kappa_0 T$ at higher temperatures. Using Fig. 6.2, we can estimate how much of a temperature increase is needed in order to observe a measurable decrease from the value $K \approx 2.5\kappa_0 T$ (*i.e.* to $K \approx 2.45\kappa_0 T$): We find the temperature has to increase from $T \approx 18 - 25\ mK$ by at least a factor of ~ 1.5, i.e., to $T \approx 35\ mK$.

7.2 Limitations and outlook

We should point out a limitation in comparing our results with the experiment: in order to calculate the thermal conductance, we assumed the temperature difference between the edge modes is small. Consequently, we considered the effects of bias in temperature and voltage only to linear order. However, in the measurements carried out by Banerjee *et al.*[37], the temperature difference is about the same order as the average temperature.

In addition, including higher order contributions can have interesting consequences. It has been argued that the interplay between the electrical and the thermal transport can generate distinct shot noise profiles along the Hall bar edge [120–123]. These noise profiles fall into three universality classes depending on the chirality structure of the edge modes. Specifically, it has been suggested that the universality class for the noise profile of the anti–Pfaffian state is different from that of the Pfaffian and the PH–Pfaffian states, and so the measurement of shot noise along the edge of the quantum Hall system at filling fraction $\nu = 5/2$ is another tool that can be used to distinguish between the different candidates.

We also point out that our results relied upon the assumption that the contacts are

ideal (Section 4.5). This assumption has not been verified explicitly in the general case where heat transfer is involved or when the edge modes are strongly interacting. And although the assumption of ideal contacts produces results that agree with the measurements of electrical conductance, one should always be wary of its limitations. This is particularly true when it is applied to the problem of thermal transport and as more experimental studies of thermal Hall conductance will be conducted in the near future.

Bibliography

[1]K. v. Klitzing, G. Dorda, and M. Pepper, "New method for high-accuracy determination of the fine-structure constant based on quantized hall resistance", Phys. Rev. Lett. **45**, 494–497 (1980).

[2]D. C. Tsui, H. L. Stormer, and A. C. Gossard, "Two-dimensional magnetotransport in the extreme quantum limit", Phys. Rev. Lett. **48**, 1559–1562 (1982).

[3]B. I. Halperin, "Quantized hall conductance, current-carrying edge states, and the existence of extended states in a two-dimensional disordered potential", Phys. Rev. B **25**, 2185–2190 (1982).

[4]R. B. Laughlin, "Quantized hall conductivity in two dimensions", Phys. Rev. B **23**, 5632–5633 (1981).

[5]X. G. Wen and A. Zee, "Classification of abelian quantum hall states and matrix formulation of topological fluids", Phys. Rev. B **46**, 2290–2301 (1992).

[6]X.-G. Wen, "Topological orders and edge excitations in fractional quantum hall states", Advances in Physics **44**, 405–473 (1995).

[7]X.-G. Wen, "Topological order and edge structure of ν=1/2 quantum hall state", Phys. Rev. Lett. **70**, 355–358 (1993).

[8]R. B. Laughlin, "Anomalous quantum hall effect: an incompressible quantum fluid with fractionally charged excitations", Phys. Rev. Lett. **50**, 1395–1398 (1983).

[9]F. D. M. Haldane, "Fractional quantization of the hall effect: a hierarchy of incompressible quantum fluid states", Phys. Rev. Lett. **51**, 605–608 (1983).

[10]B. I. Halperin, "Statistics of quasiparticles and the hierarchy of fractional quantized hall states", Phys. Rev. Lett. **52**, 1583–1586 (1984).

[11]H. L. Stormer, A. Chang, D. C. Tsui, J. C. M. Hwang, A. C. Gossard, and W. Wiegmann, "Fractional quantization of the hall effect", Phys. Rev. Lett. **50**, 1953–1956 (1983).

[12]A. M. Chang, P. Berglund, D. C. Tsui, H. L. Stormer, and J. C. M. Hwang, "Higher-order states in the multiple-series, fractional, quantum hall effect", Phys. Rev. Lett. **53**, 997–1000 (1984).

[13]J. K. Jain, *Composite fermions* (Cambridge University Press, 2007).

[14]V. J. Goldman, B. Su, and J. K. Jain, "Detection of composite fermions by magnetic focusing", Phys. Rev. Lett. **72**, 2065–2068 (1994).

[15]J. K. Jain, "Composite-fermion approach for the fractional quantum hall effect", Phys. Rev. Lett. **63**, 199–202 (1989).

[16]R. Willett, J. P. Eisenstein, H. L. Störmer, D. C. Tsui, A. C. Gossard, and J. H. English, "Observation of an even-denominator quantum number in the fractional quantum hall effect", Phys. Rev. Lett. **59**, 1776–1779 (1987).

[17]F. D. M. Haldane and E. H. Rezayi, "Spin-singlet wave function for the half-integral quantum hall effect", Phys. Rev. Lett. **60**, 956–959 (1988).

[18]G. Moore and N. Read, "Nonabelions in the fractional quantum hall effect", Nuclear Physics B **360**, 362 –396 (1991).

[19]M. Greiter, X.-G. Wen, and F. Wilczek, "Paired hall state at half filling", Phys. Rev. Lett. **66**, 3205–3208 (1991).

[20]M. Levin, B. I. Halperin, and B. Rosenow, "Particle-hole symmetry and the pfaffian state", Phys. Rev. Lett. **99**, 236806 (2007).

[21]S.-S. Lee, S. Ryu, C. Nayak, and M. P. A. Fisher, "Particle-hole symmetry and the $\nu = \frac{5}{2}$ quantum hall state", Phys. Rev. Lett. **99**, 236807 (2007).

[22]B. J. Overbosch and X.-G. Wen, *Phase transitions on the edge of the $\nu = 5/2$ pfaffian and anti-pfaffian quantum hall state*, 2008.

[23]C. Nayak, S. H. Simon, A. Stern, M. Freedman, and S. Das Sarma, "Non-abelian anyons and topological quantum computation", Rev. Mod. Phys. **80**, 1083–1159 (2008).

[24]D. T. Son, "Is the composite fermion a dirac particle?", Phys. Rev. X **5**, 031027 (2015).

[25]N. Read and D. Green, "Paired states of fermions in two dimensions with breaking of parity and time-reversal symmetries and the fractional quantum hall effect", Phys. Rev. B **61**, 10267–10297 (2000).

[26]A. H. MacDonald, D. Yoshioka, and S. M. Girvin, "Comparison of models for the even-denominator fractional quantum hall effect", Phys. Rev. B **39**, 8044–8047 (1989).

[27]K. Pakrouski, M. R. Peterson, T. Jolicoeur, V. W. Scarola, C. Nayak, and M. Troyer, "Phase diagram of the $\nu = 5/2$ fractional quantum hall effect: effects of landau-level mixing and nonzero width", Phys. Rev. X **5**, 021004 (2015).

[28]E. H. Rezayi, "Landau level mixing and the ground state of the $\nu = 5/2$ quantum hall effect", Phys. Rev. Lett. **119**, 026801 (2017).

[29]E. H. Rezayi and S. H. Simon, "Breaking of particle-hole symmetry by landau level mixing in the $\nu = 5/2$ quantized hall state", Phys. Rev. Lett. **106**, 116801 (2011).

[30]X. Lin, C. Dillard, M. A. Kastner, L. N. Pfeiffer, and K. W. West, "Measurements of quasiparticle tunneling in the $\upsilon = \frac{5}{2}$ fractional quantum hall state", Phys. Rev. B **85**, 165321 (2012).

[31]I. P. Radu, J. B. Miller, C. M. Marcus, M. A. Kastner, L. N. Pfeiffer, and K. W. West, "Quasi-particle properties from tunneling in the v = 5/2 fractional quantum hall state", Science **320**, 899–902 (2008).

[32]X. Lin, R. Du, and X. Xie, "Recent experimental progress of fractional quantum Hall effect: 5/2 filling state and graphene", National Science Review **1**, 564–579 (2014).

[33]G. Yang and D. E. Feldman, "Influence of device geometry on tunneling in the $\nu = \frac{5}{2}$ quantum hall liquid", Phys. Rev. B **88**, 085317 (2013).

[34]G. Yang and D. E. Feldman, "Experimental constraints and a possible quantum hall state at $\nu = 5/2$", Phys. Rev. B **90**, 161306 (2014).

[35]A. Bid, N. Ofek, H. Inoue, M. Heiblum, C. L. Kane, V. Umansky, and D. Mahalu, "Observation of neutral modes in the fractional quantum hall regime", Nature **466**, 585–590 (2010).

[36]Y. Gross, M. Dolev, M. Heiblum, V. Umansky, and D. Mahalu, "Upstream neutral modes in the fractional quantum hall effect regime: heat waves or coherent dipoles", Phys. Rev. Lett. **108**, 226801 (2012).

[37]M. Banerjee, M. Heiblum, V. Umansky, D. E. Feldman, Y. Oreg, and A. Stern, "Observation of half-integer thermal hall conductance", Nature **559**, 205–210 (2018).

[38]C. L. Kane and M. P. A. Fisher, "Quantized thermal transport in the fractional quantum hall effect", Phys. Rev. B **55**, 15832–15837 (1997).

[39]P. T. Zucker and D. E. Feldman, "Stabilization of the particle-hole pfaffian order by landau-level mixing and impurities that break particle-hole symmetry", Phys. Rev. Lett. **117**, 096802 (2016).

[40]C. Wang, A. Vishwanath, and B. I. Halperin, "Topological order from disorder and the quantized hall thermal metal: possible applications to the $\nu = 5/2$ state", Phys. Rev. B **98**, 045112 (2018).

[41]D. F. Mross, Y. Oreg, A. Stern, G. Margalit, and M. Heiblum, "Theory of disorder-induced half-integer thermal hall conductance", Phys. Rev. Lett. **121**, 026801 (2018).

[42]B. Lian and J. Wang, "Theory of the disordered $\nu = \frac{5}{2}$ quantum thermal hall state: emergent symmetry and phase diagram", Phys. Rev. B **97**, 165124 (2018).

[43]S. H. Simon, "Interpretation of thermal conductance of the $\nu = \mathbf{5/2}$ edge", Phys. Rev. B **97**, 121406 (2018).

[44]M. Banerjee, M. Heiblum, A. Rosenblatt, Y. Oreg, D. E. Feldman, A. Stern, and V. Umansky, "Observed quantization of anyonic heat flow", Nature **545**, 75–79 (2017).

[45]D. E. Feldman, "Comment on "interpretation of thermal conductance of the $\nu = 5/2$ edge"", Phys. Rev. B **98**, 167401 (2018).

[46]K. K. W. Ma and D. E. Feldman, "Partial equilibration of integer and fractional edge channels in the thermal quantum hall effect", Phys. Rev. B **99**, 085309 (2019).

[47]S. H. Simon and B. Rosenow, *Partial equilibration of the anti-pfaffian edge due to majorana disorder*, 2019.

[48]E. H. Hall, "On a new action of the magnet on electric currents", American Journal of Mathematics **2**, 287–292 (1879).

[49]P. Drude, "Zur elektronentheorie der metalle", Annalen der Physik **306**, 566–613 (1900).

[50]P. Drude, "Zur elektronentheorie der metalle; ii. teil. galvanomagnetische und thermomagnetische effecte", Annalen der Physik **308**, 369–402 (1900).

[51]N. Ashcroft and N. Mermin, *Solid State Physics* (Saunders College, Philadelphia, 1976).

[52]K. von Klitzing, "The quantized hall effect", Rev. Mod. Phys. **58**, 519–531 (1986).

[53]D. Tong, *Lectures on the quantum hall effect*, 2016.

[54]S. M. G. Richard E. Prange, *The quantum hall effect* (Springer-Verlag New York, 1990).

[55]D. Arovas, J. R. Schrieffer, and F. Wilczek, "Fractional statistics and the quantum hall effect", Phys. Rev. Lett. **53**, 722–723 (1984).

[56]M. Stone, *Quantum hall effect* (World Scientific Publishing Company, Incorporated, 1992).

[57]J. M. Leinaas and J. Myrheim, "On the theory of identical particles", Nuovo Cim. B **37**, 1–23 (1977).

[58]F. Wilczek, "Quantum mechanics of fractional-spin particles", Phys. Rev. Lett. **49**, 957–959 (1982).

[59]S. M. Girvin, "Particle-hole symmetry in the anomalous quantum hall effect", Phys. Rev. B **29**, 6012–6014 (1984).

[60]E. Rezayi and N. Read, "Fermi-liquid-like state in a half-filled landau level", Phys. Rev. Lett. **72**, 900–903 (1994).

[61]R. L. Willett, R. R. Ruel, K. W. West, and L. N. Pfeiffer, "Experimental demonstration of a fermi surface at one-half filling of the lowest landau level", Phys. Rev. Lett. **71**, 3846–3849 (1993).

[62]R. L. Willett, K. W. West, and L. N. Pfeiffer, "Apparent inconsistency of observed composite fermion geometric resonances and measured effective mass", Phys. Rev. Lett. **75**, 2988–2991 (1995).

[63]N Read, "Theory of the half-filled landau level", Semiconductor Science and Technology **9**, 1859–1864 (1994).

[64]B. I. Halperin, P. A. Lee, and N. Read, "Theory of the half-filled landau level", Phys. Rev. B **47**, 7312–7343 (1993).

[65]V. Pasquier and F. Haldane, "A dipole interpretation of the $\nu = 1/2$ state", Nuclear Physics B **516**, 719–726 (1998).

[66]M. Sato and Y. Ando, "Topological superconductors: a review", Reports on Progress in Physics **80**, 076501 (2017).

[67]S. M. Girvin and T. Jach, "Formalism for the quantum hall effect: hilbert space of analytic functions", Phys. Rev. B **29**, 5617–5625 (1984).

[68]R. H. Morf, "Transition from quantum hall to compressible states in the second landau level: new light on the $\nu = 5/2$ enigma", Phys. Rev. Lett. **80**, 1505–1508 (1998).

[69]M. P. Zaletel, R. S. K. Mong, F. Pollmann, and E. H. Rezayi, "Infinite density matrix renormalization group for multicomponent quantum hall systems", Phys. Rev. B **91**, 045115 (2015).

[70]M. Stone, "Edge waves in the quantum hall effect", Annals of Physics **207**, 38–52 (1991).

[71]X. G. Wen, "Chiral luttinger liquid and the edge excitations in the fractional quantum hall states", Phys. Rev. B **41**, 12838–12844 (1990).

[72]D.-H. Lee and X.-G. Wen, "Edge excitations in the fractional-quantum-hall liquids", Phys. Rev. Lett. **66**, 1765–1768 (1991).

[73]X. G. Wen, "Electrodynamical properties of gapless edge excitations in the fractional quantum hall states", Phys. Rev. Lett. **64**, 2206–2209 (1990).

[74]X. G. Wen, "Gapless boundary excitations in the quantum hall states and in the chiral spin states", Phys. Rev. B **43**, 11025–11036 (1991).

[75]N. Nagaosa, *Quantum field theory in strongly correlated electronic systems* (Springer-Verlag Berlin Heidelberg, 1999).

[76]J. von Delft and H. Schoeller, "Bosonization for beginners - refermionization for experts", Annalen der Physik **7**, 10.1002/(sici)1521-3889(199811)7:4<225::aid-andp225>3.0.co;2-l (1998).

[77]T. Giamarchi, *Quantum physics in one dimension* (Oxford, 2004).

[78]E. Miranda, "Introduction to bosonization", Brazilian Journal of Physics **33**, 10.1590/S0103-97332003000100002 (2003).

[79]E. Fradkin, *Field theories of condensed matter physics* (Cambridge University Press, 2013).

[80]R. Floreanini and R. Jackiw, "Self-dual fields as charge-density solitons", Phys. Rev. Lett. **59**, 1873–1876 (1987).

[81]L. Faddeev and R. Jackiw, "Hamiltonian reduction of unconstrained and constrained systems", Phys. Rev. Lett. **60**, 1692–1694 (1988).

[82]J. Sonnenschein, "Chiral bosons", Nuclear Physics B **309**, 752–770 (1988).

[83]N. Read, "Excitation structure of the hierarchy scheme in the fractional quantum hall effect", Phys. Rev. Lett. **65**, 1502–1505 (1990).

[84] And N. Read, "Edge excitations of paired fractional quantum hall states", Phys. Rev. B **53**, 13559–13582 (1996).

[85]C. W. J. Beenakker, "Edge channels for the fractional quantum hall effect", Phys. Rev. Lett. **64**, 216–219 (1990).

[86]C. d. C. Chamon and X. G. Wen, "Sharp and smooth boundaries of quantum hall liquids", Phys. Rev. B **49**, 8227–8241 (1994).

[87]Y. Meir, "Composite edge states in the ν=2/3 fractional quantum hall regime", Phys. Rev. Lett. **72**, 2624–2627 (1994).

[88]M. D. Johnson and A. H. MacDonald, "Composite edges in the ν=2/3 fractional quantum hall effect", Phys. Rev. Lett. **67**, 2060–2063 (1991).

[89]X. Wan, K. Yang, and E. H. Rezayi, "Reconstruction of fractional quantum hall edges", Phys. Rev. Lett. **88**, 056802 (2002).

[90]X. Wan, E. H. Rezayi, and K. Yang, "Edge reconstruction in the fractional quantum hall regime", Phys. Rev. B **68**, 125307 (2003).

[91]K. Yang, "Field theoretical description of quantum hall edge reconstruction", Phys. Rev. Lett. **91**, 036802 (2003).

[92]C. L. Kane and M. P. A. Fisher, "Impurity scattering and transport of fractional quantum hall edge states", Phys. Rev. B **51**, 13449–13466 (1995).

[93]C. L. Kane, M. P. A. Fisher, and J. Polchinski, "Randomness at the edge: theory of quantum hall transport at filling ν=2/3", Phys. Rev. Lett. **72**, 4129–4132 (1994).

[94]R. Sabo, I. Gurman, A. Rosenblatt, F. Lafont, D. Banitt, J. Park, M. Heiblum, Y. Gefen, V. Umansky, and D. Mahalu, "Edge reconstruction in fractional quantum hall states", Nature Physics **13**, 13559–13582 (2017).

[95]I. Protopopov, Y. Gefen, and A. Mirlin, "Transport in a disordered $\nu = 5/2$ fractional quantum hall junction", Annals of Physics **385**, 287 –327 (2017).

[96]J. Naud, L. P. Pryadko, and S. Sondhi, "Quantum hall bilayers and the chiral sine-gordon equation", Nuclear Physics B **565**, 572 –610 (2000).

[97]C. de C. Chamon and E. Fradkin, "Distinct universal conductances in tunneling to quantum hall states: the role of contacts", Phys. Rev. B **56**, 2012–2025 (1997).

[98]A. Würtz, R. Wildfeuer, A. Lorke, E. V. Deviatov, and V. T. Dolgopolov, "Separately contacted edge states: a spectroscopic tool for the investigation of the quantum hall effect", Phys. Rev. B **65**, 075303 (2002).

[99]B. W. Alphenaar, P. L. McEuen, R. G. Wheeler, and R. N. Sacks, "Selective equilibration among the current-carrying states in the quantum hall regime", Phys. Rev. Lett. **64**, 677–680 (1990).

[100]G. Müller, D. Weiss, A. V. Khaetskii, K. von Klitzing, S. Koch, H. Nickel, W. Schlapp, and R. Lösch, "Equilibration length of electrons in spin-polarized edge channels", Phys. Rev. B **45**, 3932–3935 (1992).

[101]C. Nosiglia, J. Park, B. Rosenow, and Y. Gefen, "Incoherent transport on the $\nu = 2/3$ quantum hall edge", Phys. Rev. B **98**, 115408 (2018).

[102]X.-G. Wen, "Edge transport properties of the fractional quantum hall states and weak-impurity scattering of a one-dimensional charge-density wave", Phys. Rev. B **44**, 5708–5719 (1991).

[103]C. L. Kane and M. P. A. Fisher, "Contacts and edge-state equilibration in the fractional quantum hall effect", Phys. Rev. B **52**, 17393–17405 (1995).

[104]C. L. Kane and M. P. A. Fisher, "Thermal transport in a luttinger liquid", Phys. Rev. Lett. **76**, 3192–3195 (1996).

[105]G. D. Mahan, *Many-particle physics*, Vol. 53 (Springer US, 1990), pp. 13559–13582.

[106]D. L. Maslov and M. Stone, "Landauer conductance of luttinger liquids with leads", Phys. Rev. B **52**, R5539–R5542 (1995).

[107]J. M. Luttinger, "Theory of thermal transport coefficients", Phys. Rev. **135**, A1505–A1514 (1964).

[108]B. Deo and S. N. Behera, "Calculation of thermal conductivity by the kubo formula", Phys. Rev. **141**, 738–741 (1966).

[109]A. Kamenev, "Many-body theory of non-equilibrium systems", Phys. Rev. B **53**, 13559–13582 (2004).

[110]A. Kamenev, *Field theory of non-equilibrium systems*, Vol. 53 (Cambridge University Press, 2011), pp. 13559–13582.

[111]T. Kita, "Introduction to nonequilibrium statistical mechanics with quantum field theory", Progress of Theoretical Physics **123**, 581–658 (2010).

[112]J. Rammer, *Quantum field theory of non-equilibrium states*, Vol. 53 (Cambridge University Press, 2007), pp. 13559–13582.

[113]E. Bocquillon, V. Freulon, J.-. M. Berroir, P. Degiovanni, B. Plaçais, A. Cavanna, Y. Jin, and G. Fève, "Separation of neutral and charge modes in one-dimensional chiral edge channels", Nature Communications **4**, 1839 (2013).

[114]N. Kumada, H. Kamata, and T. Fujisawa, "Edge magnetoplasmon transport in gated and ungated quantum hall systems", Phys. Rev. B **84**, 045314 (2011).

[115]S. H. Simon, "Reply to "comment on 'interpretation of thermal conductance of the $\nu = 5/2$ edge' "", Phys. Rev. B **98**, 167402 (2018).

[116]M. Banerjee, M. Heiblum, A. Rosenblatt, Y. Oreg, D. E. Feldman, A. Stern, and V. Umansky, "Observed quantization of anyonic heat flow", Nature **545**, 75 EP – (2017).

[117]E. V. Devyatov, "Edge states in the regimes of integer and fractional quantum hall effects", Physics-Uspekhi **50**, 197–218 (2007).

[118]C. d. C. Chamon and X. G. Wen, "Sharp and smooth boundaries of quantum hall liquids", Phys. Rev. B **49**, 8227–8241 (1994).

[119]I. L. Aleiner and L. I. Glazman, "Novel edge excitations of two-dimensional electron liquid in a magnetic field", Phys. Rev. Lett. **72**, 2935–2938 (1994).

[120]C. Spånslätt, J. Park, Y. Gefen, and A. D. Mirlin, "Topological classification of shot noise on fractional quantum hall edges", Phys. Rev. Lett. **123**, 137701 (2019).

[121]J. Park, A. D. Mirlin, B. Rosenow, and Y. Gefen, "Noise on complex quantum hall edges: chiral anomaly and heat diffusion", Phys. Rev. B **99**, 161302 (2019).

[122]C. Spånslätt, J. Park, Y. Gefen, and A. D. Mirlin, "Conductance plateaus and shot noise in fractional quantum hall point contacts", Phys. Rev. B **101**, 075308 (2020).

[123]J. Park, C. Spånslätt, Y. Gefen, and A. D. Mirlin, *Noise on the non-abelian $\nu = 5/2$ fractional quantum hall edge*, 2020.

[124]A. Cappelli, M. Huerta, and G. R. Zemba, "Thermal transport in chiral conformal theories and hierarchical quantum Hall states", Nuclear Physics B **636**, 568–582 (2002).

[125]R. H. Morf, "Transition from quantum hall to compressible states in the second landau level: new light on the $\nu = 5/2$ enigma", Phys. Rev. Lett. **80**, 1505–1508 (1998).

[126]H. Stormer, "Two-dimensional electron correlation in high magnetic fields", Physica B: Condensed Matter **177**, 401–408 (1992).

[127]Y. W. Suen, L. W. Engel, M. B. Santos, M. Shayegan, and D. C. Tsui, "Observation of a ν=1/2 fractional quantum hall state in a double-layer electron system", Phys. Rev. Lett. **68**, 1379–1382 (1992).

Appendix A

Correlation function of chiral bosons

As we demonstrated in section 3.1 the chiral bosonic fields are related to the edge density as

$$\rho(x) = \frac{1}{2\pi}\partial_x \phi(x). \tag{A.1}$$

The inverse relation is (L is the length of the edge and a is the short-distance cutoff)

$$\phi(x) = \frac{2\pi\sqrt{\nu}}{\sqrt{L}} \sum_{k>0} e^{-ak/2} \frac{1}{ik} \{e^{ikx}\rho_k - e^{-ikx}\rho_{-k}\}. \tag{A.2}$$

We can also expand $\phi(x)$ in terms of harmonic oscillator bosonic operators b_k and $b_k^\dagger$ with commutation relations

$$[b_k, b_{k'}^\dagger] = \delta_{kk'}. \tag{A.3}$$

To satisfy the correct commutation relation we need separate definitions for the right-moving fields ϕ_R ($\eta = 1$) and left-moving fields ϕ_L ($\eta = -1$)

$$\phi_R(x) = -i\sqrt{\nu}\sum_{k>0}\sqrt{\frac{2\pi}{Lk}}e^{-ak/2}\left[e^{ikx}b_k - e^{-ikx}b_k^\dagger\right] \tag{A.4}$$

$$\phi_L(x) = -i\sqrt{\nu}\sum_{k>0}\sqrt{\frac{2\pi}{Lk}}e^{-ak/2}\left[e^{ikx}b_{-k}^\dagger - e^{-ikx}b_{-k}\right]. \tag{A.5}$$

A.1 Single edge mode

The Hamiltonian of the free bosonic field Eq. 3.18 in terms of $b_k, b_k^\dagger$ is

$$H = \sum_{\eta k>0}\hbar\eta v k(b_k^\dagger b_k + \frac{1}{2}). \tag{A.6}$$

So the ground state $|GS\rangle$ is determined by

$$\forall k:\ b_k|GS\rangle = 0. \tag{A.7}$$

To find the equal time Green function we first write

$$\left\langle\phi(x)\phi(x')\right\rangle = \left\langle\phi^+(x)\phi^-(x')\right\rangle = \left\langle[\phi^+(x),\phi^-(x')]\right\rangle = [\phi^+(x),\phi^-(x')] \tag{A.8}$$

where $\phi^+/\phi^-(x)$ is the creation/annihilation part of $\phi(x)$. The last equality follows since $[\phi^+(x),\phi^-(x')]$ is a just a number. Using A.2 we find ($k = 2n\pi/L$ with $n \in \mathbb{Z}$)

$$\begin{aligned}\left\langle\phi(x)\phi(x')\right\rangle =& \frac{2k\nu}{L}\sum_{k>0}\frac{1}{k}\,\mathrm{e}^{p(-i\eta(x-x')-a)}\\ =& \nu\sum_{n=1}^{\infty}\frac{1}{n}(\mathrm{e}^{-\frac{2\pi}{L}(a+i\eta(x-x'))})^n\\ =& -\nu\ln(1-e^{-\frac{2\pi}{L}(a+i\eta(x-x'))})\\ =& -\nu\ln(\frac{2\pi}{L}(\alpha+i\eta(x-x'))).\end{aligned} \tag{A.9}$$

The last equality is valid in the $L \to \infty$ limit. Using this, it is easy to find the Green function for non-equal times. Since the field $\phi(x,t)$ is chiral we have

$$\phi(x,t) = \phi(x - \eta v t). \tag{A.10}$$

Therefore

$$\langle \phi(x,t)\phi(0,0)\rangle = -\nu \ln\left[\frac{2\pi}{L}\left(a - i(vt - \eta x)\right)\right]. \tag{A.11}$$

We can also find the correlation function at finite temperature ($\beta = 1/k_B T$. See [76])

$$\langle \phi(x,t)\phi(0,0)\rangle = -\nu \ln\Big[\frac{2\beta v}{L}\sin\frac{\pi}{\beta v}(\alpha + i(vt \mp x))\Big]. \tag{A.12}$$

We can also write down the time-ordered correlation function

$$\begin{aligned}\langle T\phi(x,t)\phi(0,0)\rangle &= \theta(t)\,\langle \phi(x,t)\phi(0,0)\rangle + \theta(-t)\,\langle \phi(0,0)\phi(x,t)\rangle \\ &= -\nu \ln\Big[\frac{2\beta v}{L}\sin\frac{\pi}{\beta v}(\alpha + i(vt \mp x))\Big].\end{aligned} \tag{A.13}$$

and the Keldysh correlation function ($\bar{T}$ denotes anti-time-ordering. See Ref. [78, 110–112])

$$\begin{aligned}\left\langle T_C \phi(x,t,s)\phi(0,0,s')\right\rangle &= \begin{pmatrix} \langle T\phi(x,t)\phi(0,0)\rangle & \langle \phi(0,0)\phi(x,t)\rangle \\ \langle \phi(x,t)\phi(0,0)\rangle & \left\langle \overline{T}\phi(x,t)\phi(0,0)\right\rangle \end{pmatrix} \\ &= -\nu \ln\Big[\frac{2\beta v}{L}\sin\frac{\pi}{\beta v}(\alpha + i\chi_{ss'}(t)(vt - \eta x))\Big] \\ \chi_{ss'} &= \begin{pmatrix} \mathrm{sgn}(t) & -1 \\ 1 & -\mathrm{sgn}(t) \end{pmatrix}.\end{aligned} \tag{A.14}$$

$s = \pm$ denotes the forward/backward direction on the Keldysh contour.

A.2 Several edge modes

When there are several edge modes interacting via the short-ranged Coulomb interaction as 3.23, we can just as easily find the correlation function. We first transform to the diagonalized fields

$$\phi_i = \sum_\alpha \Lambda_{i\alpha} \tilde{\phi}_\alpha. \tag{A.15}$$

So

$$\begin{aligned}\langle \phi_i(x,t)\phi_j(0,0)\rangle &= \sum_{\alpha\beta} \Lambda_{i\alpha}\Lambda_{j\beta} \left\langle \tilde{\phi}_\alpha(x,t)\tilde{\phi}_\beta(0,0)\right\rangle \\ &= -\sum_{\alpha\beta} \Lambda_{i\alpha}\Lambda_{j\alpha} \ln\Big[\frac{2\beta v_\beta}{L}\sin\frac{\pi}{\beta v_\alpha}(a + i(v_\alpha t - \eta_\alpha x))\Big].\end{aligned} \tag{A.16}$$

Vertex operators

We are looking to find the correlation function of vertex operators

$$\left\langle \mathrm{e}^{i\sum_i m_i\phi_i(x,t)}\, \mathrm{e}^{i\sum_i m_i'\phi_i(0,0)}\right\rangle \tag{A.17}$$

when the field ϕ_i are interacting via the short-ranged Coulomb interaction. First note that for bosonic operators B_1 and B_2 with a quadratic Hamiltonian we have

$$\begin{aligned}\left\langle \mathrm{e}^{B_1}\,\mathrm{e}^{B_2}\right\rangle &= \left\langle \mathrm{e}^{B_1+B_2}\right\rangle \mathrm{e}^{\frac{1}{2}[B_1,B_2]} \\ &= \mathrm{e}^{\frac{1}{2}\left\langle B_1^2+B_2^2+B_1B_2+B_2B_1\right\rangle}\, \mathrm{e}^{\frac{1}{2}[B_1,B_2]} \\ &= \mathrm{e}^{\frac{1}{2}\left\langle B_1^2+B_2^2+2B_1B_2\right\rangle}.\end{aligned} \tag{A.18}$$

The first equality is the result of the Baker–Campbell–Hausdorff formula and the second equality follows if the Hamiltonian is quadratic. Therefore

$$\begin{aligned}\left\langle \mathrm{e}^{i\sum_i m_i\phi_i(x,t)}\,\mathrm{e}^{-i\sum_i m_i'\phi_i(0,0)}\right\rangle &= \exp\Bigg[-\frac{1}{2}\sum_{i,j,\alpha} m_i m_j \Lambda_{i\alpha}\Lambda_{j\alpha}\left\langle\phi_\alpha(x,t)\phi_\alpha(x,t)\right\rangle \\ &\qquad -\frac{1}{2}\sum_{i,j,\alpha} m_i' m_j' \Lambda_{i\alpha}\Lambda_{j\alpha}\left\langle\phi_\alpha(0,0)\phi_\alpha(0,0)\right\rangle \\ &\qquad +\sum_{i,j,\alpha} m_i m_j' \Lambda_{i\alpha}\Lambda_{j\alpha}\left\langle\phi_\alpha(x,t)\phi_\alpha(0,0)\right\rangle\Bigg] \\ &= \prod_\alpha \frac{\left(\frac{2\beta v_\alpha}{L}\sin\frac{\pi}{\beta v_\alpha}a\right)^{\frac{1}{2}\sum_{i,j,\alpha}(m_i m_j + m_i' m_j')\Lambda_{i\alpha}\Lambda_{j\alpha}}}{\left(\frac{2\beta v_\alpha}{L}\sin\frac{\pi}{\beta v_\alpha}(a+i(\tilde{v}_\alpha t-\eta_\alpha x))\right)^{\sum_{i,j} m_i m_j'\Lambda_{i\alpha}\Lambda_{j\alpha}}}.\end{aligned} \tag{A.19}$$

Using this, we find the scaling dimension of the vertex operator $\mathcal{O}(x,t) = \mathrm{e}^{i\sum_i m_i\phi_i(x,t)}$. At zero temperature $T = 0$

$$\left\langle \mathcal{O}(x,t)\mathcal{O}^\dagger(x,t=0)\right\rangle = \prod_\alpha \left(\frac{a}{iv_\alpha t}\right)^{\sum_{i,j} m_i m_j \Lambda_{i\alpha}\Lambda_{j\alpha}} \sim t^{-2\Delta_\mathcal{O}}, \tag{A.20}$$

with scaling dimension

$$\Delta_\mathcal{O} = \frac{1}{2}\sum_{i,j,\alpha} m_i m_j \Lambda_{i\alpha}\Lambda_{j\alpha}. \tag{A.21}$$

Appendix B

Effective theory of $\Delta_{12} = 1$ fixed point

After changing variables to the charge mode $\phi_{\rho_{12}} = \frac{1}{\sqrt{2}}(\phi_1 + \phi_2)$ and the neutral mode $\phi_{\sigma_{12}} = \frac{1}{\sqrt{2}}(\phi_1 - \phi_2)$ [92] we have (we will not write expressions already defined in 5.1)

$$S = \sum_{i=\sigma_{12},\rho_{12},3,4} S_i + \sum_{i,j\in\{\sigma_{12},\rho_{12},3,4\},i\neq j} S_{ij} + S_\psi + S_{\text{tunneling},34\psi} \tag{B.1a}$$

$$S_{\rho_{12}} = -\frac{1}{4\pi}\int_{t,x} [\partial_x\phi_{\rho_{12}}(\partial_t\phi_{\rho_{12}} + v_{\rho_{12}}\partial_x\phi_{\rho_{12}}] \tag{B.1b}$$

$$S_{\sigma_{12}} = -\frac{1}{4\pi}\int_{t,x} [\partial_x\phi_{\sigma_{12}}(\partial_t\phi_{\sigma_{12}} + v_{\sigma_{12}}\partial_x\phi_{\sigma_{12}}] + \int_{t,x}\left[\xi_{12}(x)\,\mathrm{e}^{i\sqrt{2}\phi_{\sigma_{12}}} + \text{h.c.}\right] \tag{B.1c}$$

$$S_{\rho_{12},\sigma_{12}} = -\frac{2v_{\rho_{12},\sigma_{12}}}{4\pi}\int_{t,x} \partial_x\phi_{\rho_{12}}\partial_x\phi_{\sigma_{12}} \tag{B.1d}$$

$$i = 3,4 : S_{\rho_{12},i} = -\frac{2v_{\rho_{12},i}}{4\pi}\int_{t,x} \partial_x\phi_{\rho_{12}}\partial_x\phi_i \tag{B.1e}$$

$$i = 3,4 : S_{\sigma_{12},i} = -\frac{2v_{\sigma_{12},i}}{4\pi}\int_{t,x} \partial_x\phi_{\sigma_{12}}\partial_x\phi_i. \tag{B.1f}$$

When $v_{\rho_{12},\sigma_{12}} = v_{\sigma_{12},3} = v_{\sigma_{12},4} = W_{34} = 0$, $S_{\sigma_{12}}$ has an $SO(3)$ symmetry [92, 95, 96]. To see this, define current operators (a is the short-distance cutoff)

$$J^x = \frac{1}{2\pi a}\cos(\sqrt{2}\phi_{\sigma_{12}}) \tag{B.2a}$$

$$J^y = \frac{1}{2\pi a}\sin(\sqrt{2}\phi_{\sigma_{12}}) \tag{B.2b}$$

$$J^z = \frac{1}{2\pi\sqrt{2}}\partial_x\phi_{\sigma_{12}}. \tag{B.2c}$$

These operators satisfy a $\mathfrak{su}(2)_1$ similar to disordered fixed point of QHE at filling fraction $\nu = 2/3$ presented in Eq. 3.58. Similar to section 3.4.3 we eliminate the tunneling term from $S_{\sigma_{12}}$. We express the currents $\tilde{J}^a$ in terms of a new bosonic field $\tilde{\phi}_{\sigma_{12}}$, similar to B.2, and write the Hamiltonian $H_{\sigma_{12}}$ as

$$H_{\sigma_{12}} = \int \mathrm{d}x \frac{v_{\sigma_{12}}}{4\pi}(\partial_x\tilde{\phi})^2. \tag{B.3}$$

The resulting action is

$$S = \sum_{i=\sigma_{12},\rho_{12},3,4} S_i + \sum_{i,j\in\{\sigma_{12},\rho_{12},3,4\},i\neq j} S_{ij} + S_\psi + S_{\text{tunneling},34\psi} \tag{B.4a}$$

$$S_{\sigma_{12}} = -\frac{1}{4\pi}\int_{t,x}\left[\partial_x\tilde{\phi}_{\sigma_{12}}(\partial_t\tilde{\phi}_{\sigma_{12}} + v_{\sigma_{12}}\partial_x\tilde{\phi}_{\sigma_{12}}\right] \tag{B.4b}$$

$$S_{\sigma_{12},i} = -\frac{2v_{\sigma_{12},i}}{4\pi}\int_{t,x}\partial_x\phi_i\left(\frac{\sqrt{2}}{a}O^{zx}\cos(\sqrt{2}\tilde{\phi}_{\sigma_{12}}) + \frac{\sqrt{2}}{a}O^{zy}\sin(\sqrt{2}\tilde{\phi}_{\sigma_{12}}) + O^{zz}\partial_x\tilde{\phi}_{\sigma_{12}}\right), \tag{B.4c}$$

for $i = \rho_{12}, 3, 4$. Here, we also used the following transformation in order to eliminate the terms proportional to $h^z(x)$

$$\phi_i(x,t) \to \phi_i(x,t) + 2\sqrt{2}\pi\frac{v_{\sigma_{12},i}}{v_i}\int_{-\infty}^{x}\mathrm{d}x\ h^z(x) \tag{B.5}$$

for $i = \rho_{12}, 3, 4$.

Appendix C

Derivation of conductivity coefficients

C.1 Electrical conductivity coefficient

We want to compute tunneling between a set of chiral modes described by the free field Hamiltonian $H_F = \sum_\alpha H_\alpha$, due to interactions of the form

$$V = \int \mathrm{d}x \; \xi(x) \prod_\alpha X_\alpha(x) + \text{h.c.} \tag{C.1}$$

in the presence of a chemical potential bias

$$H_\mu = -\int \mathrm{d}x \; \sum_\alpha \mu_\alpha n_\alpha(x), \qquad n_\alpha = \frac{1}{2\pi}\partial_x \phi_\alpha. \tag{C.2}$$

The bosonic fields ϕ_α satisfy the commutation relations $[\phi_\alpha(x), \phi_\beta(x'')] = \delta_{\alpha\beta}\pi i \frac{\eta_\alpha}{k_\alpha}\,\mathrm{sign}(x - x')$. Chiral fermions will be described by chiral bosons. Here X_α is only a function of ϕ_α and $\xi(x)$ is Gaussian-correlated disorder satisfying $\overline{\xi(x)\xi(x')} = W_V \delta(x - x')$. The continuity

equation for each number current I_α is

$$-\partial_x I_\alpha(x,t) = \partial_t n_\alpha(x,t) = i[H, n_\alpha(x)](t). \tag{C.3}$$

For the Hamiltonian $H = H_F + H_\mu + V$

$$-\partial_x I_\alpha(t) = -\eta_\alpha v_\alpha \partial_x n_\alpha(x,t) + i \int \mathrm{d}x'\ \xi(x')[X_\alpha(x'), n_\alpha(x)] \prod_{\beta\neq\alpha} X_\alpha(x') + \text{h.c.}\ . \tag{C.4}$$

As we discussed in section 4.3.1, this equation should be understood as the continuous limit of a series of point contact tunnelings [97, 103]. Different tunnelings are assumed incoherent so that each mode comes to local equilibrium between consecutive tunnelings. It follows that $n_\alpha = \frac{1}{2\pi}\frac{1}{k_\alpha v_\alpha}\mu_\alpha$ can be assume constant and so we drop the $\partial_x n_\alpha$ term.

We calculate the expectation value of $\partial_x I_\alpha$ using the Keldysh technique

$$\partial_x \langle I_\alpha(x,t)\rangle = \frac{1}{2}\sum_{\sigma_{12}} \left\langle T_C\ \partial_x I_{i,H_0}(x,t,s)\, \mathrm{e}^{i\sum_{s'} s' \int \mathrm{d}t' V(t',s')_{H_0}} \right\rangle, \tag{C.5}$$

$$H_0 \equiv H_F + H_\mu, \tag{C.6}$$

where T_C indicates "time" ordering along the Keldysh contour. Expanding the exponential to first order in ξ and taking disorder average

$$\begin{aligned}\partial_x \langle I_\alpha(x,t)\rangle &= \frac{i}{2}\sum_{ss'} s' \int \mathrm{d}t' \left\langle T_C\ \partial_x I_\alpha(x,t,s)_{H_F} V(t',s')_{H_0}\right\rangle \\ &= \frac{1}{2} W_V \sum_{ss'} s' \int \mathrm{d}x' \int \mathrm{d}t' \left\langle T_C\ [X_\alpha(x'), n_\alpha(x)](t,s) X_\alpha^\dagger(x',t',s')\right\rangle \\ &\qquad \times \prod_{\beta\neq\alpha} \left\langle T_C\ X_\beta(x',t,s) X_\beta^\dagger(x',t',s')\right\rangle + \text{h.c.}\ .\end{aligned} \tag{C.7}$$

We look at two cases separately.

C.1.1 Random tunneling

Operators that tunnel electrons/quasiparticles between edge channels of a fractional quantum Hall state have the form $\mathrm{e}^{i\sum_i m_i\phi_i}$, where ϕ_i with Latin index represents a chiral boson mode carrying charge ν_i and chirality η_i with commutation relation $[\phi_i(x),\phi_j(x')] = \delta_{ij}\pi i\eta_i\nu_i\,\mathrm{sign}(x-x')$. This term also has a coefficient $\frac{1}{(2\pi a)^{N_e}}$, with a the UV distance cut-off and N_e the number of electrons transferred, which we will retain at the end of our calculations. Here conservation of electric charge implies $\sum_i \eta_i m_i \nu_i = 0$. In case there are Coulomb interactions between these fractional modes we use a transformation $\phi_i = \Lambda_{i\alpha}\phi_\alpha$ to diagonalize the quadratic part of the action. In terms of the diagonal basis ϕ_α (which are indexed by Greek letters), the electron/quasi-particle tunneling operator is $\mathrm{e}^{i\sum_\alpha \lambda_\alpha\phi_\alpha} = \prod_\alpha X_\alpha$ with $X_\alpha \equiv \mathrm{e}^{i\lambda_\alpha\phi_\alpha}$ and $\lambda_\alpha = \sum_i m_i\Lambda_{i\alpha}$.

From the Heisenberg equation of motion for ϕ_α, evolved with H_0,

$$\partial_t\phi_\alpha = -\eta_\alpha v_\alpha\partial_x\phi_\alpha + \frac{\eta_\alpha}{k_\alpha}\mu_\alpha \tag{C.8}$$

$$\to X_\alpha(x,t)_{H_0} = \mathrm{e}^{i\eta_\alpha\lambda_\alpha\mu_\alpha t/k_\alpha}\,X_\alpha(x,t)_{H_F}. \tag{C.9}$$

Also,

$$[X_\alpha(x'),n_\alpha(x)] = \frac{\eta_\alpha\lambda_\alpha}{k_\alpha}X_\alpha(x)\delta(x-x'). \tag{C.10}$$

So (from now all the time dependencies are with respect to H_F)

$$\partial_x\langle I_\alpha(x,t)\rangle = \frac{1}{2}\frac{\eta_\alpha\lambda_\alpha}{k_\alpha}W_V\sum_{ss'}s'\int \mathrm{d}t'\prod_\beta \mathrm{e}^{i\eta_\beta\lambda_\beta\mu_\beta(t-t')/k_\beta}\left\langle T_C X_\beta(x,t,s)X_\beta^\dagger(x,t',s')\right\rangle - \text{h.c.} \tag{C.11}$$

$$= i\frac{\eta_\alpha\lambda_\alpha}{k_\alpha}W_V\sum_{ss'}s'\int \mathrm{d}t'\sin\left(\Omega(t-t')\right)\prod_\beta\left\langle T_C X_\beta(t,s)X_\beta^\dagger(t',s')\right\rangle$$

where $\mu_\beta = 0$ if β is a Majorana mode and we defined $\Omega \equiv \sum_\beta \frac{\eta_\beta \lambda_\beta}{k_\beta} \mu_\beta$. The Keldysh Green function of a chiral operator X_α is

$$\left\langle T_C X_\alpha(x,t,s) X_\alpha^\dagger(0,t',s') \right\rangle = \left(\frac{A_\alpha T_\alpha}{v_\alpha \sin \frac{\pi T_\alpha}{v_\alpha}(a + i\chi_{ss'}(t-t')(v_\alpha(t-t') - \eta_\alpha x)} \right)^{2d_\alpha} \tag{C.12}$$

where v_α,T_α and d_α are the velocity, temperature, and scaling dimension of operator X_α. A_α is a constant ($A_\alpha = 2$ for Majorana fermions, $A_\alpha = \pi a$ for a vertex operator, and $A_\alpha = \frac{\pi}{k_\alpha}$ for a boson density operator $\partial_x \phi_\alpha$) and

$$\chi_{ss'}(t) = \begin{pmatrix} \operatorname{sgn}(t) & -1 \\ 1 & -\operatorname{sgn}(t) \end{pmatrix}. \tag{C.13}$$

Substituting in the appropriate Green functions, assuming all modes are at the same temperature,

$$\begin{aligned} \partial_x \langle I_\alpha \rangle &= i \frac{\eta_\alpha \lambda_\alpha}{k_\alpha} . W_V . \prod_\beta (\frac{A_\beta}{v_\beta})^{2d_\beta} . T^{2\Delta} \sum_{ss'} s' \int \mathrm{d}t' \frac{\sin(\Omega(t-t'))}{\prod_\beta \sin\left(\frac{\pi T_\beta}{v_\beta}(a + i\chi_{ss'} v_\beta (t-t'))\right)^{2d_\beta}} \\ &= i \frac{\eta_\alpha \lambda_\alpha}{k_\alpha} . W_V . \prod_\beta (\frac{A_\beta}{v_\beta})^{2d_\beta} . T^{2\Delta} \sum_{s} s \int \mathrm{d}t' \frac{\sin(\Omega t')}{\prod_\beta \sin\left(\frac{\pi T}{v_\beta}(a + i s v_\beta t')\right)^{2d_\beta}}, \end{aligned} \tag{C.14}$$

where in the last equality we dropped the odd terms when $s = s'$. Changing variables to $t' = -s(t + i/2T)$ and dropping a's assuming $\forall \beta : aT/v_\beta < 1$

$$\begin{aligned} \partial_x \langle I_\alpha \rangle &= i \frac{\eta_\alpha \lambda_\alpha}{k_\alpha} . W_V . \prod_\beta (\frac{A_\beta}{v_\beta})^{2d_\beta} . T^{2\Delta} \times \\ &\qquad \sum_s s \int \mathrm{d}t \frac{-s(\sin(\Omega t)\, cosh\,(\Omega/2T) + i\cos(\Omega t)\sinh(\Omega/2T))}{\cosh(\pi T t)^{2\Delta}} \\ &= 2 \frac{\eta_\alpha \lambda_\alpha}{k_\alpha} . W_V . \prod_\beta (\frac{A_\beta}{v_\beta})^{2d_\beta} . T^{2\Delta} \sinh\left(\frac{\Omega}{2T}\right) \int \mathrm{d}t \frac{\cosh(i\Omega t)}{\cosh(\pi T t)^{2\Delta}} \\ &= \frac{\eta_\alpha \lambda_\alpha}{\pi k_\alpha} . W_V . \prod_\beta (\frac{A_\beta}{v_\beta})^{2d_\beta} . 2^{2\Delta} T^{2\Delta - 1} \sinh\left(\frac{\Omega}{2T}\right) B(\Delta + i\frac{\Omega}{2\pi T}, \Delta - i\frac{\Omega}{2\pi T}), \end{aligned} \tag{C.15}$$

where $\Delta = \sum_\beta d_\beta$ is the scaling dimension of $\prod_\beta X_\beta$. So in the ohmic regime when $\Omega \ll T$ we have (we're also retaining the $\frac{1}{(2\pi a)^{N_e}}$ factor)

$$\partial_x \langle I_\alpha \rangle = \sigma_0 g_V \frac{\eta_\alpha \lambda_\alpha}{k_\alpha} \sum_\beta \frac{\eta_\beta \lambda_\beta}{k_\beta} \mu_\beta(x), \qquad g_V = W_V . \frac{(2\pi a)^{2(\Delta - N_e)}}{\prod_\gamma v_\gamma^{2d_\gamma}} . \frac{\Gamma(\Delta)^2}{\Gamma(2\Delta)} T^{2\Delta - 2}. \quad \text{(C.16)}$$

Assuming local equilibrium we have $\langle I_\beta \rangle = \eta_\beta \sigma_0 \mu_\alpha / k_\beta$. We can write these set of equations in terms of the original modes $I_i = \Lambda_{i\alpha} I_\alpha$ as

$$\partial_x \langle I_i \rangle = -g_V \eta_i \nu_i m_i \sum_j m_j \langle I_j(x) \rangle . \quad \text{(C.17)}$$

C.1.2 Random density-density

For concreteness let's look at the example of the disordered fixed point of the $\nu = 2$ quantum Hall edge state. This is the theory that we derived in Appendix B if we only focus on the ϕ_1 and ϕ_2 modes and ignore the rest:

$$S = S_1 + S_2 + S_{12} + S_{\text{tunneling},12} \quad \text{(C.18a)}$$

$$i = 1, 2 : S_i = -\frac{1}{4\pi} \int_{t,x} [\partial_x \phi_i (\eta_i \partial_t \phi_i + v_i \partial_x \phi_i)] \quad \text{(C.18b)}$$

$$S_{12} = -\frac{v_{12}}{4\pi} \int_{t,x} \partial_x \phi_1 \partial_x \phi_2 \quad \text{(C.18c)}$$

$$S_{\text{tunneling},12} = -\int_{t,x} \left[\xi_{12}(x) \, \mathrm{e}^{i(\phi_1 - \phi_2)} + \text{h.c.} \right] . \quad \text{(C.18d)}$$

We first change the basis to the charge mode $\phi_\rho = \frac{1}{\sqrt{2}}(\phi_1 + \phi_2)$ and the neutral mode $\phi_\sigma = \frac{1}{\sqrt{2}}(\phi_1 - \phi_2)$ and then perform a gauge transformation $O(x)$ to eliminate the random

tunneling term. Now, we can write down the Hamiltonian for the disordered fixed point as

$$H_F = H_\rho + H_\sigma \tag{C.19a}$$

$$H_\rho = \frac{v_\rho}{4\pi}\int \mathrm{d}x\ (\partial_x\phi_\rho)^2 \tag{C.19b}$$

$$H_\sigma = \int \mathrm{d}x\ \frac{2\pi v_\sigma}{3}\tilde{\boldsymbol{J}}_\sigma^2 \tag{C.19c}$$

where current operators $\tilde{J}^a$ are defined as in (3.57). The residual density-density interaction between the charge mode ϕ_ρ and the new neutral mode $\tilde{\phi}_\sigma$ is

$$V = H_{\rho\sigma} = \frac{1}{2\pi}\int \mathrm{d}x\partial_x\phi_\rho(\boldsymbol{\xi}_\sigma.\tilde{\boldsymbol{J}}(x)), \qquad \xi_\sigma^a \equiv 2\pi\sqrt{2}v_{\rho\sigma}O^{za}(x). \tag{C.20}$$

ξ_σ^a is a quenched random variable, the auto-correlation of which decays on the length scales of $\sim v_\sigma^2/W_{12}$. This renders V irrelevant. Assuming v_σ^2/W_{12} is small enough, for simplicity we take ξ_σ to have Gaussian correlation $\overline{\xi_\sigma^a(x)\xi_\sigma^b(x')} = \delta^{ab}W_\sigma\delta(x-x')$ where $W_\sigma \approx 8\pi^2 v_{\rho\sigma}^2 v_\sigma^2/W_{12}$.

In order to find the tunneling current between the charge and neutral modes we bias the modes with chemical potential by introducing the interaction

$$H_\mu = -\int \mathrm{d}x\,[\mu_\rho n_\rho(x) + \tilde{\mu}_\sigma\tilde{n}_\sigma(x)] \tag{C.21}$$

with the charge density $n_\rho = \frac{1}{2\pi}\partial_x\phi_\rho$ and the new neutral denstiy $\tilde{n}_\sigma = \frac{1}{2\pi}\partial_x\tilde{\phi}_\sigma = \sqrt{2}\tilde{J}^z$. The charge mode is conserved

$$-\partial_x I_\rho = \partial_t n_\rho = -\eta_\rho v_\rho \partial_x n_\rho \tag{C.22}$$

while for the neutral mode we have

$$\begin{aligned}-\partial_x\tilde{I}_\sigma(x,t) = \partial_t\tilde{n}_\sigma(x,t) &= -\eta_\sigma v_\sigma\partial_x\tilde{n}_\sigma + i[H_{\rho\sigma}, \sqrt{2}\tilde{J}^z(x,t)] \\ &= -\eta_\sigma v_\sigma\partial_x\tilde{n}_\sigma + \sqrt{2}n_\rho(x,t)\left(\xi_\sigma^x(x)\tilde{J}^y(x,t) - \xi_\sigma^y(x)\tilde{J}^x(x,t)\right).\end{aligned} \tag{C.23}$$

Similarly as before, we assume the modes are in local equilibrium so we have $n_\rho(x) = \frac{1}{2\pi v_\rho}\mu_\rho$ and $\tilde{n}_\sigma(x) = \frac{1}{2\pi v_\sigma}\tilde{\mu}_\sigma$. Note that since the density $\tilde{n}_\sigma(x)$ decays only due to the interaction term C.20, we expect this density and its conjugate chemical potential $\tilde{\mu}_\sigma$ to vary slowly at low temperatures. Therefore, we drop the terms $\partial_x n_\rho$ and $\partial_x \tilde{n}_\sigma$ in the above equations. Therefore we drop To leading order in W_σ, the expectation value of this operator is

$$\partial_x \left\langle \tilde{I}_\sigma(x,t) \right\rangle = -\frac{i}{\sqrt{2}} W_\sigma \sum_{s,s'} \int \mathrm{d}t' \left\langle n_\rho(x,t,s)_{H_0} n_\rho(x,t',s')_{H_0} \right\rangle \tag{C.24}$$
$$\times \left[\left\langle \tilde{J}^y(x,t,s)_{H_0} \tilde{J}^x(x,t',s')_{H_0} \right\rangle - \left\langle \tilde{J}^x(x,t,s)_{H_0} \tilde{J}^y(x,t',s')_{H_0} \right\rangle \right].$$

The equation of motion for $\tilde{J}^a(x)$, evolved with H_0, is

$$\partial_t \tilde{J}^x(x,t) = -\eta_\sigma v_\sigma \partial_x \tilde{J}^x(x,t) - \sqrt{2}\tilde{\mu}_\sigma \tilde{J}^y(x,t) \tag{C.25a}$$

$$\partial_t \tilde{J}^y(x,t) = -\eta_\sigma v_\sigma \partial_x \tilde{J}^y(x,t) + \sqrt{2}\tilde{\mu}_\sigma \tilde{J}^x(x,t) \tag{C.25b}$$

with solutions

$$\tilde{J}^x(x,t) = \tilde{J}^x(x - \eta_\sigma v_\sigma t)\cos(\sqrt{2}\tilde{\mu}_\sigma t) - \tilde{J}^y(x - \eta_\sigma v_\sigma t)\sin(\sqrt{2}\tilde{\mu}_\sigma t) \tag{C.26a}$$

$$\tilde{J}^y(x,t) = \tilde{J}^y(x - \eta_\sigma v_\sigma t)\cos(\sqrt{2}\tilde{\mu}_\sigma t) + \tilde{J}^x(x - \eta_\sigma v_\sigma t)\sin(\sqrt{2}\tilde{\mu}_\sigma t). \tag{C.26b}$$

Using this solution we have

$$\partial_x \left\langle \tilde{I}_\sigma(x,t) \right\rangle = -\frac{i}{\sqrt{2}} W_\sigma \sum_{s,s'} \int \mathrm{d}t' \sin(\sqrt{2}\tilde{\mu}_\sigma(t-t')) \left\langle n_\rho(x,t,s)_{H_F} n_\rho(x,t',s')_{H_F} \right\rangle \tag{C.27}$$
$$\left[\left\langle \tilde{J}^x(x,t,s)_{H_F} \tilde{J}^x(x,t',s')_{H_F} \right\rangle + \left\langle \tilde{J}^y(x,t,s)_{H_F} \tilde{J}^y(x,t',s')_{H_F} \right\rangle \right].$$

We proceed similarly as before to find

$$\partial_x \left\langle \tilde{I}_\sigma \right\rangle = -\frac{1}{2\pi} \frac{\sqrt{2} W_\sigma}{v_\rho^2 v_\sigma^2} T^{2\Delta - 1} \sinh\left(\frac{\sqrt{2}\tilde{\mu}_\sigma}{2T} \right) B(\Delta + i\frac{\sqrt{2}\tilde{\mu}_\sigma}{2\pi T}, \Delta - i\frac{\sqrt{2}\tilde{\mu}_\sigma}{2\pi T}), \tag{C.28}$$

with $\Delta = 2$. To linear order in $\tilde{\mu}_\sigma$

$$\partial_x \left\langle \tilde{I}_\sigma \right\rangle = -g_\sigma \sigma_0 \tilde{\mu}_\sigma, \qquad g_\sigma = \frac{W_\sigma}{12 v_\rho^2 v_\sigma^2} T^2 = \frac{2\pi^2 v_{\rho\sigma}^2}{3 v_\rho^2 W_{12}} T^2. \tag{C.29}$$

We can express this equation along with $\partial_x I_\rho = 0$ in a basis similar to the original fractional modes. We define

$$I_1' = \frac{1}{\sqrt{2}}(I_\rho + \tilde{I}_\sigma) \tag{C.30a}$$

$$I_2' = \frac{1}{\sqrt{2}}(I_\rho - \tilde{I}_\sigma). \tag{C.30b}$$

These new modes mix only due the irrelevant interactions such as C.20 and so are expected to vary slowly at low temperatures. In this basis the kinetic equations are

$$\partial_x \left\langle I_i' \right\rangle = -\sigma_0 g_\sigma \eta_i m_i \sum_j m_j I_j'(x) \tag{C.31}$$

with $m_1 = 1$ and $m_2 = -1$. While this expression looks similar to C.17, the conductivity coefficient is different and reflects the disordered fixed point.

C.2 Thermal conductivity coefficient

Similarly, we can find the heat currents exchanged between the edge modes. Here, we work to linear order in the temperature bias and assume zero chemical potential bias. From the Heisenberg equation of motion with total Hamiltonian $H = \sum_\alpha H_\alpha + V$:

$$\begin{aligned} -\partial_x J_\alpha(t) &= \partial_t \mathcal{H}_\alpha(x,t) = i[H, \mathcal{H}_\alpha(x)](t) \\ &= -\eta_\alpha v_\alpha \partial_x \mathcal{H}_\alpha(x,t) + i \int \mathrm{d}x' \; \xi(x') [X_\alpha(x'), \mathcal{H}_\alpha(x)] \prod_{\beta \neq \alpha} X_\alpha(x') + \text{h.c.}, \end{aligned} \tag{C.32}$$

where $\mathcal{H}_\alpha$ is the energy density of mode α. This equation should be understood as change in heat current due to a series of incoherent tunnelings. Local equilibrium implies $\langle \mathcal{H}_\alpha \rangle =$

$\frac{1}{2v_\alpha}\kappa_0 T_\alpha^2$ so to leading order we can drop the first term on the right hand side. We will find the expectation value of $\partial_x J_\alpha$ using the Keldysh technique ($H_F = \sum_\alpha H_\alpha$),

$$\langle \partial_x J_\alpha(x,t)\rangle = \frac{1}{2}\sum_s \left\langle T_C\ \partial_x J_\alpha(x,t,s)_{H_F}\, \mathrm{e}^{i\sum_{s'} s' \int \mathrm{d}t' V(t',s')_{H_F}} \right\rangle . \tag{C.33}$$

Expanding the slow evolution operator to first order

$$\begin{aligned}\partial_x \langle J_\alpha(x,t)\rangle &= \frac{-i}{2}\sum_{ss'} s' \int \mathrm{d}t' \left\langle T_C \partial_x J_\alpha(x,t,s)_{H_F} V(t',s')_{H_F}\right\rangle \\ &= \frac{1}{2} W_V \sum_{ss'} s' \int \mathrm{d}x' \int \mathrm{d}t' \left\langle T_C [X_\alpha(x'), \mathcal{H}_\alpha(x)](t,s) X_\alpha^\dagger(x',t',s')\right\rangle \\ &\qquad \times \prod_{\beta\neq\alpha} \left\langle T_C X_\beta(x',t,s) X_\beta^\dagger(x',t',s')\right\rangle + \text{h.c.}\end{aligned} \tag{C.34}$$

where we dropped the H_F index after the second equality and also took the disorder average. We assume the modes are in local equilibrium so that the temperatures T_α are actually local temperatures at point x. Using $[X_\alpha(x'), \mathcal{H}_\alpha(x)](t)_{H_F} = i\delta(x-x')\partial_t X_\alpha(x,t)_{H_F}$ we get

$$\begin{aligned}\partial_x \langle J_\alpha\rangle = \frac{1}{2} W_V (2\pi d_\alpha T_\alpha) \prod_\beta \left(\frac{A_\beta T_\beta}{v_\beta}\right)^{2d_\beta} \times \\ \sum_{ss'} s' \int \mathrm{d}t' \chi_{ss'}(t-t') \frac{\cot\frac{\pi T_\alpha}{v_\alpha}(a + i\chi_{ss'} v_\alpha (t-t'))}{\prod_\beta \sin\left(\frac{\pi T_\beta}{v_\beta}(a + i\chi_{ss'} v_\beta (t-t'))\right)^{2d_\beta}} + \text{h.c.}\end{aligned} \tag{C.35}$$

$\chi_{ss}(t)$ is an odd function of t so $t\chi_{ss}(t)$ is even and so the integral vanishes for $s = s'$. Therefore, ($\chi_{s,-s} = -s$)

$$\partial_x \langle J_\alpha\rangle = W_V . \pi d_\alpha T_\alpha . \prod_\beta \left(\frac{A_\beta T_\beta}{v_\beta}\right)^{2d_\beta} . \sum_s \int \mathrm{d}t' \frac{\cot\frac{\pi T_\alpha}{v_\alpha}(a + i s v_\alpha t')}{\prod_\beta \sin\left(\frac{\pi T_\beta}{v_\beta}(a + i s v_\beta t')\right)^{2d_\alpha}} + \text{h.c.} \tag{C.36}$$

Ignoring a's (assuming $aT_\beta/v_\beta < 1$) and changing variables to $t' = -s(t + i\frac{1}{2T_\alpha})$,

$$\begin{aligned}\partial_x \langle J_\alpha\rangle = W_V . \pi d_\alpha T_\alpha . \prod_\beta \left(\frac{A_\beta T_\beta}{v_\beta}\right)^{2d_\beta} \times \\ \sum_s \int \mathrm{d}t \frac{i \sinh(\pi T_\alpha t)}{\cosh(s\pi T_\alpha t)^{2d_\alpha+1} \prod_{\beta\neq\alpha} \sin\left(\frac{\pi T_\beta}{2T_\alpha} - i\pi T_\alpha t)\right)^{2d_\beta}} + \text{h.c.}\end{aligned} \tag{C.37}$$

Expanding the integrand to first order in $\tau_{\beta\alpha} \equiv T_\beta - T_\alpha$

$$\partial_x \langle J_\alpha \rangle = W_V . \pi d_\alpha . \prod_\beta (\frac{A_\beta T_\beta}{v_\beta})^{2d_\beta} . \sum_s \int \mathrm{d}t \frac{i \sinh(\pi T_\alpha t)}{\cosh(\pi T_\alpha t)^{\sum_\beta 2d_\beta + 1}} . \left(1 - i \tanh(\pi T_\alpha t) . (\frac{\pi}{2T_\alpha} - i\pi T_\alpha t) \sum_{\beta \neq \alpha} 2d_\beta \tau_{\beta\alpha} \right) + \text{h.c.} \tag{C.38}$$

Dropping the odd terms in the integrand

$$\begin{aligned} \partial_x \langle J_\alpha \rangle &= 2\pi d_\alpha W_V . \prod_\beta (\frac{A_\beta}{v_\beta})^{2d_\beta} . T^{2\Delta - 2} . \frac{\pi}{2T} \sum_{j \neq i} 2d_\beta \tau_{\beta\alpha} . \sum_s \int \mathrm{d}t \frac{\sinh(\pi T_\alpha t)^2}{\cosh(s\pi T_\alpha t)^{\sum_\beta 2d_\beta + 2}} \\ &= \kappa_0 \sum_{\beta \neq \alpha} g^Q_{\alpha\beta} \frac{T_\beta^2 - T_\alpha^2}{2}, \qquad g^Q_{\alpha\beta} \equiv g_V \frac{12 d_\alpha d_\beta}{1 + 2\Delta} \end{aligned} \tag{C.39}$$

with g_V defined in (C.16).